Delft University of Technology
Faculty of Electrical Engineering, Mathematics and Computer Science
& Faculty of Applied Sciences

Influence of the partial closure of estuaries on the residual sediment transport and trapping

Thesis for fulfilling the requirements
of the degrees of

BACHELOR OF SCIENCE
in
APPLIED MATHEMATICS AND APPLIED PHYSICS

BY

Ferhat Sindy

Delft, The Netherlands
August 2020

Abstract

In this thesis the water motion and sediment dynamics are investigated in a periodically closed and opened estuary. The water motion in an estuary is mainly driven by the semi-diurnal tide with an period of 12h25m and river discharge. An example of such an estuary is the Ems-Dollard estuary. Recent observations show an increase in tidal range (height difference between high and low tide), suspended sediment concentration and the depletion of oxygen levels (consequently harming the ecosystem). A possible solution, periodically closing and opening the estuary, is investigated. The water motion in a periodically opened and closed estuary is described by the linearised cross-sectionally averaged equations which give the sea-surface elevations and tidal velocity when solved with the eigenfunction expansion method. It was found that the sea-surface elevations and tidal velocity for a periodically opened and closed estuary are again 12h25m periodic. For the sediment transport, when no overtide is considered the residual sediment transport is seaward directed if the estuary is closed at low water and landward directed if the estuary is closed at high water. The barrier location determines the magnitude of the residual sediment. When overtide is included in the forcing of the system no relation is found between the direction of the residual sediment transport and the closing height and closing position. The location of the barrier and closing height both determine the magnitude of the residual sediment transport and direction. By introducing a barrier that periodically closes and opens we intended to achieve a seaward directed residual sediment transport in the Ems-Dollard estuary. The results suggest that this is not possible. Further research is needed with more extensive models to confirm this. For future Research I recommend to extend the model to a two-dimensional model with the eigenfunction expansion method. Other possibilities may be to consider a spatial dependent erodible bed.

Contents

Chapter 1

Introduction

In this thesis we will study the water motion and sediment dynamics in an estuary. According to Pritchard (1967) an estuary is defined as "a partially enclosed coastal body of brackish water with one or more rivers or streams flowing into it, and with a free connection to the open sea". Estuaries trap sediment as a result of the land inward flow at the bottom Meade (1969).
The water motion is driven by the tides and river discharge. In this thesis the semi-diurnal tide, with an angular frequency of $\sigma = 2\pi/12\text{h}25\text{m}$ and the first overtide, with angular frequency 2σ is considered. Due to the water motion, sediment is being transported, resulting in specific places where it accumulates. These locations are called Estuarine Turbidity Maxima (see Burchard et al. (2018)).

Figure 1.1: Muddy Ems-Dollard estuary. From defotograaf.eu, van Houdt

Human interventions influence the water motion and sediment trapping hence the optimal functioning of estuarine ecosystems. This could possibly cause adverse environmental and societal implications Boesch et al. (1994). An example of an estuary where major changes took place over the past 25 years is the Ems-Dollard estuary, located on the border between The Netherlands and Germany. Recent observations on the river Ems show an increase in tidal range (height difference between high and low tide) and suspended sediment concentration and the depletion of oxygen levels (consequently harming the ecosystem) between 1980 and the present as a response to maintenance dredging and deepening Krebs et al. (2008). The tidal river has also shifted from a sandy bed to a silty bed Krebs et al. (2008) see Figure 1.1. Different possible solutions

have been proposed. An example is the introduction of a horizontally movable time dependent barrier de Jongh (2020). In this thesis a different possible solution is investigated. By using a barrier the estuary is completely closed for a specific period of time. The main mathematical tool used to investigate this is the eigenfunction expansion method instead of a time stepping approach. This results in the following research question:

Can the sea surface elevation/tidal velocity in an estuary that is periodically opened and closed be accurately modeled with a limited number of Fourier modes in time?

The second research question concerns the residual sediment transport which is defined as "The local (Eularian) averaged sediment transport within a tidal period" Wang et al. (1999):

What is the influence of introducing a barrier on the residual sediment transport of an estuary?

In order to answer these questions, an one-dimensional model for the water motion is derived in chapter 2. The model consist of the cross-sectionally averaged momentum and continuity equation that describe the sea-surface elevations and tidal velocity in the estuary. The opening and closing of the barrier is introduced and the resulting equations are solved with the eigenfunction expansion method in chapter 3. The results that follow from varying the free parameters in the model, namely the closing height and closing position, are discussed, analyzed and applied on the Ems-Dollard estuary to investigate its influence on the magnitude and direction of the residual sediment transport in chapter 4 and finally the research questions are answered in chapter 5.

Chapter 2

Derivation of the linearised cross-sectionally averaged equations

In this chapter a derivation of the cross-sectionally averaged shallow water equations is given following chapter 2 of Rozendaal (2019) and appendix B.4 of Ter Brake (2011). The starting point is the system of equations consisting of the incompressible continuity equation and the three dimensional Navier stokes equations given in equation (2.1).

$$\begin{cases} \dfrac{\partial u}{\partial x} + \dfrac{\partial v}{\partial y} + \dfrac{\partial w}{\partial z} = 0, & \text{(2.1a)} \\ \dfrac{\partial u}{\partial t} + u\dfrac{\partial u}{\partial x} + v\dfrac{\partial u}{\partial y} + w\dfrac{\partial u}{\partial z} + f_* w - fv = -\dfrac{1}{\rho}\dfrac{\partial p}{\partial x} + \nu\left(\dfrac{\partial^2 u}{\partial x^2} + \dfrac{\partial^2 u}{\partial y^2} + \dfrac{\partial^2 u}{\partial z^2}\right), & \text{(2.1b)} \\ \dfrac{\partial v}{\partial t} + u\dfrac{\partial v}{\partial x} + v\dfrac{\partial v}{\partial y} + w\dfrac{\partial v}{\partial z} + fu = -\dfrac{1}{\rho}\dfrac{\partial p}{\partial y} + \nu\left(\dfrac{\partial^2 v}{\partial x^2} + \dfrac{\partial^2 v}{\partial y^2} + \dfrac{\partial^2 v}{\partial z^2}\right), & \text{(2.1c)} \\ \dfrac{\partial w}{\partial t} + u\dfrac{\partial w}{\partial x} + v\dfrac{\partial w}{\partial y} + w\dfrac{\partial w}{\partial z} - f_* u = -\dfrac{1}{\rho}\dfrac{\partial p}{\partial z} + \nu\left(\dfrac{\partial^2 w}{\partial x^2} + \dfrac{\partial^2 w}{\partial y^2} + \dfrac{\partial^2 w}{\partial z^2}\right) - g. & \text{(2.1d)} \end{cases}$$

In equation (2.1) the variables u,v,w are the flow velocity in Cartesian coordinates, ρ is the fluid density, ν is the kinematic viscosity and g is the gravitational acceleration. $f = 2\Omega\cos(\phi)$ and $f^* = 2\Omega\sin(\phi)$ are Coriolis parameters where Ω is the angular frequency of the Earth and ϕ is the geographic latitude. The Coriolis parameters are only valid if the coordinate system is chosen such that the x-axis is pointing Eastward, the y-axis is pointing to the North and the z-axis is pointing upwards to obtain a right hand side coordinate system. Keep in mind that u,v,w,p are a function of x,y,z,t.
In section (2.1) the unsteady Reynolds averaged Navier Stokes equations are derived and subsequently the three dimensional shallow water equations. In section (2.2) the two dimensional shallow water equations are obtained by integrating over the depth and finally in section (2.3) the one dimensional shallow water equation is derived by integrating over the width. To obtain the linearised cross-sectionally averaged equations , the one dimensional shallow water equations are scaled.

2.1 Derivation of the three dimensional shallow water equation

Equations (2.1) are used to model flows including the length and time scales. For the estuary dynamics we are interested in large time scales therefore a Reynolds Decomposition is applied. Reynolds Decomposition decomposes the velocity in a mean and turbulent part, denoted by $\langle\cdot\rangle$

and $\cdot'$ respectively. In equation (2.2) the Reynold Decomposition is shown for the flow velocity u along with some important averaging $\langle\cdot\rangle$ properties:

$$\begin{aligned} &u = \langle u\rangle + u', \\ &\langle u'\rangle = 0, \quad \langle\langle u\rangle\rangle = \langle u\rangle, \quad \langle u+v\rangle = \langle u\rangle + \langle v\rangle, \quad \langle\langle u\rangle v\rangle = \langle u\rangle\langle v\rangle, \quad \left\langle \frac{\partial u}{\partial s}\right\rangle = \frac{\partial}{\partial s}\langle u\rangle. \end{aligned} \tag{2.2}$$

Applying the Reynold decomposition to the continuity equation (2.1a) and using the averaging properties the Reynolds averaged continuity equation is derived:

$$\frac{\partial\langle u\rangle}{\partial x} + \frac{\partial\langle v\rangle}{\partial y} + \frac{\partial\langle w\rangle}{\partial z} = 0.$$

Equivalently for the Navier Stokes equations the Reynolds decomposition can be applied. To illustrate this, the Reynolds averaged Navier Stokes equation in the x-direction is derived next. Before applying the Reynolds decomposition, the Navier Stokes equation (2.1b) must be written in its conservative form. This is done by multiplying the continuity equation (2.1a) with the flow velocity u and adding it to the Navier Stokes equation (2.1b) and using the chain rule:

$$\frac{\partial u}{\partial t} + \frac{\partial}{\partial x}\left(u^2\right) + \frac{\partial}{\partial y}(uv) + \frac{\partial}{\partial z}(uw) + f_* w - fv = -\frac{1}{\rho}\frac{\partial p}{\partial x} + \nu\left(\frac{\partial^2 u}{\partial x^2} + \frac{\partial^2 u}{\partial y^2} + \frac{\partial^2 u}{\partial z^2}\right).$$

Applying the Reynolds decomposition results in:

$$\begin{aligned} &\frac{\partial\langle u\rangle}{\partial t} + \frac{\partial}{\partial x}\langle u\rangle^2 + \frac{\partial}{\partial y}\langle u\rangle\langle v\rangle + \frac{\partial}{\partial z}\langle u\rangle\langle w\rangle + f_*\langle w\rangle - f\langle v\rangle \\ &\qquad = -\frac{1}{\rho}\frac{\partial\langle p\rangle}{\partial x} + \nu\left(\frac{\partial^2\langle u\rangle}{\partial x^2} + \frac{\partial^2\langle u\rangle}{\partial y^2} + \frac{\partial^2\langle u\rangle}{\partial z^2}\right) - \frac{\partial}{\partial x}\left\langle u'^2\right\rangle - \frac{\partial}{\partial y}\left\langle u'v'\right\rangle - \frac{\partial}{\partial z}\left\langle u'w'\right\rangle. \end{aligned}$$

This equation can be rewritten by using the chain rule combined with the Reynolds averaged continuity equation.

$$\begin{aligned} &\frac{\partial\langle u\rangle}{\partial t} + \langle u\rangle\frac{\partial\langle u\rangle}{\partial x} + \langle v\rangle\frac{\partial\langle u\rangle}{\partial y} + \langle w\rangle\frac{\partial\langle u\rangle}{\partial z} + f_*\langle w\rangle - f\langle v\rangle, \\ &\qquad = -\frac{1}{\rho}\frac{\partial\langle p\rangle}{\partial x} + \frac{\partial}{\partial x}\left(\nu\frac{\partial\langle u\rangle}{\partial x} - \left\langle u'^2\right\rangle\right) + \frac{\partial}{\partial y}\left(\nu\frac{\partial\langle u\rangle}{\partial y} - \left\langle u'v'\right\rangle\right) + \frac{\partial}{\partial z}\left(\nu\frac{\partial\langle u\rangle}{\partial z} - \left\langle u'w'\right\rangle\right). \end{aligned} \tag{2.3}$$

The equation above still has correlations of the unknown turbulent fluctuations $\langle u'^2\rangle$, $\langle v'^2\rangle$, $\langle w'^2\rangle$, $\langle u'v'\rangle$, $\langle u'w'\rangle$ and $\langle v'w'\rangle$. By choosing an appropriate closure the Reynolds stress equations can be expressed in averaged quantities here a first order closure is chosen for convenience. The closures are shown in equation (2.4), where A_h and A_v are the horizontal and vertical eddy viscosity coefficients respectively. A distinction is made between the vertical and horizontal eddy viscosity term because the turbulent flow is much larger in the horizontal dimension for the flows we consider Cushman-Roisin and Beckers (2011).

$$\begin{aligned} &\langle u'^2\rangle = -2A_\mathrm{h}\frac{\partial\langle u\rangle}{\partial x}, && \langle v'^2\rangle = -2A_\mathrm{h}\frac{\partial\langle v\rangle}{\partial y}, && \langle w'^2\rangle = -2A_\mathrm{v}\frac{\partial\langle w\rangle}{\partial z}, \\ &\langle u'v'\rangle = -A_\mathrm{h}\left(\frac{\partial\langle u\rangle}{\partial y} + \frac{\partial\langle v\rangle}{\partial x}\right), && \langle u'w'\rangle = -A_\mathrm{v}\frac{\partial\langle u\rangle}{\partial z} - A_\mathrm{h}\frac{\partial\langle w\rangle}{\partial x}, && \langle v'w'\rangle = -A_\mathrm{v}\frac{\partial\langle v\rangle}{\partial z} - A_\mathrm{h}\frac{\partial\langle w\rangle}{\partial y}. \end{aligned} \tag{2.4}$$

Substituting these expressions in the Reynolds averaged Navier Stokes equation and defining $\mathcal{A}_\mathrm{h} = \nu + A_\mathrm{h}$ and $\mathcal{A}_\mathrm{v} = \nu + A_\mathrm{v}$, the so-called effective eddy viscosity coefficients, results in:

$$\begin{cases} \dfrac{\partial u}{\partial x} + \dfrac{\partial v}{\partial y} + \dfrac{\partial w}{\partial z} = 0, & \text{(2.5a)} \\ \dfrac{\partial u}{\partial t} + u\dfrac{\partial u}{\partial x} + v\dfrac{\partial u}{\partial y} + w\dfrac{\partial u}{\partial z} + f_* w - fv = -\dfrac{1}{\rho}\dfrac{\partial p}{\partial x} + \dfrac{\partial}{\partial x}\left(\mathcal{A}_\mathrm{h}\dfrac{\partial u}{\partial x}\right) + \dfrac{\partial}{\partial y}\left(\mathcal{A}_\mathrm{h}\dfrac{\partial u}{\partial y}\right) + \dfrac{\partial}{\partial z}\left(\mathcal{A}_\mathrm{v}\dfrac{\partial u}{\partial z}\right), & \text{(2.5b)} \\ \dfrac{\partial v}{\partial t} + u\dfrac{\partial v}{\partial x} + v\dfrac{\partial v}{\partial y} + w\dfrac{\partial v}{\partial z} + fu = -\dfrac{1}{\rho}\dfrac{\partial p}{\partial y} + \dfrac{\partial}{\partial x}\left(\mathcal{A}_\mathrm{h}\dfrac{\partial v}{\partial x}\right) + \dfrac{\partial}{\partial y}\left(\mathcal{A}_\mathrm{h}\dfrac{\partial v}{\partial y}\right) + \dfrac{\partial}{\partial z}\left(\mathcal{A}_\mathrm{v}\dfrac{\partial v}{\partial z}\right), & \text{(2.5c)} \\ \dfrac{\partial w}{\partial t} + u\dfrac{\partial w}{\partial x} + v\dfrac{\partial w}{\partial y} + w\dfrac{\partial w}{\partial z} - f_* u = -\dfrac{1}{\rho}\dfrac{\partial p}{\partial z} + \dfrac{\partial}{\partial x}\left(\mathcal{A}_\mathrm{h}\dfrac{\partial w}{\partial x}\right) + \dfrac{\partial}{\partial y}\left(\mathcal{A}_\mathrm{h}\dfrac{\partial w}{\partial y}\right) + \dfrac{\partial}{\partial z}\left(\mathcal{A}_\mathrm{v}\dfrac{\partial w}{\partial z}\right) - g, & \text{(2.5d)} \end{cases}$$

where the brackets $\langle\cdot\rangle$ are left out for convenience (so u is the turbulent averaged velocity in the x-direction). Comparing the above equation with equation (2.1) the only difference is that the flow velocities are replaced by their Reynolds average and the viscosity coefficients are replaced by their effective eddy viscosity. The final step in deriving the three dimensional shallow water equation follows from scaling the equations. We introduce L,H,U,V as the horizontal-, vertical length scale, horizontal- and vertical flow scale respectively. The scaling of the Reynolds averaged continuity equation is given by:

$$\begin{matrix} \dfrac{\partial u}{\partial x} & + & \dfrac{\partial v}{\partial y} & + & \dfrac{\partial w}{\partial z} & = 0. \\ \dfrac{U}{L} & & \dfrac{U}{L} & & \dfrac{W}{H} & \end{matrix}$$

Now three cases can be considered:
1. $\frac{U}{L} < \frac{W}{H}$: For this approximation the leading order balance is given by $\partial w/\partial x = 0$. This means that the flow in the vertical direction is constant in z. Therefore the supply of vertical flow must come from the horizontal direction, However the horizontal flows are small and therefore it is not possible to provide for such a vertical flow. In short this balance is infeasible.
2. $\frac{U}{L} > \frac{W}{H}$: For this approximation the leading order balance is given by $\partial u/\partial x + \partial v/\partial y = 0$. This means that the convergence of the flow in the horizontal direction is compensated by the divergence of the flow in the other horizontal direction. However, for the kinematic boundary conditions to hold one has to regulate that $W \sim UH/L$ holds, therefore $W < U\frac{H}{L}$ is also infeasible.
3. $\frac{U}{L} \sim \frac{W}{H}$: For this approximation the leading order balance is given as $\partial u/\partial x + \partial v/\partial y + \partial w/\partial z = 0$. This is a three way balance and therefore a feasible leading order balance.

To simplify the momentum equation. I assume that the water is shallow , i.e. $H << L$. Applying this to the continuity equation, it follows that $W << U$. Therefore the vertical flow is smaller than the horizontal flow. Applying the order balance analysis on the vertical momentum equation (2.5d), results in (For a detailed derivation see Pedlosky (2013):

$$\frac{\partial p}{\partial z} = -\rho g,$$

the so-called hydro static balance equation. Furthermore the Coriolis term proportional to f_* is negligible compared to the other components in the equation Cushman-Roisin and Beckers (2011). The resulting three dimensional shallow water equations read:

$$\begin{cases} \dfrac{\partial u}{\partial x}+\dfrac{\partial v}{\partial y}+\dfrac{\partial w}{\partial z}=0, & \text{(2.6a)}\\ \dfrac{\partial u}{\partial t}+u\dfrac{\partial u}{\partial x}+v\dfrac{\partial u}{\partial y}+w\dfrac{\partial u}{\partial z}-fv=-\dfrac{1}{\rho}\dfrac{\partial p}{\partial x}+\dfrac{\partial}{\partial x}\left(\mathcal{A}_{\mathrm{h}}\dfrac{\partial u}{\partial x}\right)+\dfrac{\partial}{\partial y}\left(\mathcal{A}_{\mathrm{h}}\dfrac{\partial u}{\partial y}\right)+\dfrac{\partial}{\partial z}\left(\mathcal{A}_{v}\dfrac{\partial u}{\partial z}\right), & \text{(2.6b)}\\ \dfrac{\partial v}{\partial t}+u\dfrac{\partial v}{\partial x}+v\dfrac{\partial v}{\partial y}+w\dfrac{\partial v}{\partial z}+fu=-\dfrac{1}{\rho}\dfrac{\partial p}{\partial y}+\dfrac{\partial}{\partial x}\left(\mathcal{A}_{\mathrm{h}}\dfrac{\partial v}{\partial x}\right)+\dfrac{\partial}{\partial y}\left(\mathcal{A}_{\mathrm{h}}\dfrac{\partial v}{\partial y}\right)+\dfrac{\partial}{\partial z}\left(\mathcal{A}_{v}\dfrac{\partial v}{\partial z}\right), & \text{(2.6c)}\\ \dfrac{\partial p}{\partial z}=-\rho g. & \text{(2.6d)} \end{cases}$$

In short, the assumption that the water is shallow results in a significant reduction of the z-direction momentum equation of the Reynolds averaged Navier Stokes equation.

2.2 Derivation of the two dimensional shallow water equation

In this section the two dimensional shallow water equation are derived. First the geometry and boundary conditions are derived. Subsequently equation (2.6) is integrated over the height to obtain the two dimensional shallow water equation.

2.2.1 Geometry and boundary conditions

In the schematic figure below a cross sectional view of a water column is shown, where $z = H+\zeta$ is the free surface, ζ is the sea-surface elevation, H is the reference height and h denotes the location of the erodible bed:

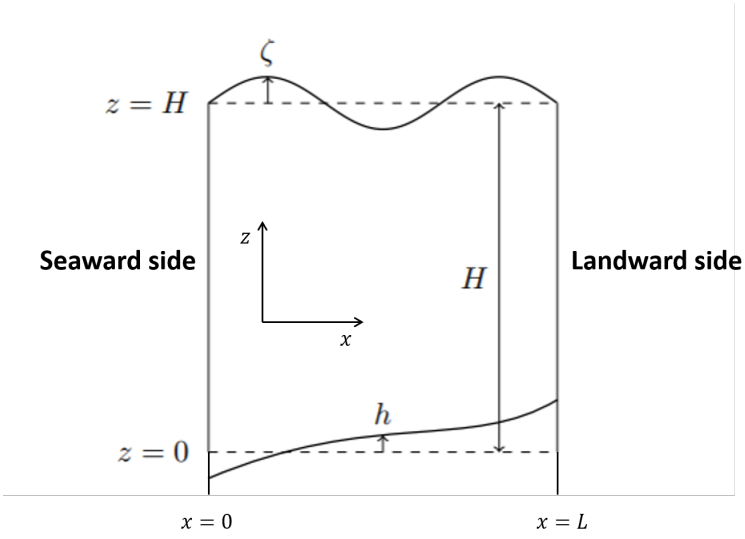

Figure 2.1: Cross-sectional view of estuary

At the seaward side, the watermotion is forced by a semi-diurnal tidal signal and is given by:

$$\zeta(0,y,t) = \mathrm{A(y)cos}(\sigma t),$$

where σ is the angular frequency of the semidiurnal tide and $A(y)$ is the amplitude of the tide at the open boundary. At the closed boundary, the transport of water is assumed to vanish. two kinematic boundary conditions have to be imposed, one at the free surface and one at the erodible bed. The kinematic boundary condition ensures that a fluid particles at the free

surface always remains part of the free surface. The kinematic boundary condition for the top and bottom are given by:

$$\begin{aligned} w &= \frac{\partial \zeta}{\partial t} + u\frac{\partial \zeta}{\partial x} + v\frac{\partial \zeta}{\partial y} \quad \text{at} \quad z = H + \zeta, \\ w &= \frac{\partial h}{\partial t} + u\frac{\partial h}{\partial x} + v\frac{\partial h}{\partial y} \quad \text{at} \quad z = h. \end{aligned} \tag{2.7}$$

Finally there are still two dynamic boundary conditions have to be imposed, one at the sea surface and one at the seabed. Ignoring the wind shear stress i.e., $\tau_{\text{wind},x} = \tau_{\text{wind},y} = 0$, the dynamic boundary condition at the surface reduce to the shear stress condition. At the seabed we prescribe a bed shear stress which is given by:

$$\frac{\tau_{\text{bed},x}}{\rho} = \begin{bmatrix} \mathcal{A}_\text{h}\frac{\partial u}{\partial x} \\ \mathcal{A}_\text{h}\frac{\partial u}{\partial y} \\ \mathcal{A}_\text{v}\frac{\partial u}{\partial z} \end{bmatrix} \cdot \begin{bmatrix} -\frac{\partial h}{\partial x} \\ -\frac{\partial h}{\partial y} \\ 1 \end{bmatrix} = -\mathcal{A}_\text{h}\frac{\partial u}{\partial x}\frac{\partial h}{\partial x} - \mathcal{A}_\text{h}\frac{\partial u}{\partial y}\frac{\partial h}{\partial y} + \mathcal{A}_\text{v}\frac{\partial u}{\partial z} \quad \text{at} \quad z = h.$$

A similar derivation holds for $\tau_{\text{bed},y}$. Both observations and dimensional arguments indicate that the bottom shear stress is quadratic in the local velocity De Swart (2006). the quadratic bottom stress law is given by:

$$\frac{\tau_{\text{bed},x}}{\rho} = C_d\sqrt{u_\text{b}^2 + v_\text{b}^2}u_\text{b}, \quad \text{and} \quad \frac{\tau_{\text{bed},y}}{\rho} = C_d\sqrt{u_\text{b}^2 + v_\text{b}^2}v_\text{b},$$

where C_d is the drag coefficient with a typical value of 0.00025 and u_b and v_b are the flows at the seabed. The quadratic bottom stress law gives a non linear interaction, these are quite complicated. A solution was proposed by Lorentz. Lorentz argued that the bottom stress law yields the correct tidally averaged dissipation of energy in the estaury. Lorentz therefore substituted the bottom stress with a linear bottom stress that yield an equivalent tidally averaged dissipation of energy. By applying Lorentz linearisation, the bottom shear stress reduces to:

$$\frac{\tau_{\text{bed},x}}{\rho} = \hat{r}u_\text{b}, \quad \text{and} \quad \frac{\tau_{\text{bed},y}}{\rho} = \hat{r}v_\text{b} \tag{2.8}$$

, where $\hat{r}$ for periodic flows is given by Vreugdenhil (2013):

$$\hat{r} = \frac{8}{3\pi}C_\text{d}u.$$

2.2.2 Depth averaged shallow water equation

First the Reynolds averaged continuity equation given in equation (2.6a) is integrated over the depth:

$$\begin{aligned} &\int_h^{H+\zeta}\left(\frac{\partial u}{\partial x} + \frac{\partial v}{\partial y} + \frac{\partial w}{\partial z}\right)dz = 0, \\ &\int_h^{H+\zeta}\frac{\partial u}{\partial x}dz + \int_h^{H+\zeta}\frac{\partial v}{\partial y}dz + [w]_h^{H+\zeta} = 0. \end{aligned}$$

To further simplify the above equation the Leibniz integration rule is needed, which is valid for a general function $f(x, y, z, t)$ and upper and lower limit $-\infty < a(x)$ and $b(x) < \infty$:

$$\frac{\partial}{\partial x}\left(\int_a^b f dz\right) = \int_a^b \frac{\partial f}{\partial x}dz + f|_b\frac{\partial b}{\partial x} - f|_a\frac{\partial a}{\partial x}. \tag{2.9}$$

Applying the Leibniz rule results in:

$$\frac{\partial}{\partial x}\left(\int_h^{H+\zeta} u dz\right)+\frac{\partial}{\partial y}\left(\int_h^{H+\zeta} v dz\right)+\left[u\frac{\partial h}{\partial x}+v\frac{\partial h}{\partial y}-w\right]_h-\left[u\frac{\partial \zeta}{\partial x}+v\frac{\partial \zeta}{\partial y}-w\right]_{H+\zeta}=0.$$

Defining the depth average flow velocity $\bar{u}$, $\bar{v}$ as:

$$\bar{u}=\frac{1}{H+\zeta-h}\int_h^{H+\zeta} u dz, \qquad \bar{v}=\frac{1}{H+\zeta-h}\int_h^{H+\zeta} v dz.$$

Substituting the defined depth averaged flows $\bar{u}$, $\bar{v}$ and the kinematic boundary conditions (2.7) results in the depth averaged continuity equation:

$$\frac{\partial \zeta}{\partial t}-\frac{\partial h}{\partial t}+\frac{\partial}{\partial x}[(H+\zeta-h)\bar{u}]+\frac{\partial}{\partial y}[(H+\zeta-h)\bar{v}]=0. \tag{2.10}$$

Next the momentum equations have to be depth averaged. To illustrate this procedure, the depth averaging of the momentum equation in the x direction (2.6b) is shown. First the momentum equation has to be written in conservative form. Recall that this has been done before in section (2.1) for the Navier Stokes equation prior to applying the Reynolds decomposition. To write the momentum equation in its conservative form the continuity equation is multiplied by the flow velocity u and added to the momentum equation; resulting in

$$\frac{\partial u}{\partial t}+\frac{\partial}{\partial x}\left(u^2\right)+\frac{\partial}{\partial y}(uv)+\frac{\partial}{\partial z}(uw)-fv=-\frac{1}{\rho}\frac{\partial p}{\partial x}+\frac{\partial}{\partial x}\left(\mathcal{A}_{\mathrm{h}}\frac{\partial u}{\partial x}\right)+\frac{\partial}{\partial y}\left(\mathcal{A}_{\mathrm{h}}\frac{\partial u}{\partial y}\right)+\frac{\partial}{\partial z}\left(\mathcal{A}_{v}\frac{\partial u}{\partial z}\right).$$

Now the left hand side is integrated over the depth and the Leibniz rule is applied:

$$\begin{aligned}\int_h^{H+\zeta}&\frac{\partial u}{\partial t}+\frac{\partial}{\partial x}\left(u^2\right)+\frac{\partial}{\partial y}(uv)+\frac{\partial}{\partial z}(uw)-fvdz\\ &=\frac{\partial}{\partial t}\left(\int_h^{H+\zeta} u dz\right)+\frac{\partial}{\partial x}\left(\int_h^{H+\zeta} u^2 dz\right)+\frac{\partial}{\partial y}\left(\int_h^{H+\zeta} uv dz\right)-f\int_h^{H+\zeta} v dz\\ &+u|_h\left[\frac{\partial h}{\partial t}+u\frac{\partial h}{\partial x}+v\frac{\partial h}{\partial y}-w\right]_h-u|_{H+\zeta}\left[\frac{\partial \zeta}{\partial t}+u\frac{\partial \zeta}{\partial x}+v\frac{\partial \zeta}{\partial y}-w\right]_{H+\zeta}.\end{aligned}$$

The last two terms vanish by applying the kinematic boundary condition. The velocities are decomposed in a similar fashion as with the Reynolds decomposition namely in a depth average velocity mean and fluctuating part denoted by a bar $\bar{\cdot}$ and tilde $\tilde{\cdot}$ respectively. Furthermore the following relation holds:

$$\int_h^{H+\zeta}\tilde{u}dz=0.$$

Applying this decomposition, $u=\bar{u}+\tilde{u}$ and $v=\bar{v}+\tilde{v}$, gives:

$$\begin{aligned}&\frac{\partial}{\partial t}\left(\int_h^{H+\zeta} u dz\right)+\frac{\partial}{\partial x}\left(\int_h^{H+\zeta} u^2 dz\right)+\frac{\partial}{\partial y}\left(\int_h^{H+\zeta} uv dz\right)-f\int_h^{H+\zeta} v dz=\\ &\frac{\partial}{\partial t}[(H+\zeta-h)\bar{u}]+\frac{\partial}{\partial x}\left[(H+\zeta-h)\bar{u}^2+\int_h^{H+\zeta}\tilde{u}^2 dz\right]+\frac{\partial}{\partial y}\left[(H+\zeta-h)\bar{u}\bar{v}+\int_h^{H+\zeta}\tilde{u}\tilde{v}dz\right]\\ &-(H+\zeta-h)f\bar{v}.\end{aligned}$$

As before in section (2.1) the nonlinear terms are parameterised as an extra viscosity term Nihoul (2011), resulting in:

$$\int_h^{H+\zeta} \tilde{u}^2 dz = -\tilde{A}_\mathrm{h}(H+\zeta-h)\frac{\partial \bar{u}}{\partial x}, \quad \text{and} \quad \int_h^{H+\zeta} \tilde{u}\tilde{v} dz = -\tilde{A}_\mathrm{h}(H+\zeta-h)\frac{\partial \bar{u}}{\partial y}. \tag{2.11}$$

Taking this all together results in:

$$\begin{aligned}
&\frac{\partial}{\partial t}[(H+\zeta-h)\bar{u}] + \frac{\partial}{\partial x}\left[(H+\zeta-h)\bar{u}^2 + \int_h^{H+\zeta}\tilde{u}^2 dz\right] + \frac{\partial}{\partial y}\left[(H+\zeta-h)\bar{u}\bar{v} + \int_h^{H+\zeta}\tilde{u}\tilde{v}dz\right] \\
&- (H+\zeta-h)f\bar{v} \\
&= (H+\zeta-h)\left(\frac{\partial \bar{u}}{\partial t} + \bar{u}\frac{\partial \bar{u}}{\partial x} + \bar{v}\frac{\partial \bar{u}}{\partial y} - f\bar{v}\right) - \frac{\partial}{\partial x}\left(\tilde{A}_\mathrm{h}(H+\zeta-h)\frac{\partial \bar{u}}{\partial x}\right) - \frac{\partial}{\partial y}\left(\tilde{A}_\mathrm{h}(H+\zeta-h)\frac{\partial \bar{u}}{\partial y}\right).
\end{aligned} \tag{2.12}$$

Before integrating the right hand side the hydrostatic balance (2.6d) is integrated over the depth under the assumption that the water density ρ is independent of the water depth z this is justified for a well mixed estuary ("A well-mixed estuary is a system in which the water column is completely mixed, making the estuary vertically homogeneous." Cavalcante (2016)), to obtain the hydrostatic pressure relationship:

$$p = p_\mathrm{a} + \rho g(H+\zeta-z),$$

where p_a is the atmospheric pressure which is assumed to be constant at the sea surface. Integrating the right-hand side of the momentum equation (2.6b) substituting the hydrostatic pressure relationship, using the Leibniz's integral rule, applying the fundamental theorem of calculus and rearranging yields:

$$\begin{aligned}
\int_h^{H+\zeta}\Big(-\frac{1}{\rho}\frac{\partial p}{\partial x} + \frac{\partial}{\partial x}\left(\mathcal{A}_\mathrm{h}\frac{\partial u}{\partial x}\right) + \frac{\partial}{\partial y}\left(\mathcal{A}_\mathrm{h}\frac{\partial u}{\partial y}\right) + \frac{\partial}{\partial z}\left(\mathcal{A}_v\frac{\partial u}{\partial z}\right)\Big)dz \\
= -(H+\zeta-h)g\frac{\partial \zeta}{\partial x} + \frac{\partial}{\partial x}\left(\int_h^{H+\zeta}\mathcal{A}_\mathrm{h}\frac{\partial u}{\partial x}dz\right) + \frac{\partial}{\partial y}\left(\int_h^{H+\zeta}\mathcal{A}_\mathrm{h}\frac{\partial u}{\partial y}dz\right) \\
+ \left[\mathcal{A}_\mathrm{h}\frac{\partial u}{\partial x}\frac{\partial h}{\partial x} + \mathcal{A}_\mathrm{h}\frac{\partial u}{\partial y}\frac{\partial h}{\partial y} - \mathcal{A}_v\frac{\partial u}{\partial z}\right]_h - \left[\mathcal{A}_\mathrm{h}\frac{\partial u}{\partial x}\frac{\partial \zeta}{\partial x} + \mathcal{A}_\mathrm{h}\frac{\partial u}{\partial y}\frac{\partial \zeta}{\partial y} - \mathcal{A}_\mathrm{v}\frac{\partial u}{\partial z}\right]_{H+\zeta}.
\end{aligned}$$

The Lorentz linearised bottom stresses in equation (2.8) are parametrised in terms of the depth-averaged velocities:

$$\frac{\tau_{\mathrm{bed},x}}{\rho} = r^*\bar{u}, \quad \text{and} \quad \frac{\tau_{\mathrm{bed},y}}{\rho} = r^*\bar{v}. \tag{2.13}$$

Note a new friction coefficient r^* is introduced. Assuming that the horizontal eddy viscosity is uniform over the depth and substituting the new bottom stresses from equation (2.13) the right hand side of the depth averaged momentum equation in the x-direction is derived:

$$\begin{aligned}
&-(H+\zeta-h)g\frac{\partial \zeta}{\partial x} + \frac{\partial}{\partial x}\left(\mathcal{A}_\mathrm{h}(H+\zeta-h)\frac{\partial \bar{u}}{\partial x}\right) + \frac{\partial}{\partial y}\left(\mathcal{A}_\mathrm{h}(H+\zeta-h)\frac{\partial \bar{u}}{\partial y}\right) + \frac{\tau_{\mathrm{wind},x}}{\rho} - \frac{\tau_{\mathrm{bed},x}}{\rho} \\
&= -(H+\zeta-h)g\frac{\partial \zeta}{\partial x} + \frac{\partial}{\partial x}\left(\mathcal{A}_\mathrm{h}(H+\zeta-h)\frac{\partial \bar{u}}{\partial x}\right) + \frac{\partial}{\partial y}\left(\mathcal{A}_\mathrm{h}(H+\zeta-h)\frac{\partial \bar{u}}{\partial y}\right) - r^*\bar{u}.
\end{aligned} \tag{2.14}$$

Combining both the right and left hand side and introducing a new effective eddy viscosity coefficient, $\hat{\mathcal{A}}_\mathrm{h} = \mathcal{A}_\mathrm{h} + \tilde{A}_\mathrm{h}$, the depth averaged momentum equation in the x-direction reads:

$$\frac{\partial \bar{u}}{\partial t}+\bar{u}\frac{\partial \bar{u}}{\partial x}+\bar{v}\frac{\partial \bar{u}}{\partial y}-f\bar{v} = -g\frac{\partial \zeta}{\partial x}+\frac{1}{H+\zeta-h}\left[-r^*\bar{u}+\frac{\partial}{\partial x}\left(\hat{\mathcal{A}}_\mathrm{h}(H+\zeta-h)\frac{\partial \bar{u}}{\partial x}\right)+\frac{\partial}{\partial y}\left(\hat{\mathcal{A}}_\mathrm{h}(H+\zeta-h)\frac{\partial \bar{u}}{\partial y}\right)\right].$$

Now scaling analysis is applied for further simplification. From the conservation of mass of the two dimensional depth averaged continuity equation (2.10) and the tidal forcing the dominant balance is given by:

$$\sigma A \sim \frac{HU}{L}.$$

Using the dispersion of the shallow water $\lambda = \sqrt{gH}/\sigma$ gives:

$$\frac{g}{\sigma U}\frac{\partial \zeta}{\partial x} \sim \frac{gA}{\sigma U L} \sim \left(\frac{\lambda}{L}\right)^2.$$

Scaling each term in the depth averaged momentum equation and dividing by σU, using the typical values from Schuttelaars and De Swart (1996), the leading order balance reads:

$$\frac{\partial \bar{u}}{\partial t}+\bar{u}\frac{\partial \bar{u}}{\partial x}+\bar{v}\frac{\partial \bar{u}}{\partial y}-f\bar{v} = -g\frac{\partial \zeta}{\partial x}-\frac{1}{H+\zeta-h}\left[r^*\bar{u}-\frac{\partial}{\partial x}\left(\hat{\mathcal{A}}_\mathrm{h}(H+\zeta-h)\frac{\partial \bar{u}}{\partial x}\right)-\frac{\partial}{\partial y}\left(\hat{\mathcal{A}}_\mathrm{h}(H+\zeta-h)\frac{\partial \bar{u}}{\partial y}\right)\right].$$

1	$\frac{U}{\sigma L}$	$\frac{U}{\sigma L}$	$\frac{f}{\sigma}$	$\frac{\lambda^2}{L^2}$	$\frac{r}{\sigma H}$	$\frac{\mathcal{A}_h}{\sigma L^2}$	$\frac{\mathcal{A}_h}{\sigma L^2}$
1	0.07	0.07	0.7	16	0.2	0.0002	0.0002

From the leading order balance it is clear that the horizontal eddy viscosities are negligible. The two dimensional shallow water equations are now given by:

$$\begin{cases} \dfrac{\partial \zeta}{\partial t} - \dfrac{\partial h}{\partial t} + \dfrac{\partial}{\partial x}[(H+\zeta-h)\bar{u}] + \dfrac{\partial}{\partial y}[(H+\zeta-h)\bar{v}] = 0, & \text{(2.15a)} \\ \dfrac{\partial \bar{u}}{\partial t} + \bar{u}\dfrac{\partial \bar{u}}{\partial x} + \bar{v}\dfrac{\partial \bar{u}}{\partial y} - f\bar{v} = -g\dfrac{\partial \zeta}{\partial x} - \dfrac{r^*\bar{u}}{H+\zeta-h}, & \text{(2.15b)} \\ \dfrac{\partial \bar{v}}{\partial t} + \bar{u}\dfrac{\partial \bar{v}}{\partial x} + \bar{v}\dfrac{\partial \bar{v}}{\partial y} + f\bar{u} = -g\dfrac{\partial \zeta}{\partial y} - \dfrac{r^*\bar{v}}{H+\zeta-h}. & \text{(2.15c)} \end{cases}$$

The $\bar{\cdot}$ denotes the depth average of the corresponding variable. Note that the Reynolds average symbol $\langle\cdot\rangle$ was already omitted for readability. The first equation represents the conservation of mass and the last two equations represent the conservation of momentum in the x and y direction.

2.3 Derivation of the one dimensional shallow water equation

In this section the one dimensional shallow water equation are derived. First the geometry and boundary conditions are derived. Subsequently the equations are integrated over the width to obtain the one dimensional shallow water equation after scaling.

2.3.1 Geometry and boundary conditions

In the schematic figure below the top view of the channel is shown, where $B_1(x)$ and $B_2(x)$ are the boundaries.

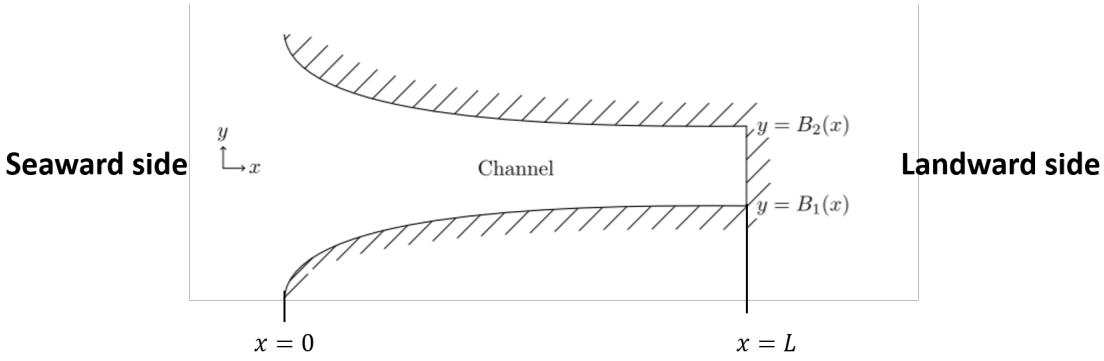

Figure 2.2: Top view of a channel

For both physical boundaries $B_1(x)$ and $B_2(x)$ the impermeable wall boundary conditions hold. This condition ensures that there is no transport trough the boundary. Translating this condition into a mathematical condition gives:

$$\begin{aligned} \overline{\boldsymbol{u}} \cdot \boldsymbol{n} = 0 \Longrightarrow \begin{bmatrix} \bar{u} \\ \bar{v} \end{bmatrix} \cdot \begin{bmatrix} \frac{dB_1}{dx} \\ -1 \end{bmatrix} = 0 \Longrightarrow \bar{u}\frac{dB_1}{dx} - \bar{v} = 0 \quad \text{at} \quad y = B_1, \\ \Longrightarrow \begin{bmatrix} \bar{u} \\ \bar{v} \end{bmatrix} \cdot \begin{bmatrix} -\frac{dB_2}{dx} \\ 1 \end{bmatrix} = 0 \Longrightarrow -\bar{u}\frac{dB_2}{dx} + \bar{v} = 0 \quad \text{at} \quad y = B_2. \end{aligned} \tag{2.16}$$

2.3.2 Width averaging

We start with the width averaging of the conservation of mass equation (2.15a):

$$\int_{B_1}^{B_2} \frac{\partial \zeta}{\partial t} - \frac{\partial h}{\partial t} + \frac{\partial}{\partial x}[(H + \zeta - h)\bar{u}] + \frac{\partial}{\partial y}[(H + \zeta - h)\bar{v}]dy = 0.$$

Since $B_1(x)$ and $B_2(x)$ are both a function of x the Leibniz rule of integration stated in equation (2.9) is applied:

$$\begin{aligned} &\frac{\partial}{\partial t}\left(\int_{B_1}^{B_2} \zeta dy\right) - \frac{\partial}{\partial t}\left(\int_{B_1}^{B_2} h dy\right) + \frac{\partial}{\partial x}\left(\int_{B_1}^{B_2} (H + \zeta - h)\bar{u} dy\right) \\ &+ \left[(H + \zeta - h)\left(\bar{u}\frac{dB_1}{dx} - \bar{v}\right)\right]_{B_1} - \left[(H + \zeta - h)\left(\bar{u}\frac{dB_2}{dx} - \bar{v}\right)\right]_{B_2} = 0. \end{aligned} \tag{2.17}$$

We define the width averages as follow:

$$\hat{\zeta} = \frac{1}{B_2 - B_1}\int_{B_1}^{B_2} \zeta dy, \quad \hat{h} = \frac{1}{B_2 - B_1}\int_{B_1}^{B_2} h dy, \quad \hat{\bar{u}} = \frac{1}{B_2 - B_1}\int_{B_1}^{B_2} \bar{u} dy. \tag{2.18}$$

Using the width averages (equation (2.18)) and the boundary conditions (equation (2.16)) Equation (2.17) reduces to:

$$\frac{\partial}{\partial t}\left[(B_2 - B_1)\,\hat{\zeta}\right] - \frac{\partial}{\partial t}\left[(B_2 - B_1)\,\hat{h}\right] + \frac{\partial}{\partial x}\left(\int_{B_1}^{B_2} (H + \zeta - h)\bar{u} dy\right) = 0. \tag{2.19}$$

We can further reduce the above equation by splitting ζ in a width mean part $\hat{\zeta}$ and a width fluctuating part $\tilde{\zeta}$. The width averages are already defined in equation (2.18). The width fluctuating part is defined as $\tilde{\zeta} = \zeta - \hat{\zeta}$ with:

$$\int_{B_1}^{B_2} \tilde{\zeta} dy = 0.$$

A similar decomposition is used for $h = \hat{h} + \tilde{h}$ and $\bar{u} = \hat{\bar{u}} + \tilde{\bar{u}}$. Substituting this decomposition in the last term of equation (2.19) gives:

$$\int_{B_1}^{B_2} (H + \zeta - h)\bar{u} dy = (B_2 - B_1)\,(H + \hat{\zeta} - \hat{h})\hat{\bar{u}} + \int_{B_1}^{B_2} (\tilde{\zeta} - \tilde{h})\tilde{\bar{u}} dy. \tag{2.20}$$

If the flow $\bar{u}$ is uniform and the shape of the domain is nearly rectangular then the width fluctuations are very small and the product even smaller. Therefore the last term of the above equation is omitted. As a result the width averaged conservation of mass is reads:

$$\frac{\partial}{\partial t}\left[(B_2 - B_1)\,\hat{\zeta}\right] - \frac{\partial}{\partial t}\left[(B_2 - B_1)\,\hat{h}\right] + \frac{\partial}{\partial x}\left[(B_2 - B_1)\,(H + \hat{\zeta} - \hat{h})\hat{\bar{u}}\right] = 0.$$

If we assume that the channel width is constant the equation reduces even more:

$$\frac{\partial \hat{\zeta}}{\partial t} - \frac{\partial \hat{h}}{\partial t} + \frac{\partial}{\partial x}[(H + \hat{\zeta} - \hat{h})\hat{u}] = 0.$$

Next momentum equations (2.15b) and (2.15c) are width averaged. As an example equation (2.15b) is averaged over the width. Before we start we need to rewrite the equation in its conservative form. The conservative form is already derived in equation (2.12) and equation (2.14) for the LHS and RHS respectively. According to Pedlosky (2013) rotational effects are negligible if a channel is narrow, an assumption we make from now on. Furthermore, the horizontal viscous terms are small. Applying the latter two assumptions the conservative depth form of the averaged momentum equation is reduced to:

$$\frac{\partial}{\partial t}[(H + \zeta - h)\bar{u}] + \frac{\partial}{\partial x}\left[(H + \zeta - h)\bar{u}^2\right] + \frac{\partial}{\partial y}[(H + \zeta - h)\bar{v}\bar{u}] = -(H + \zeta - h)g\frac{\partial \zeta}{\partial x} + r^*\bar{u}.$$

Next the LHS is integrated over the width and the Leibniz rule stated in equation (2.9) is used together with the fundamental theory of calculus:

$$\int_{B_1}^{B_2} \left\{\frac{\partial}{\partial t}[(H + \zeta - h)\bar{u}] + \frac{\partial}{\partial x}\left[(H + \zeta - h)\bar{u}^2\right] + \frac{\partial}{\partial y}[(H + \zeta - h)\bar{v}\bar{u}]\right\} dy = \frac{\partial}{\partial t}\left(\int_{B_1}^{B_2} (H + \zeta - h)\bar{u} dy\right)$$
$$+ \frac{\partial}{\partial x}\left(\int_{B_1}^{B_2} (H + \zeta - h)\bar{u}^2 dy\right) + \left[(H + \zeta - h)\bar{u}\left(\bar{u}\frac{dB_1}{dx} - \bar{v}\right)\right]_{B_1} - \left[(H + \zeta - h)\bar{u}\left(\bar{u}\frac{dB_2}{dx} - \bar{v}\right)\right]_{B_2}.$$

Substituting the boundary conditions and decomposing h, $\bar{u}$, ζ and $\bar{v}$ in a width mean part and a width fluctuating part gives

$$\frac{\partial}{\partial t}\left(\int_{B_1}^{B_2} (H + \zeta - h)\bar{u} dy\right) + \frac{\partial}{\partial x}\left(\int_{B_1}^{B_2} (H + \zeta - h)\bar{u}^2 dy\right) =$$
$$\frac{\partial}{\partial t}\left[(B_2 - B_1)\,(H + \hat{\zeta} - \hat{h})\hat{\bar{u}} + \int_{B_1}^{B_2} (\tilde{\zeta} - \tilde{h})\tilde{\bar{u}} dy\right]$$
$$+ \frac{\partial}{\partial x}\left[(B_2 - B_1)\,(H + \hat{\zeta} - \hat{h})\hat{\bar{u}}^2 + (H + \hat{\zeta} - \hat{h})\int_{B_1}^{B_2} \bar{\bar{u}}^2 dy + 2\hat{\bar{u}}\int_{B_1}^{B_2} (\tilde{\zeta} - \tilde{h})\tilde{\bar{u}} dy + \int_{B_1}^{B_2} (\tilde{\zeta} - \tilde{h})\tilde{\bar{u}}^2 dy\right].$$

If the flows are uniform and the shape of the domain is nearly rectangular then the width fluctuations are very small and the products even smaller. Therefore the covariance terms of the above equation are omitted. As a result the LHS of the width averaged conservation of momentum is reduced to:

$$\frac{\partial}{\partial t}\left[(B_2-B_1)\,(H+\hat{\zeta}-\hat{h})\hat{\bar{u}}\right]+\frac{\partial}{\partial x}\left[(B_2-B_1)\,(H+\hat{\zeta}-\hat{h})\hat{\bar{u}}\hat{\bar{u}}\right]=$$
$$(B_2-B_1)\,(H+\hat{\zeta}-\hat{h})\left(\frac{\partial\hat{\bar{u}}}{\partial t}+\hat{\bar{u}}\frac{\partial\hat{\bar{u}}}{\partial x}\right)$$
$$+\hat{\bar{u}}\left(\frac{\partial}{\partial t}\left[(B_2-B_1)\,\hat{\zeta}\right]-\frac{\partial}{\partial t}\left[(B_2-B_1)\,\hat{h}\right]+\frac{\partial}{\partial x}\left[(B_2-B_1)\,(H+\hat{\zeta}-\hat{h})\hat{\bar{u}}\right]\right).$$

The last term is zero due to the width averaged conservation of mass. The RHS of the depth averaged conservation of momentum equation is derived in a similar fashion. Combining both the LHS and RHS gives:

$$\frac{\partial\hat{\bar{u}}}{\partial t}+\hat{\bar{u}}\frac{\partial\hat{\bar{u}}}{\partial x}=-g\frac{\partial\hat{\zeta}}{\partial x}-\frac{r^*\hat{\bar{u}}}{H+\hat{\zeta}-\hat{h}}.$$

The conservation of mass and the conservation of momentum together give the cross sectionally averaged shallow water equations, where $\bar{\cdot}$ denotes the depth average of the corresponding variable and $\hat{\cdot}$ denotes the width averaging. From now on we assume that all variables are cross-sectionally averaged and the symbols $\bar{\cdot}$ and $\hat{\cdot}$ will be omitted. Note that the Reynolds average symbol $\langle\cdot\rangle$ was already omitted for readability. The first equation represents the conservation of mass and the last equation represent the conservation of momentum :

$$\begin{cases}\dfrac{\partial\zeta}{\partial t}-\dfrac{\partial h}{\partial t}+\dfrac{\partial}{\partial x}[(H+\zeta-h)u]=0, & \text{(2.21a)}\\[2ex] \dfrac{\partial u}{\partial t}+u\dfrac{\partial u}{\partial x}=-g\dfrac{\partial\zeta}{\partial x}-\dfrac{r^*u}{H+\zeta-h}. & \text{(2.21b)}\end{cases}$$

2.4 Scaling

By using a scaling analysis we will analyse under what condition the non-linear terms are small. First equation (2.21a) is made dimensionless by making the independent and dependent variables dimensionless as follow:

$$x=Lx^*,\quad t=t^*\sigma^{-1},\quad u=Uu^*,\quad \zeta=\frac{HU}{\sigma L}\zeta^*,\quad h=Hh^*,$$

where the variables with an asterisk $\cdot^*$ are dimensionless variable. In addition L,H,U,σ are the characteristic values given on p.9 of Schuttelaars and De Swart (1997). Substituting the dimensionless variables and using the chain rule in equation (2.21a) gives:

$$\frac{\sigma HU}{\sigma L}\frac{\partial\zeta^*}{\partial t^*}-\sigma H\frac{\partial h^*}{\partial x^*}+\frac{\partial}{\partial x^*}\frac{U}{L}\left[\left(\frac{HU}{\sigma L}\zeta^*+H-Hh^*\right)u^*\right]=0.$$

Dividing by $\frac{HU}{L}$ and substituting $\epsilon=\frac{U}{\sigma L}$ result in:

$$\frac{\partial\zeta^*}{\partial t^*}-\frac{1}{\epsilon}\frac{\partial h^*}{\partial t^*}+\frac{\partial}{\partial x^*}\left[(\epsilon\zeta^*+1-h^*)\,u^*\right]=0,$$

with $\epsilon << 1$. Here we use that the bed we consider is flat and does not change on the timescales we consider. This allows us to choose the erodible bed $h = 0$. The dimensionless equation is reduced to:

$$\frac{\partial \zeta^*}{\partial t^*} + \frac{\partial u^*}{\partial x^*} = 0.$$

Making the equation dimensional again results in:

$$\frac{\partial \zeta}{\partial t} + H\frac{\partial u}{\partial x} = 0. \tag{2.22}$$

In a similar fashion equation (2.21b) is made non-dimensional. First the variables are made dimensionless and the chain rule is applied:

$$U\sigma\frac{\partial u^*}{\partial t^*} + \frac{U^2}{L}u^*\frac{\partial u^*}{\partial x^*} + \frac{r^*Uu^*}{(H\epsilon\zeta^* + H - Hh^*)} = -\frac{gH\epsilon}{L}\frac{\partial \zeta^*}{\partial x^*}.$$

Dividing by $U\sigma$ and substituting $\epsilon = \frac{U}{\sigma L}$ and $\Lambda^2 = \frac{gH}{\sigma^2 L^2}$ results in:

$$\frac{\partial u^*}{\partial t^*} + \epsilon u^*\frac{\partial u^*}{\partial x^*} + \frac{r^*}{\sigma H}\frac{u^*}{(\epsilon\zeta^* + 1 - h^*)} = -\Lambda^2\frac{\partial \zeta^*}{\partial x^*}.$$

Again, using that $\epsilon << 1$, and that we only consider h = 0, the dimensionless equation is reduced to:

$$\frac{\partial u^*}{\partial t^*} + \frac{r^*}{\sigma H}u^* = -\Lambda^2\frac{\partial \zeta^*}{\partial x^*}.$$

Making the equation dimensional again results in:

$$\frac{\partial u}{\partial t} = -g\frac{\partial \zeta}{\partial x} - \frac{r^*}{H}u. \tag{2.23}$$

Both equation (2.22) and equation (2.23) together are called the linearised cross-sectionally averaged equations:

$$\begin{cases} \dfrac{\partial u}{\partial t} = -g\dfrac{\partial \zeta}{\partial x} - \lambda u, & \text{(2.24a)} \\ \dfrac{\partial \zeta}{\partial t} + H\dfrac{\partial u}{\partial x} = 0. & \text{(2.24b)} \end{cases}$$

Chapter 3

Solution Method

In this chapter the solution method to obtain the water motion in a periodically closed and opened estuary is described, considering an open estuary i.e. an estuary with the water motion forced at the entrance, a closed estuary i.e. an estuary where the watermotion only results from initial pertubations and an estuary that is opened and closed periodically during a tidal cycle.

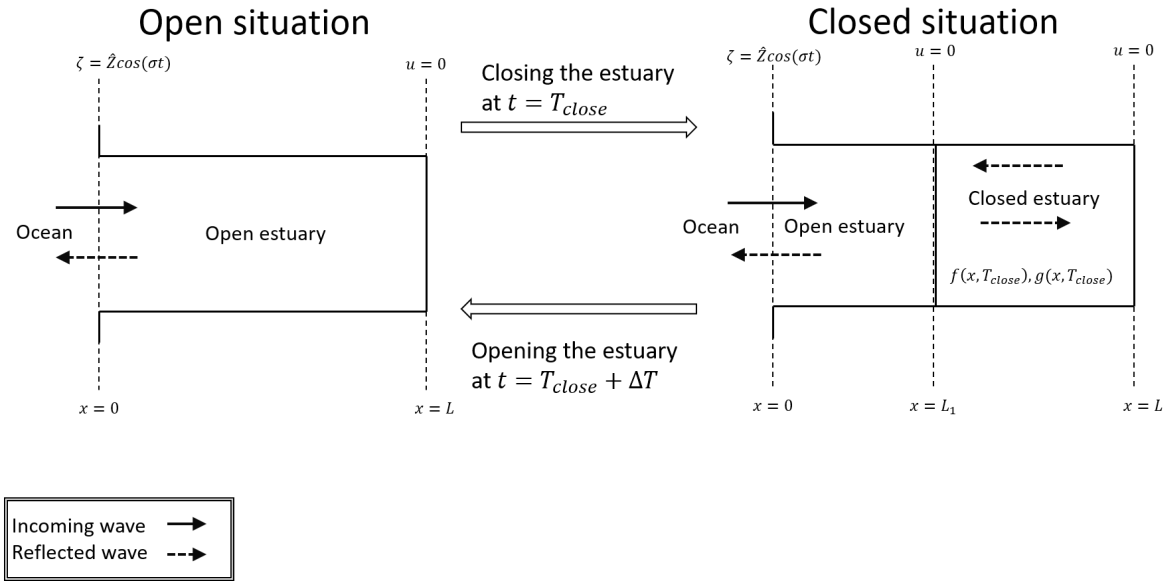

Figure 3.1: At the left an estuary is shown in which the water motion is forced by the tides at $x = 0$. We call this estuary the "open" estuary. At the right an estuary is shown in which a barrier is closed at $t = T_{close}$ and $x = L_1$. This estuary consists of an open part from $x = 0$ to $x = L_1$ and a closed part from $x = L_1$ to $x = L$. The closed part is driven by the initial conditions $f(x, T_{close})$ and $g(x, T_{close})$. At the top the boundary conditions are shown.

The solution method is schematically pictured in Figure 3.1. We have an open estuary with length L and an incoming wave at the seaward boundary with tidal elevation $\zeta = \hat{Z}\cos(\sigma t)$, where $\sigma = 2\pi/12\text{h}25\text{m}$ is the angular frequency of the semi-diurnal tide M_2 and $\hat{Z}$ the tidal amplitude. The incoming wave is reflected at the coast and travels back in the seaward direction. After a certain time T_{close} the estuary is closed at the position $x = L_1$ with a sea-surface elevation $\zeta(L_1, T_{close}) = H_1$. We now have an estuary consisting of two parts: a closed part and a part connected to the sea. After a certain time ΔT, the time between opening and closing,

the sea-surface elevation in the open estuary has reached height H_1 again and the barrier is removed. We end up where we started with a completely open estuary. This process is iterated. We are going to use two different methods namely an analytic one and an eigenfunction expansion method (which is sometimes referred to as the spectral method throughout the chapter) to solve the linearised cross-sectionally averaged equations derived in chapter 2. In sections 3.3 and 3.4 we take a closer look at closing and opening an estuary. In section 3.5 the first overtide M_4 is introduced so in the previous sections only a M_2 tide was considered and, finally the residual sediment transport is considered in section 3.6.

3.1 Analytic solution for the open estuary

In this section the tidal velocity and sea-surface elevation are derived analytically for an open estuary. The equations for an open estuary with their corresponding boundary conditions are given below.

$$\begin{cases} \dfrac{\partial u}{\partial t} = -g\dfrac{\partial \zeta}{\partial x} - \lambda u, & \text{(3.1a)} \\ \dfrac{\partial \zeta}{\partial t} + H\dfrac{\partial u}{\partial x} = 0, & \text{(3.1b)} \\ \zeta = \hat{Z}\cos(\sigma t) \quad \text{at} \quad x = 0, & \text{(3.1c)} \\ u = 0 \quad \text{at} \quad x = L. & \text{(3.1d)} \end{cases}$$

Note that in equation (3.1) no initial conditions are specified, since we are looking for asymptotic solutions (i.e. $t \to \infty$ behaviour) see Appendix (A) for an explanation. Note that the water motion is only forced by an M_2 tidal elevation at $x = 0$. First a single equation for the sea-surface elevations ζ is derived by applying the operator $(\frac{\partial}{\partial t} + \lambda)$ on the continuity equation (3.1b) and substituting the momentum equation (3.1a):

$$\begin{aligned} &\left(\frac{\partial}{\partial t} + \lambda\right)\left(\frac{\partial \zeta}{\partial t} + H\frac{\partial u}{\partial x} = 0\right), \\ &\frac{\partial^2 \zeta}{\partial t^2} + H\frac{\partial}{\partial x}\frac{\partial u}{\partial t} + \lambda\frac{\partial \zeta}{\partial t} + H\lambda\frac{\partial u}{\partial x} = 0, \\ &\frac{\partial^2 \zeta}{\partial t^2} + H\frac{\partial}{\partial x}\left(-g\frac{\partial \zeta}{\partial x} - \lambda u\right) + \lambda\frac{\partial \zeta}{\partial t} + H\lambda\frac{\partial u}{\partial x} = 0, \\ &\frac{\partial^2 \zeta}{\partial t^2} + \lambda\frac{\partial \zeta}{\partial t} - gH\frac{\partial^2 \zeta}{\partial x^2} = 0. \end{aligned}$$

Re-using the boundary condition stated in equation (3.1c) and substituting the boundary condition stated in equation (3.1d) in equation (3.1a) the single partial differential equation (PDE) for the sea-surface elevation reads:

$$\begin{aligned} &\frac{\partial^2 \zeta}{\partial t^2} + \lambda\frac{\partial \zeta}{\partial t} - c_0^2\frac{\partial^2 \zeta}{\partial x^2} = 0, \quad c_0^2 = gH, \\ &\zeta = \Re\left\{\hat{Z}e^{-i\sigma t}\right\} \quad \text{at} \quad x = 0, \\ &\frac{\partial \zeta}{\partial x} = 0 \quad \text{at} \quad x = L. \end{aligned} \tag{3.2}$$

The same is done for the tidal velocity:

$$\begin{aligned} &\frac{\partial^2 u}{\partial t^2} + \lambda \frac{\partial u}{\partial t} - c_0^2 \frac{\partial^2 u}{\partial x^2} = 0, \quad c_0^2 = gH, \\ &\frac{\partial u}{\partial t} = \Re\left\{ \frac{i\sigma \tilde{Z} e^{-i\sigma t}}{H} \right\} \quad \text{at} \quad x = 0, \\ &u = 0 \quad \text{at} \quad x = L. \end{aligned} \tag{3.3}$$

Since the system is linear and forced by a time-periodic function at the open boundary the solutions are also oscillatory. This approach assumes that the effects of the initial conditions go to zero as $t \to \infty$, hence an asymptotic solution is obtained. The solutions are of the following form: $\zeta = \Re\left\{Z(x)e^{-i\sigma t}\right\}$ and $u = \Re\left\{U(x)e^{-i\sigma t}\right\}$. First the sea-surface elevations $\zeta(x,t)$ is derived by substituting $\zeta = \Re\left\{Z(x)e^{-i\sigma t}\right\}$ in equation (3.2).

$$\frac{\partial^2}{\partial t^2}\left\{Z(x)e^{-i\sigma t}\right\} + \lambda \frac{\partial}{\partial t}\left\{Z(x)e^{-i\sigma t}\right\} - c_0^2 \frac{\partial^2}{\partial x^2}\left\{Z(x)e^{-i\sigma t}\right\} = 0,$$

Reducing equation (3.2) to a second order ordinary differential equation:

$$\begin{aligned} &\frac{d^2 Z}{dx^2} + k_*^2 Z = 0, \quad k_*^2 = \frac{\sigma^2}{c_0^2}(1 + i\hat{\lambda}), \qquad \hat{\lambda} = \frac{\lambda}{\sigma}, \\ &Z = \hat{Z} \quad \text{at} \quad x = 0, \quad \frac{dZ}{dx} = 0 \quad \text{at} \quad x = L. \end{aligned} \tag{3.4}$$

The solution is given by:

$$Z(x) = \frac{\hat{Z}}{\cos(k_* L)} \cos\left[k_*(L - x)\right]. \tag{3.5}$$

The solution for the velocity $U(x)$ is derived by substituting $u = \Re\left\{U(x)e^{-i\sigma t}\right\}$ and $\zeta = \Re\left\{Z(x)e^{-i\sigma t}\right\}$ in the momentum equation (3.1a):

$$\begin{aligned} &\frac{\partial}{\partial t}\left\{U(x)e^{-i\sigma t}\right\} = -g\frac{\partial}{\partial x}\left\{Z(x)e^{-i\sigma t}\right\} - \lambda\{U(x)e^{-i\sigma t}\}, \\ &-i\sigma U(x) = -g\frac{dZ(x)}{dx} - \lambda U(x), \\ &U(x) = \frac{-ig}{\sigma + i\lambda}\frac{dZ(x)}{dx}, \end{aligned}$$

resulting in:

$$U(x) = \frac{-ig\hat{Z}}{c_0(1 + i\hat{\lambda})^{1/2}} \frac{\sin\left[k_*(L - x)\right]}{\cos(k_* L)}. \tag{3.6}$$

To better understand the solution of the sea-surface elevation and tidal velocity, k^* is split in an imaginary and real part, $k_* = k_r + ik_i$ with k_r and k_i defined by:

$$k_r = \frac{\sigma}{c_0}\left\{\frac{1}{2} + \frac{1}{2}\left(1 + \hat{\lambda}^2\right)^{\frac{1}{2}}\right\}^{\frac{1}{2}}, \quad k_i = \frac{\sigma}{c_0}\left\{-\frac{1}{2} + \frac{1}{2}\left(1 + \hat{\lambda}^2\right)^{\frac{1}{2}}\right\}^{\frac{1}{2}}.$$

The full solution for the sea-surface elevation ζ and velocity u are stated in equation (3.7), from which it is clear that the solution consists of an incoming wave and reflected wave.

$$\zeta = \mathrm{Re}\left\{ \frac{\hat{Z}}{\cos(k_* L)} \left(\underbrace{\frac{1}{2} e^{k_i(L-x)} e^{i(k_r x - \sigma t - k_r L)}}_{\longrightarrow} + \underbrace{\frac{1}{2} e^{-k_i(L-x)} e^{-i(k_r x + \sigma t - k_r L)}}_{\longleftarrow} \right) \right\}$$

$$u = \mathrm{Re}\left\{ \frac{-ig\hat{Z}}{c_0(1+i\hat{\lambda})^{\frac{1}{2}} \cos(k_* L)} \left(\underbrace{\frac{1}{2i} e^{k_i(L-x)} e^{i(k_r x - \sigma t - k_r L)}}_{\longrightarrow} + \underbrace{\frac{1}{2i} e^{-k_i(L-x)} e^{-i(k_r x + \sigma t - k_r L)}}_{\longleftarrow} \right) \right\} \tag{3.7}$$

3.2 Eigenfunction expansion method

In this section the linearised cross-sectionally averaged equations for an open and closed estuary are solved with the eigenfunction expansion method explained in chapter 8 of Haberman (1983). To solve for the water motion, equation (3.2) and (3.3) are going to be solved to obtain the sea surface elevations and the tidal velocity.

3.2.1 The open estuary

First the sea-surface elevation is considered by solving the following PDE:

$$\begin{aligned} &\frac{\partial^2 \zeta}{\partial t^2} + \lambda \frac{\partial \zeta}{\partial t} - c_0^2 \frac{\partial^2 \zeta}{\partial x^2} = 0, \quad c_0^2 = gH \\ &\zeta = \hat{Z}\cos(\sigma t) \quad \text{at} \quad x = 0, \quad \frac{\partial \zeta}{\partial x} = 0 \quad \text{at} \quad x = L, \\ &\zeta(x,t) = f(x) \quad \text{at} \quad t = 0, \quad \zeta_t(x,t) = g(x) \quad \text{at} \quad t = 0, \end{aligned} \tag{3.8}$$

where arbitrary initial conditions can be prescribed. To compare with the analytical solution, the initial conditions are obtained by using the analytic solution in equation (3.7) at $t = 0$. Note that the boundary conditions are not homogeneous therefore summation and integration are not interchangeable which is necessary in deriving the solution. To solve this we define $s = \zeta - \hat{Z}\cos(\sigma t)$. Substituting $\zeta = s + \hat{Z}\cos(\sigma t)$ and taking the new boundary and initial conditions into account the PDE is rewritten to:

$$\begin{aligned} &\frac{\partial^2 s}{\partial t^2} + \lambda \frac{\partial s}{\partial t} - c_0^2 \frac{\partial^2 s}{\partial x^2} = \hat{Z}\sigma^2 \cos(\sigma t) + \lambda \hat{Z}\sigma \sin(\sigma t), \quad c_0^2 = gH, \\ &s = 0 \quad \text{at} \quad x = 0, \\ &\frac{\partial s}{\partial x} = 0 \quad \text{at} \quad x = L, \\ &s(x,t) = f(x) - \hat{Z}, \quad s_t(x,t) = g(x) \quad \text{at} \quad t = 0. \end{aligned} \tag{3.9}$$

To obtain the eigenfunctions, the corresponding eigenvalue problem, given by:

$$\begin{aligned} &\frac{d^2\phi(x)}{dx^2} = -\lambda\phi(x), \\ &\phi(x) = 0 \quad \text{at} \quad x = 0, \\ &\frac{d\phi(x)}{dx} = 0 \quad \text{at} \quad x = L, \end{aligned}$$

has to be solved. The resulting eigenfunctions $\phi_n(x)$ and eigenvalues λ_n read:

$$\phi_n = \sin\left(\frac{\pi(2n-1)}{2L}x\right) \quad n = 1, 2, \ldots,$$
$$\lambda_n = \left(\frac{\pi(2n-1)}{2L}\right)^2 \quad n = 1, 2, \ldots.$$

With the above information the eigenfunction expansion method can be applied, assuming that:

$$s = \sum_{n=1}^{\infty} B_n(t)\phi_n(x),$$

where $B_n(t)$ are the time dependent coefficients to be determined. Substituting the eigenfunction expansion and the eigenvalue problem in equation (3.9) gives:

$$\sum_{n=1}^{\infty} \frac{d^2B_n}{dt^2}(t)\phi_n(x) + \lambda\sum_{n=1}^{\infty} \frac{dB_n(t)}{dt}\phi_n(x) + c_0^2\sum_{n=1}^{\infty} B_n\lambda_n\phi_n = \hat{Z}\sigma^2\cos(\sigma t) + \lambda\hat{Z}\sigma\sin(\sigma t).$$

Next the left and right hand side are multiplied with an eigenfunction ϕ_p and integrated over the domain. Furthermore the boundary conditions of equation (3.9) and the eigenvalue problem are both homogeneous therefore summation and integration can be interchanged. Next, using the orthogonality of the eigenfunctions results in:

$$\frac{d^2B_p(t)}{dt^2}\int_0^L \phi_p(x)\phi_p(x)dx + \lambda\frac{dB_p(t)}{dt}\int_0^L \phi_p(x)\phi_p(x)dx + c_0^2B_p(t)\lambda_p\int_0^L \phi_p\phi_p dx = \left(\hat{Z}\sigma^2\cos(\sigma t) + \lambda\hat{Z}\sigma\sin(\sigma t)\right)\int_0^L \phi_p dx.$$

Evaluating the integral $\int_0^L \phi_p(x)\phi_p(x)dx = \frac{L}{2}$ gives:

$$\frac{d^2B_n}{dt^2}(t) + \lambda\frac{dB_n(t)}{dt} + c_0^2B_n(t)\lambda_n = \left(\hat{Z}\sigma^2\cos(\sigma t) + \lambda\hat{Z}\sigma\sin(\sigma t)\right)\frac{2}{L}\int_0^L \phi_n dx.$$

The solution of the non-homogeneous ODE stated above is the sum of the homogeneous solution and a particular solution. The homogeneous solution is given by

$$B_n^H(t) = A_n e^{\left(-\frac{\lambda}{2}+\frac{1}{2}\sqrt{\lambda^2-4c_0^2\lambda_n}\right)t} + C_n e^{\left(-\frac{\lambda}{2}-\frac{1}{2}\sqrt{\lambda^2-4c_0^2\lambda_n}\right)t}, \quad n = 1, 2, \ldots.$$

To find the particular solution the method of undetermined coefficients is used. We assume that the particular solution has the following form:

$$B_n^P(t) = \tilde{A}_n\cos(\sigma t) + \tilde{C}_n\sin(\sigma t).$$

Substituting the above assumption gives the following system of equations:

$$\begin{pmatrix} -\sigma^2+\lambda_n c_0^2 & \sigma\lambda \\ -\sigma\lambda & -\sigma^2+\lambda_n c_0^2 \end{pmatrix}\begin{pmatrix} \tilde{A}_n \\ \tilde{C}_n \end{pmatrix} = \frac{2}{L}\int_0^L \phi_n dx \begin{pmatrix} \hat{Z}\sigma^2 \\ \lambda\hat{Z}\sigma \end{pmatrix}. \tag{3.10}$$

Solving the above system of equation gives the coefficients $\tilde{A}_n$, $\tilde{C}_n$. The full solution of equation (3.9) is now given by:

$$s(x,t) = \sum_{n=1}^{\infty} \left(\tilde{A}_n \cos(\sigma t) + \tilde{C}_n \sin(\sigma t) + A_n e^{s_{n_+} t} + C_n e^{s_{n_-} t} \right) \phi_n$$

,where $s_{n_+} = -\frac{\lambda}{2} + \frac{1}{2}\sqrt{\lambda^2 - 4c_0^2\lambda_n}$ and $s_{n_-} = -\frac{\lambda}{2} - \frac{1}{2}\sqrt{\lambda^2 - 4c_0^2\lambda_n}$. Since the coefficients $\tilde{A}_n$ and $\tilde{C}_n$ follow from equation (3.10) only the coefficients A_n and C_n have to be determined. This is done by using the principle of orthogonality and the initial conditions. First the initial conditions are multiplied by the eigenfunction $\phi_p(x)$ and subsequently integrated over the domain. For the initial sea surface elevations, this results in:

$$\sum_{n=1}^{\infty} \left(A_n + C_n + \tilde{A}_n \right) \int_0^L \phi_n(x)\phi_p(x)dx = \int_0^L (f(x) - \hat{Z})\phi_p(x)dx,$$

using the principle of orthogonality:

$$A_p + C_p + \tilde{A}_n = \frac{2}{L} \int_0^L (f(x) - \hat{Z})\phi_p(x)dx.$$

For the time-derivative of the initial sea surface elevations, one finds

$$\sum_{n=1}^{\infty} \left(s_{n_+} A_n + s_{n_-} C_n + \sigma \tilde{C}_n \right) \int_0^L \phi_n(x)\phi_p(x)dx = \int_0^L g(x)\phi_p(x)dx,$$

again using the principle of orthogonality:

$$s_{p_+} A_p + s_{p_-} C_p + \sigma \tilde{C}_n = \frac{2}{L} \int_0^L g(x)\phi_p(x)dx.$$

The coefficient A_n and C_n are determined by solving the following system of equations:

$$\begin{pmatrix} 1 & 1 \\ s_n^+ & s_n^- \end{pmatrix} \begin{pmatrix} A_n \\ C_n \end{pmatrix} = \begin{pmatrix} \frac{2}{L}\int_0^L (f(x) - Z)\,\phi_n dx - \tilde{A}_n \\ \frac{2}{L}\int_0^L g(x)\phi_n dx - \sigma\tilde{C}_n \end{pmatrix}.$$

The full solution of the sea-surface elevations in an open estuary is now given by:

$$\zeta(x,t) = \sum_{n=1}^{\infty} \left(\tilde{A}_n \cos(\sigma t) + \tilde{C}_n \sin(\sigma t) + A_n e^{s_{n_+} t} + C_n e^{s_{n_-} t} \right) \phi_n + \hat{Z} \cos \sigma t. \tag{3.11}$$

Similarly, the tidal velocity is derived resulting in:

$$u(x,t) = \sum_{n=1}^{\infty} \left(\tilde{A}_n \cos(\sigma t) + \tilde{C}_n \sin(\sigma t) + A_n e^{s_{n_+} t} + C_n e^{s_{n_-} t} \right) \phi_n + (x - L)\frac{\sigma \hat{Z}}{H} \sin(\sigma t), \tag{3.12}$$

where the coefficients are determined by solving the following two system of equations:

$$\begin{pmatrix} -\sigma^2 + \lambda_n c_0^2 & \sigma\lambda \\ -\sigma\lambda & -\sigma^2 + \lambda_n c_0^2 \end{pmatrix} \begin{pmatrix} \tilde{A}_n \\ \tilde{C}_n \end{pmatrix} = \frac{2}{L}\int_0^L (x - L)\phi_n dx \begin{pmatrix} -\frac{\hat{Z}\lambda\sigma^2}{H} \\ \frac{\sigma^3 \hat{Z}}{H} \end{pmatrix},$$

$$\begin{pmatrix} 1 & 1 \\ s_n^+ & s_n^- \end{pmatrix} \begin{pmatrix} A_n \\ C_n \end{pmatrix} = \begin{pmatrix} \frac{2}{L}\int_0^L f(x)\phi_n dx - \tilde{A}_n \\ \frac{2}{L}\int_0^L \left(g(x) - \frac{(x-L)\sigma^2\hat{Z}}{H} \right) \phi_n dx - \sigma\tilde{C}_n \end{pmatrix}.$$

Comparison to the analytical solution

Since the analytic solution is known for both the sea-surface elevations and tidal velocity a comparison is made between the analytical solution, and the solution obtained with the eigenfunction expansion method, with the appropriate initial condition. In Figure 3.2 the results are shown using an approximation of n = 25 modes. The chosen values for the parameters are listed in Table 3.1.

Parameter		Value
Gravitational acceleration	g	9.81 ms^{-2}
Height of Estuary	H	10 m
Angular frequency of semi-diurnal tide	σ	1.424E-4 $rad{\cdot}s^{-1}$
Length of estuary	L	6.6E4 m
Frictional damping	λ	1.424E-4
Amplitude of semi-diurnal tide	$\hat{Z}$	1.5m
Number of modes	n	100

Table 3.1: List of values for the parameters that are used for the numerical computation.

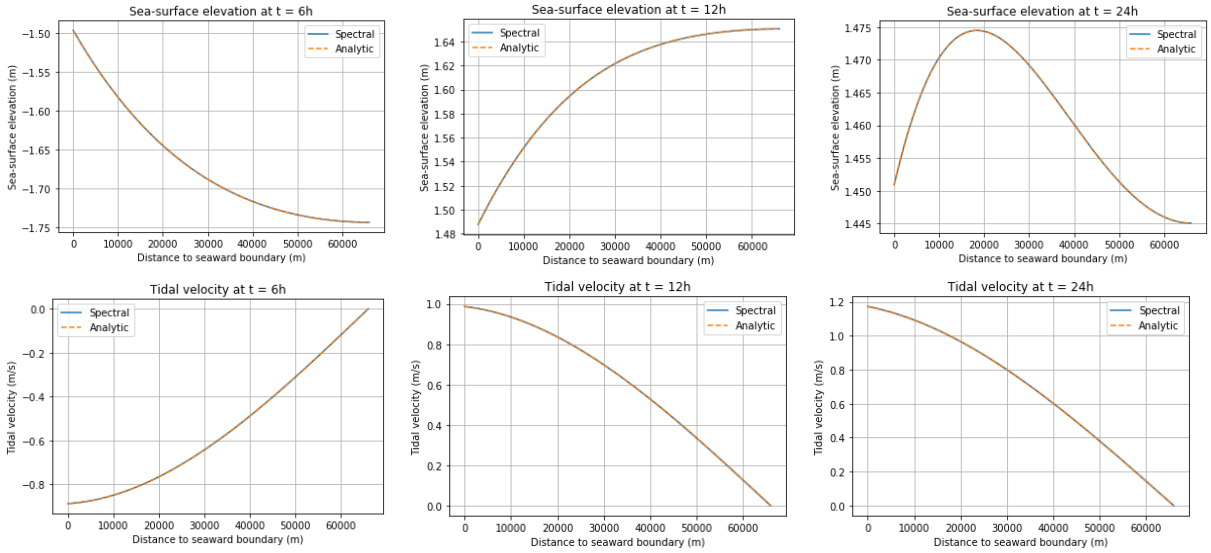

Figure 3.2: In the first row the sea-surface elevations in meters is plotted against the distance to the seaward boundary in meters at different moments in the tidal cycle. In the second row the tidal velocity in meters per second is plotted.

Moving to the error analysis in Figure 3.3 the L_2 norm of the error is shown for 25 and 100 modes. We have a smaller error for 100 modes which is what we expect.

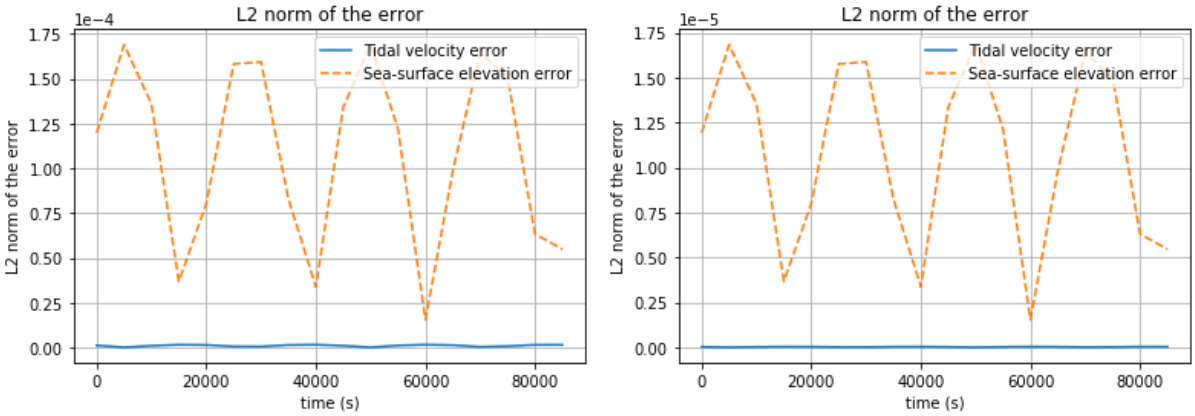

Figure 3.3: The L_2 norm of the error for the tidal velocity (blue line) and the sea-surface elevations (orange dashed line) is plotted against the time in seconds. At the left the error is shown for 25 modes and at the right for 100 modes.

3.2.2 The closed estuary

When considering a closed estuary, a barrier is placed between the sea and the landward side. At this barrier the tidal velocity has to be zero as well. Assuming the barrier is placed at $x = L_1$. The sea-surface elevation reads:

$$\begin{aligned}
&\frac{\partial^2\zeta}{\partial t^2} + \lambda\frac{\partial\zeta}{\partial t} - c_0^2\frac{\partial^2\zeta}{\partial x^2} = 0, \quad c_0^2 = gH,\\
&\frac{\partial\zeta}{\partial x} = 0 \quad \text{at} \quad x = L_1,\\
&\frac{\partial\zeta}{\partial x} = 0 \quad \text{at} \quad x = L,\\
&\zeta(x,t) = f(x) \quad \text{at} \quad t = 0, \quad \zeta_t(x,t) = g(x) \quad \text{at} \quad t = 0.
\end{aligned} \tag{3.13}$$

Again the method of eigenfunctions expansion is considered. To find the eigenfunctions and eigenvalues the following eigenvalue problem has to be solved:

$$\begin{aligned}
&\frac{d^2\phi(x)}{dx^2} = -\lambda\phi(x),\\
&\frac{d\phi(x)}{dx} = 0 \quad \text{at } x = L_1 \quad \text{and} \quad \text{at } x = L,
\end{aligned} \tag{3.14}$$

Resulting in the following eigenvalues λ_n and eigenfunctions $\phi_n(x)$

$$\begin{aligned}
\phi_n(x) &= \cos\left(\frac{\pi n(x-L)}{L_1 - L}\right) \qquad n = 0, 1, 2, \ldots,\\
\lambda_n &= \left(\frac{\pi n}{L_1 - L}\right)^2 \qquad n = 0, 1, 2, \ldots.
\end{aligned}$$

Expanding the sea-surface elevation in its eigenfunctions reads:

$$\zeta = \sum_{n=0}^{\infty} B_n(t)\phi_n(x),$$

and substituting the expansion in equation (3.13) gives:

$$\sum_{n=0}^{\infty} \frac{d^2 B_n}{dt^2}(t)\phi_n(x) - c_0^2 \sum_{n=0}^{\infty} B_n(t)\frac{d^2\phi_n(x)}{dx^2} + \lambda \sum_{n=0}^{\infty} \frac{dB_n(t)}{dt}\phi_n(x) = 0.$$

Using the eigenvalue problem, the term $\frac{d^2\phi_n(x)}{dx^2}$ can be reduced to $-\lambda_n\phi_n(x)$. Furthermore the equation is reduced to an ODE by using the orthogonality of the eigenfunctions. Note that the boundary conditions of the eigenvalue problem and our original are both zero, allowing for the interchange of integration and summation. Applying the above gives the following ODE:

$$\frac{d^2 B_n}{dt^2}(t) + c_0^2 B_n(t)\lambda_n + \lambda \frac{dB_n(t)}{dt} = 0.$$

The solutions of this ODE are exponential functions. Note that the differential equations simplifies for $n = 0$ since $\lambda_0 = 0$:

$$\begin{aligned} B_n(t) &= A_n e^{\left(-\frac{\lambda}{2}+\frac{1}{2}\sqrt{\lambda^2-4c_0^2\lambda_n}\right)t} + C_n e^{\left(-\frac{\lambda}{2}-\frac{1}{2}\sqrt{\lambda^2-4c_0^2\lambda_n}\right)t} \quad n = 1, 2, \ldots, \\ B_0(t) &= A_0 + C_0 e^{-\lambda t}. \end{aligned}$$

hence, the sea-surface elevation in a closed estuary is given by:

$$\zeta(x,t) = A_0 + C_0 e^{-\lambda t} + \sum_{n=1}^{\infty} \left[A_n e^{s_{n_+} t} + C_n e^{s_{n_-} t}\right] \phi_n(x), \tag{3.15}$$

where $s_{n_+} = -\frac{\lambda}{2} + \frac{1}{2}\sqrt{\lambda^2 - 4c_0^2\lambda_n}$ and $s_{n_-} = -\frac{\lambda}{2} - \frac{1}{2}\sqrt{\lambda^2 - 4c_0^2\lambda_n}$. The unknown coefficients A_0, C_0, A_n and C_n are derived using the principle of orthogonality and the initial conditions. First A_0 and C_0 are derived by multiplying the initial conditions with the eigenfunction $\phi_0(x) = 1$ and integrate over the domain:

$$\begin{aligned} \int_{L_1}^{L} \zeta(x,0)\cdot 1 dx = \int_{L_1}^{L} f(x)\cdot 1 dx \quad &\Longrightarrow \quad A_0 + C_0 = \frac{1}{L-L_1}\int_{L_1}^{L} f(x)dx, \\ \int_{L_1}^{L} \zeta_t(x,0)\cdot 1 dx = \int_{L_1}^{L} g(x)\cdot 1 dx \quad &\Longrightarrow \quad C_0 = -\frac{1}{\lambda(L-L_1)}\int_{L_1}^{L} g(x)dx, \\ &\qquad\qquad A_0 = \frac{1}{L-L_1}\int_{L_1}^{L} f(x)dx + \frac{1}{\lambda(L-L_1)}\int_{L_1}^{L} g(x)dx. \end{aligned}$$

Similarly, A_n and C_n are obtained by multiplying with $\phi_p(x)$ and integrate over the domain. Using the initial sea surface elevation, one finds that

$$\sum_{n=1}^{\infty} (A_n + C_n) \int_{L_1}^{L} \phi_n(x)\phi_p(x)dx = \int_{L_1}^{L} f(x)\phi_p(x)dx$$

resulting in

$$A_p + C_p = \frac{2}{L-L_1}\int_{L_!}^{L} f(x)\phi_p(x)dx,$$

Similarly for the time derivative of the initial condition of the sea-surface elevation, one finds

$$\sum_{n=1}^{\infty} \left(s_{n_+}A_n + s_{n_-}C_n\right) \int_{L_1}^{L} \phi_n(x)\phi_p(x)dx = \int_{L_1}^{L} g(x)\phi_p(x)dx$$

resulting in

$$s_{p_+} A_p + s_{p_-} C_p = \frac{2}{L - L_1} \int_{L_1}^{L} g(x)\phi_p(x)dx.$$

Combining these two expression, the coefficients A_n and C_n can be determined by solving the following system of equations:

$$\begin{pmatrix} 1 & 1 \\ s_n^+ & s_n^- \end{pmatrix} \begin{pmatrix} A_n \\ C_n \end{pmatrix} = \begin{pmatrix} \frac{2}{L-L_1} \int_{L_!}^{L} f(x)\phi_p(x)dx \\ \frac{2}{L-L_1} \int_{L_1}^{L} g(x)\phi_p(x)dx \end{pmatrix}.$$

Similarly, the tidal velocity can be obtained (Note that there is no λ_0 since the eigenfunction $\phi_0 = 0$), resulting in

$$u(x,t) = \sum_{n=1}^{\infty} \left[A_n e^{\left(-\frac{\lambda}{2} + \frac{1}{2}\sqrt{\lambda^2 - 4c_0^2\lambda_n}\right)t} + C_n e^{\left(-\frac{\lambda}{2} - \frac{1}{2}\sqrt{\lambda^2 - 4c_0^2\lambda_n}\right)t} \right] \phi_n(x), \tag{3.16}$$

where the coefficients A_n and C_n follow from

$$\begin{pmatrix} 1 & 1 \\ s_n^+ & s_n^- \end{pmatrix} \begin{pmatrix} A_n \\ C_n \end{pmatrix} = \begin{pmatrix} \frac{2}{L-L_1} \int_{L_!}^{L} f(x)\phi_p(x)dx \\ \frac{2}{L-L_1} \int_{L_1}^{L} g(x)\phi_p(x)dx \end{pmatrix}.$$

To test the correctness of the eigenfunction expansion method for a closed estuary, a specific eigenfunction is used as initial condition and the ratio between the initial condition and the resulting sea-surface elevation after a specific time is checked to be constant. The plots of the ratio of the eigenfunctions are shown in Figure 3.4. We see that the output of the eigenfunction expansion method gives a re-scaled eigenfunction back, suggesting the eigenfunction expansion method gives correct results.

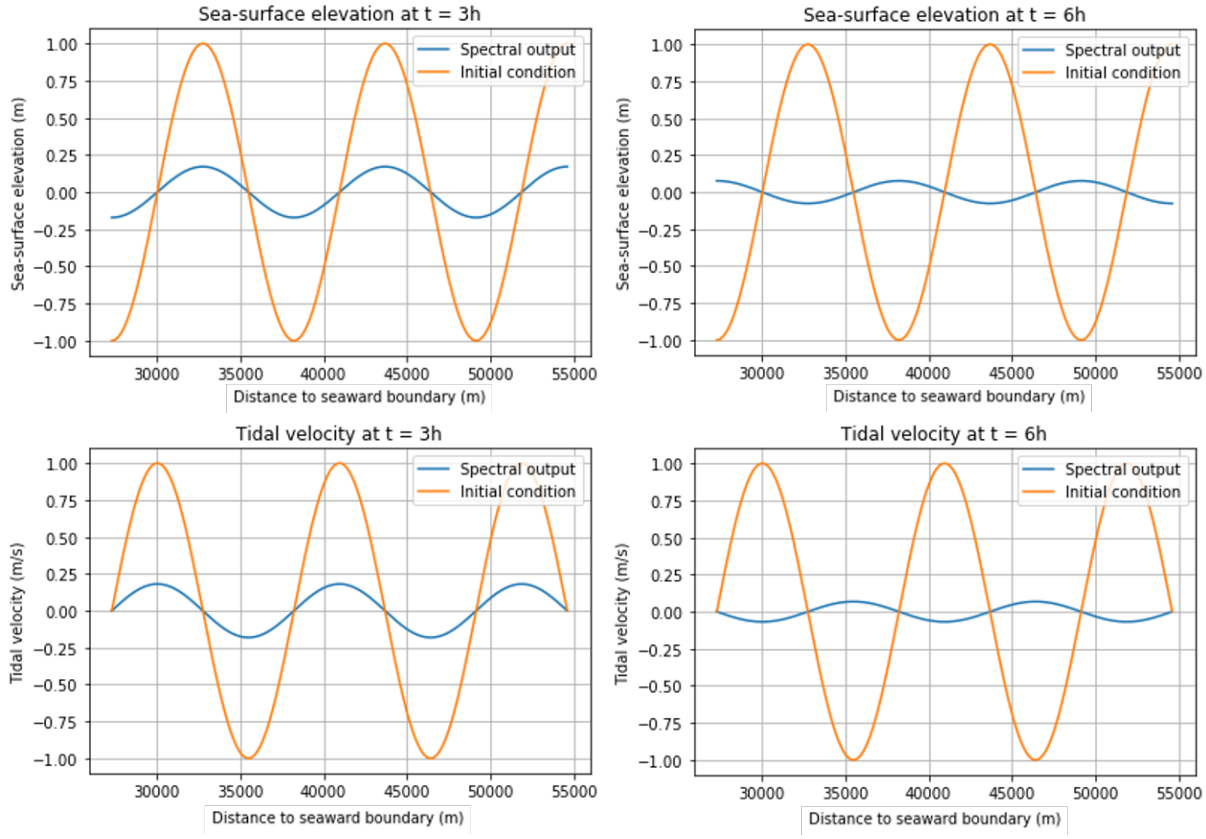

Figure 3.4: In the first row the sea-surface elevations, colored orange, is plotted with its corresponding eigenfunctions with mode number $n = 5$, colored blue, as initial condition. In the second row the same is done for the tidal velocity

3.3 Closing the Estuary

In this section the mathematical modelling of closing an estuary is explained in detail. Implementing the solution method described in section 3.2.2 gives rise to several problems when the estuary is closed at an arbitrarily location L_1. Indeed after closing the barrier, a new initial value problem has to be defined and the initial conditions must obey the boundary conditions, assuming a balance between the local acceleration u_t and the viscosity terms. However, at $x = z$, the velocity is usually not zero where the barrier is closed. In real life the estuary is not closed instantaneous, but it takes a certain time. A so called boundary layer with width L_b will be formed that ensures that the boundary conditions are met. The thickness of this boundary layer follows from scaling analysis done in the derivation of the linearised cross-sectionally averaged equations. The horizontal eddy viscosity were omitted after scaling, but this is not valid as the boundary closes. The thickness of L_b reads

$$\left.\begin{aligned} u_t &\sim \frac{U}{T} \\ \hat{\mathcal{A}}_h \frac{\partial^2 u}{\partial x^2} &\sim \hat{\mathcal{A}}_h \frac{U}{L_b^2} \end{aligned}\right\} \Rightarrow \frac{U}{T} \sim \hat{\mathcal{A}}_h \frac{U}{L_b^2} \Rightarrow L_b \sim \sqrt{\hat{\mathcal{A}}_h T} \Rightarrow L_b \sim \sqrt{100 \frac{m^2}{s} \cdot 44500 s} \Rightarrow L_b \sim 2000 m.$$

To parametrically include this adjustment in our initial condition when closing the estuary, we consider the following example. A barrier is placed at $L_1 = \frac{1}{2}L$ where the tidal velocity should

be $u = 0$. To get $u = 0$ at $x = L_1$, we multiply the tidal velocity with the van Albada 1 function van Albada et al. (1982):

$$\phi_{va1}(r) = \frac{r^2 + r}{r^2 + 1},$$

which becomes zero at $r = 0$ and $\lim_{r\to\infty} \phi_{va1}(r) = 1$. Given the tidal velocity before closing the estuary $u(x)$, the tidal velocity u_{closed} after closing is then given by:

$$u_{closed}(x) = \begin{cases} u(x)\phi_{va1}(\frac{-x + L_1}{400}) & x < L_1, \\ u(x)\phi_{va1}(\frac{x - L_1}{400}) & x \geq L_1. \end{cases}$$

For the sea surface elevations, one has to require that $\frac{\partial \zeta}{\partial x} = 0$ at $x = L_1$, the sea-surface elevations ζ_{closed} is related to the sea-surface elevation before closing $\zeta(x)$:

$$\zeta_{closed}(x) = \begin{cases} \zeta(x) & x < L_1 - \epsilon, \\ \zeta(L_1 - \epsilon) & L_1 - \epsilon \leq x < \epsilon, \\ \zeta(L_1 + \epsilon) & L_1 \leq x \leq L_1 + \epsilon, \\ \zeta(x) & x > L_1 + \epsilon, \end{cases}$$

where ϵ is a small parameter. This is summarized in Figure 3.5:

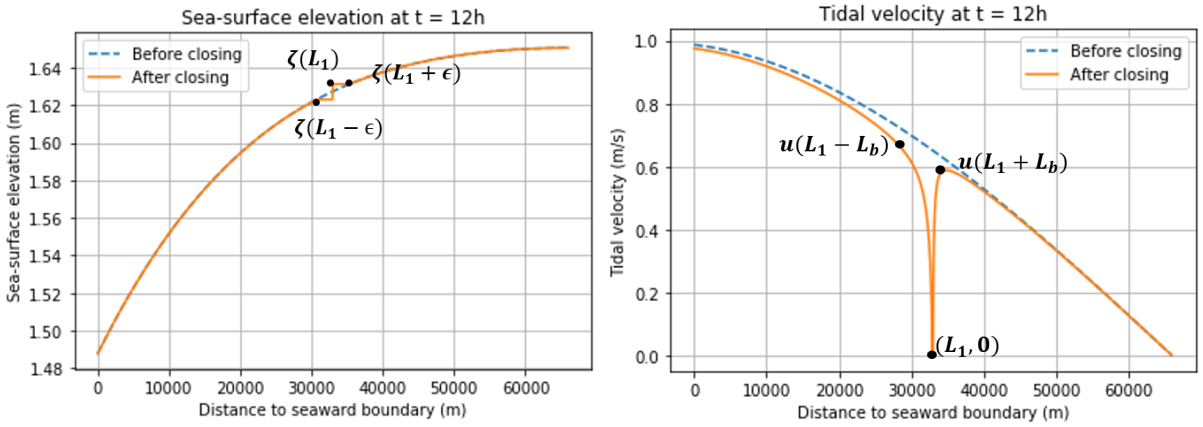

Figure 3.5: At the left the boundary layer is implemented for the sea-surface elevations and at the right for the tidal velocity.

With the above information the estuary can now be closed and we can check if the amount of water is conserved in the closed estuary when using the eigenfunction expansion method. In Table 3.2 the integral over the domain of the sea-surface elevation in a closed estuary is calculated at different time t. From Table (3.2) we conclude that the amount of water is conserved in the spectral method.

time in hours	Area under ζ in m^2 (Spectral)
0h	94791.7729272578
6h	94791.7729272579
12h	94791.772927257

Table 3.2: The area under $\zeta(x,t)$ is shown for different time t.

3.4 Opening the estuary

In this section the opening of an estuary is modeled. Throughout this section we consider an estuary that has been closed at time $t = T_{close}$ for a duration of ΔT and will be re-opened. Again we need to realize that in the real world the estuary is not opened instantaneously, therefore we need to smooth out the solution we obtained after the estuary is closed for a certain time ΔT. We still have a boundary layer L_b. In this boundary layer the solution obtained before opening the estuary is smoothed. For the tidal velocity u_{open} we define:

$$u_{open}(x) = \begin{cases} u(x) & x < L_1 - L_b, \\ (u(L_1 - L_b) - \bar{u}) \tanh \dfrac{x - L_1}{1000} + \bar{u} & L_1 - L_b \leq x \leq L_1 + L_b, \\ u(x) & x > L_1 + L_b, \end{cases} \tag{3.17}$$

where $\bar{u} = \frac{1}{2}\left(u(L_1 - L_b) + u(L_1 + L_b)\right)$ and $u(x)$ is the tidal velocity before opening the estuary. For the sea-surface elevations a similar function is used:

$$\zeta_{open}(x,i) = \begin{cases} \zeta(x) & x < L_1 - L_b, \\ (\zeta(L_1 - L_b) - \bar{\zeta}) \tanh \dfrac{x - L_1 + i}{1000} + \bar{\zeta} & L_1 - L_b \leq x \leq L_1 + L_b, \\ \zeta(x) & x > L_1 + L_b, \end{cases} \tag{3.18}$$

where $\bar{\zeta} = \frac{1}{2}\left(\zeta(L_1 - L_b) + u(L_1 + L_b)\right)$ and $\zeta(x)$ is the sea-surface elevation before opening the estuary. Note that in contrast with equation (3.17) the equation for ζ_{open} has an additional variable i. This additional variable ensures that the amount of water before and after opening is conserved. The variable i is determined with the following iterative scheme:

Iterative scheme

$i = L_1 - L_b$
Δx =gridstepsize
ϵ = allowed error
$\text{Area}_1 = \int_{L_1-L_b}^{L_1+L_b} \zeta(x)dx$
$\text{Area}_2 = \text{Area}_1 + \epsilon + 1$
while $|\text{Area}_1 - \text{Area}_2| > \epsilon$ **and** $L_1 - L_b \leq i \leq L_1 + L_b$:
    $\text{Area}_2 = \int_{L_1-L_b}^{L_1+L_b} \zeta_{open}(x, i)dx$
    i = i+Δx
    if $i = L_1 + L_b$:
        return $\zeta_{open}(x, L_1)$
return $\zeta_{open}(x, i)$

The methods are illustrated in figure (3.6).

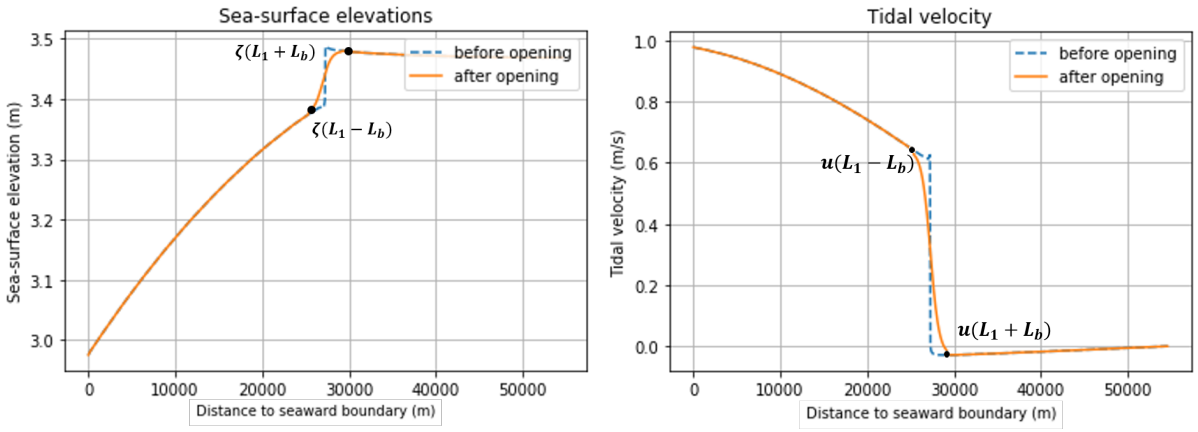

Figure 3.6: At the left the sea-surface elevation is shown before opening, blue line, and after opening, orange line, and at the right the same is shown for the tidal velocity.

3.5 Overtide

Until now, The water motion was only forced by a semi-diurnal constituents, the so-called M_2 tidal component. In this subsection the first overtide, with an angular frequency of 2σ, is implemented along with the semi-diurnal tide. This implicates that at $x = 0$, the boundary condition consists of a forced semi-diurnal tide and its first overtide:

$$\zeta = \hat{Z}_1 \cos \sigma t + \hat{Z}_2 \cos (2\sigma t - \phi_\zeta), \tag{3.19}$$

where $\hat{Z}_1$, $\hat{Z}_2$ are the amplitudes of respectively the semi-diurnal tide and overtide and ϕ_ζ is the phase difference between the semi-diurnal tide and overtide at $x = 0$. This boundary condition influences the estuarine region connected to the seaward side therefore we only need to resolve the following PDE

$$\begin{aligned}
&\frac{\partial^2\zeta}{\partial t^2} + \lambda\frac{\partial\zeta}{\partial t} - c_0^2\frac{\partial^2\zeta}{\partial x^2} = 0, \quad c_0^2 = gH,\\
&\zeta = \Re\left\{\hat{Z}_1 e^{-i\sigma t}\right\} + \Re\left\{\hat{Z}_2 e^{i\phi_\zeta} e^{-i2\sigma t}\right\} \quad \text{at} \quad x = 0, \quad \frac{\partial\zeta}{\partial x} = 0 \quad \text{at} \quad x = L,\\
&\zeta(x,t) = f(x) \quad \text{at} \quad t = 0, \quad \zeta_t(x,t) = g(x) \quad \text{at} \quad t = 0.
\end{aligned} \tag{3.20}$$

Since the PDE is linear the solution of equation (3.20) can be rewritten as the sum of ζ_1 and ζ_2, where ζ_1 and ζ_2 are obtained by solving equation (3.21) and (3.22) respectively.

$$\begin{aligned}
&\frac{\partial^2\zeta_1}{\partial t^2} + \lambda\frac{\partial\zeta_1}{\partial t} - c_0^2\frac{\partial^2\zeta_1}{\partial x^2} = 0, \quad c_0^2 = gH,\\
&\zeta_1 = \Re\left\{\hat{Z}_1 e^{-i\sigma t}\right\} \quad \text{at} \quad x = 0, \quad \frac{\partial\zeta_1}{\partial x} = 0 \quad \text{at} \quad x = L,\\
&\zeta_1(x,t) = f(x) \quad \text{at} \quad t = 0, \quad \zeta_{1_t}(x,t) = g(x) \quad \text{at} \quad t = 0,
\end{aligned} \tag{3.21}$$

$$\begin{aligned}
&\frac{\partial^2\zeta_2}{\partial t^2} + \lambda\frac{\partial\zeta_2}{\partial t} - c_0^2\frac{\partial^2\zeta_2}{\partial x^2} = 0, \quad c_0^2 = gH,\\
&\zeta_2 = \Re\left\{\hat{Z}_2 e^{i\phi_\zeta} e^{-i2\sigma t}\right\} \quad \text{at} \quad x = 0, \quad \frac{\partial\zeta_2}{\partial x} = 0 \quad \text{at} \quad x = L,\\
&\zeta_2(x,t) = f(x) \quad \text{at} \quad t = 0, \quad \zeta_{2_t}(x,t) = g(x) \quad \text{at} \quad t = 0.
\end{aligned} \tag{3.22}$$

The solution procedure for equations (3.21) and (3.22) is already discussed in section (3.2.1) and will not be repeated here. The same reasoning is applied for the tidal velocity.

3.6 Residual sediment transport

Before introducing the residual sediment transport two important technical terms are explained, namely:

Estuarine Turbidity Maximum (ETM)	A region along an estuary with a localized maximum in tidally and cross-sectionally averaged SPM concentration.
Suspended Particulate Matter (SPM)	Inorganic and organic fractions of particulate matter suspended in the water column, the largest fraction of which is generally sediment of lithogenic origin.

There are several mechanism that cause residual sedimentation transport. In this thesis only the tidal co-variance transport is considered, "E.g., up-estuarine transport due to higher depth-mean SPM concentration during flood than during ebb; often referred to as tidal pumping" Burchard et al. (2018). In this thesis we ignore the horizontal diffusivity and source/sinks, and we start with the following transport equation Schuttelaars and De Swart (2000):

$$\frac{\partial C}{\partial t} + \frac{\partial(uC)}{\partial x} = F_e - F_s, \tag{3.23}$$

where C is the depth–integrated concentration, u the depth–averaged velocity, F_e the erosion flux and F_s the settling flux. The settling flux F_s can be parameterised as $F_s = \gamma C$ with γ the deposition parameter, the erosion flux F_e can be parameterised as $F_e = \alpha u^2$ with α the erosion parameter. We consider sediments with a settling time scale much shorter than the tidal time scale. This allows us to neglect local inertia, resulting in the following equation:

$$0 = \alpha u^2 - \gamma C, \tag{3.24}$$

Allowing for an explicit expression of C in terms of u. The resulting residual sediment transport is proportional to $\langle uC \rangle$, where $\langle \cdot \rangle$ denotes tidal averaging. Now consider the following tidal velocity:

$$u = U_{\mathrm{M}_2} \cos(\sigma t) + U_{\mathrm{M}_4} \cos(2\sigma t - \phi_u), \tag{3.25}$$

with σ the M2 tidal frequency, U_{M_2} and U_{M_4} the amplitudes of the depth–averaged M2 and M4 velocities, and ϕ_u the relative phase between the two velocity components. The residual sediment transport for overtide is determined by substituting equation (3.25) in the sediment transport equation $\langle UC \rangle$:

$$\begin{aligned}
\langle uC \rangle &= \frac{\alpha}{\gamma} \langle u^3 \rangle, \\
&= \frac{\alpha}{\gamma} \langle (U_{\mathrm{M}_2} \cos(\sigma t) + U_{\mathrm{M}_4} \cos(2\sigma t - \phi_u))^3 \rangle, \\
&= \frac{\alpha}{\gamma} \langle ((U_{\mathrm{M}_2} \cos(\sigma t))^3 \rangle + \frac{\alpha}{\gamma} \langle (U_{\mathrm{M}_4} \cos(2\sigma t - \phi_u)))^3 \rangle \\
&+ \frac{3\alpha}{\gamma} \langle U_{\mathrm{M}_2} U_{\mathrm{M}_4} \cos(\sigma t) \cos(2\sigma t - \phi_u)(U_{\mathrm{M}_2} \cos(\sigma t) + U_{\mathrm{M}_4} \cos(2\sigma t - \phi_u)) \rangle, \\
&= \frac{3\alpha}{\gamma} \langle U_{\mathrm{M}_2} \cos(\sigma t) U_{\mathrm{M}_4} \cos(2\sigma t - \phi_u)((U_{\mathrm{M}_2} \cos(\sigma t) + U_{\mathrm{M}_4} \cos(2\sigma t - \phi_u)) \rangle, \\
&= \frac{3\alpha}{2\gamma} U_{\mathrm{M}_2} U_{\mathrm{M}_4} \langle (\cos(3\sigma t - \phi_u) + \cos(-\sigma t + \phi_u))((U_{\mathrm{M}_2} \cos(\sigma t) + U_{\mathrm{M}_4} \cos(2\sigma t - \phi_u)) \rangle, \\
&= \frac{3\alpha}{4\gamma} U_{\mathrm{M}_2} U_{\mathrm{M}_4} \langle U_{\mathrm{M}_2} \cos(4\sigma t - \phi_u) + U_{\mathrm{M}_2} \cos(2\sigma t - \phi_u) + \\
&\qquad U_{\mathrm{M}_4} \cos(5\sigma t - 2\phi_u) + U_{\mathrm{M}_4} \cos(\sigma t) + \\
&\qquad U_{\mathrm{M}_2} \cos(\phi_u) + U_{\mathrm{M}_2} \cos(-2\sigma t + \phi_u) + \\
&\qquad U_{\mathrm{M}_4} \cos(\sigma t) + U_{\mathrm{M}_4} \cos(-3\sigma t + 2\phi_u) \rangle,
\end{aligned}$$

resulting in:

$$\frac{3\alpha}{4\gamma} U_{\mathrm{M}_2}^2 U_{\mathrm{M}_4} \cos(\phi_u). \tag{3.26}$$

Note that the residual sediment transport of the overtide is zero for $\phi_u = \pi/2, -\pi/2$. If only the semi-diurnal tide, with tidal velocity $u = U_{M_2} \cos(\sigma t)$, is considered the transport reduces to zero (since $U_{M_4} = 0$). Equation (3.27) will be used as a proxy for the residual sediment transport in the next chapter.

$$\langle u^3 \rangle. \tag{3.27}$$

Chapter 4

Results and discussion

In this chapter the results concerning the water motion and sediment transport are presented. In section 4.1 the periodically opened and closed estuary with only a semi-diurnal tidally forced estuary is considered and in section 4.2 the overtide is included as a more representative forcing for the Ems-Dollard estuary. For both models the eigenfunction expansion method is used together with the parameters listed in Table 3.1 for the semi-diurnal forced model and Table 4.3 for the overtide forced model.

4.1 Semi-diurnal tides

In subsection 4.1.1 the completely open estuary is considered and in section 4.1.2 the results concerning periodically opened and closed estuary, described in Figure 3.1, are discussed. Our aim is to obtain periodic solutions of ζ and u and to determine what the influence of periodically opening and closing an estuary is on the residual sediment transport.

4.1.1 Open estuary

The open estuary is our reference case. Using the variables listed in Table 3.1 and equation (3.11) and (3.12), the tidal velocity and sea-surface elevations for $t = 0$h until $t = T = 12$h25m is calculated and shown in Figure 4.1.

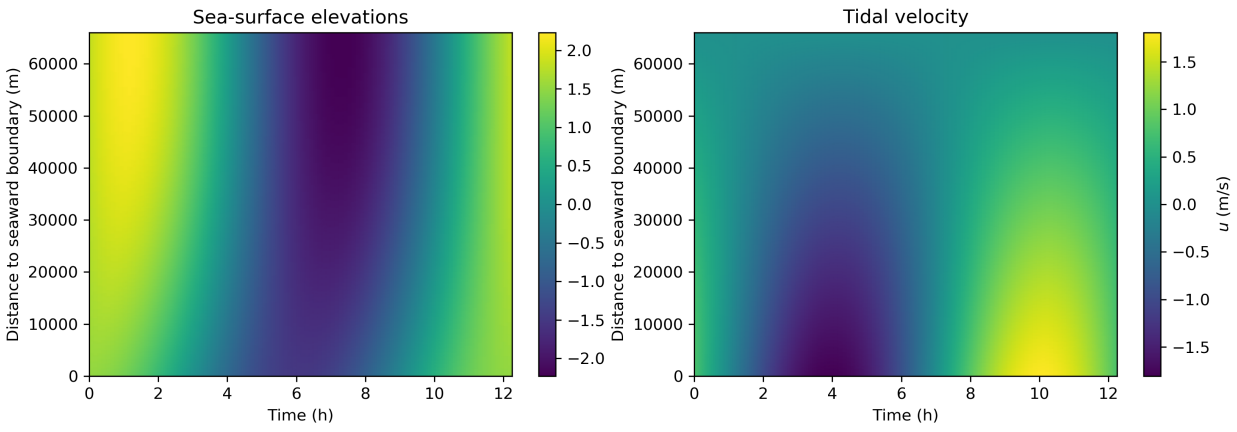

Figure 4.1: Plot of the sea-surface elevations at the left and tidal velocity at the right. On the vertical axis the distance to the seaward boundary is shown and on the horizontal axis the time in hours.

The solutions in Figure 4.1 are oscillatory. To determine the angular frequency the Fast Fourier Transform (FFT) of ζ and u is calculated. Figure 4.2 shows the corresponding amplitude of each frequency, obtained by multiplying the absolute value of the FFT by 2 and dividing by the number of time-steps. From now on, all the FFT plots are manipulated in the same way to obtain the amplitudes. Figure 4.2 concludes that the angular frequency of ζ and u equals σ. This corresponds with the theory since the analytic solution of ζ and u is of the form $\Re\{A(x)e^{-i\sigma t}\}$. The amplitude of ζ increases towards the landward side due to resonance. The amplitude of u decreases to zero towards the landward side, since our defined boundary condition is zero at the landward boundary.

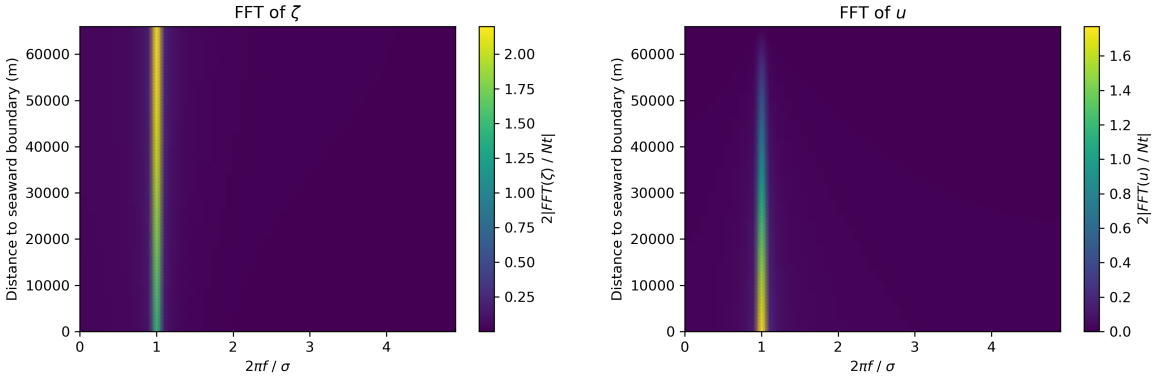

Figure 4.2: Plot of the FFT of the sea-surface elevations and tidal velocity. On the vertical axis the distance to the seaward boundary is shown and on the horizontal axis the non-dimensional angular frequency is shown.

Using the obtained tidal velocity, the residual sediment transport is given by equation (3.27), and shown in Figure 4.3.

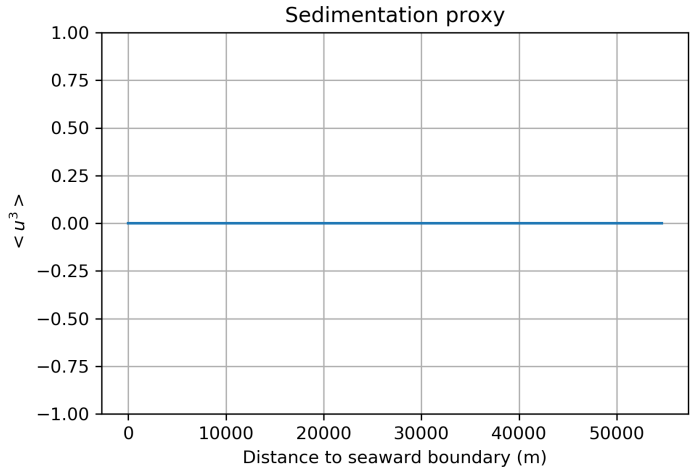

Figure 4.3: Plot of the sedimentation proxy which is given by $\langle u^3 \rangle$ as shown on the vertical axis. Furthermore on the horizontal axis the distance to the seaward boundary is shown.

The proxy is zero for all positions in the estuary, indicating that the residual sediment transport is zero, as shown in section 3.6.

4.1.2 periodically opening and closing the estuary

In this subsection the periodically opened and closed estuary shown schematically in Figure 3.1 is considered. The parameters are listed in Table 3.1. Furthermore there are still three free parameters to be chosen:

The opening and closing position	L_1	L_1 denotes the location of closing and opening in meters. $L_1 = 0$ means that the estuary is closed at the seaward boundary. $L_1 = L$ means the estuary is closed at the landward boundary.
The time between opening and closing	ΔT	ΔT denotes how long the estuary is closed in a time-period of 12h25m. $\Delta T = 0$ means that the estuary is not closed, this is our reference case. $\Delta T = 2$h means that the estuary is closed for 2 hours and open for 10h25m in a period of 12h25m.
The opening and closing height	H_1	H_1 denotes at what sea-surface elevation ζ the estuary is closed and opened.

Table 4.1: Table of all free parameters of the model.

Note that ΔT is related to H_1 and L_1. For example let $L_1 = 0.5L$ and $H_1 = 1$ m then ΔT is fixed. This is illustrated in Figure 4.4.

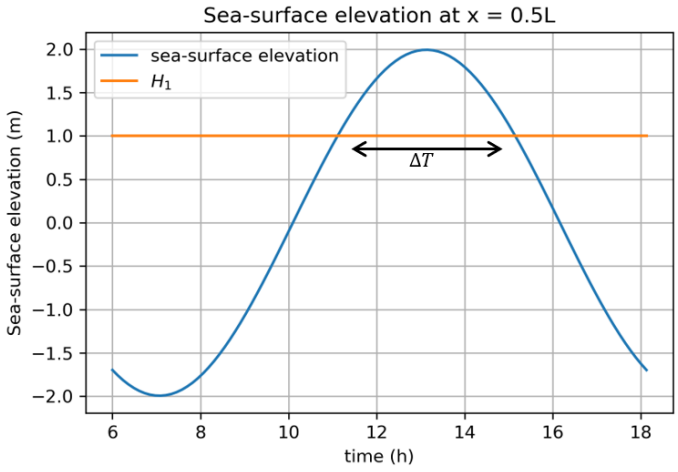

Figure 4.4: Sea-surface elevation in an open estuary at $x = 0.5L$ and 6h$\leq t \leq$18h.

To determine ΔT, the Numpy package in Python is used. First $1 - \zeta(x = H_1, t))$ is calculated with the corresponding signs using numpy.sign. Applying numpy.diff reveals all the locations, where the sign changes. Using numpy.argwhere gives us the exact indices and consequently the closing time T_{close} and opening time T_{open}. Let $x = L_1$ and $\zeta = H_1$ then the closing time T_{close} and opening time T_{open} are given by:

$$T_{close}, T_{open} = \text{numpy.argwhere(numpy.diff(numpy.sign(1 - } \zeta(\text{x} = H_1, t))$$

, Using the closing and opening time $\Delta T = T_{open} - T_{close}$ is determined. Using the parameters in Table 3.1, together with $L_1 = 0.5L$, $H_1 = 1$ m and $\Delta T = 4.06$h (in other words closing the

estuary at high water as shown in Figure 4.4) gives the following sea-surface elevation ζ and tidal velocity u at $x = 0.25L$ and $x = 0.75L$ seen in Figures 4.5 and 4.6 (see Figures C.4 and C.5 for convergence of the solution in terms of the number of modes):

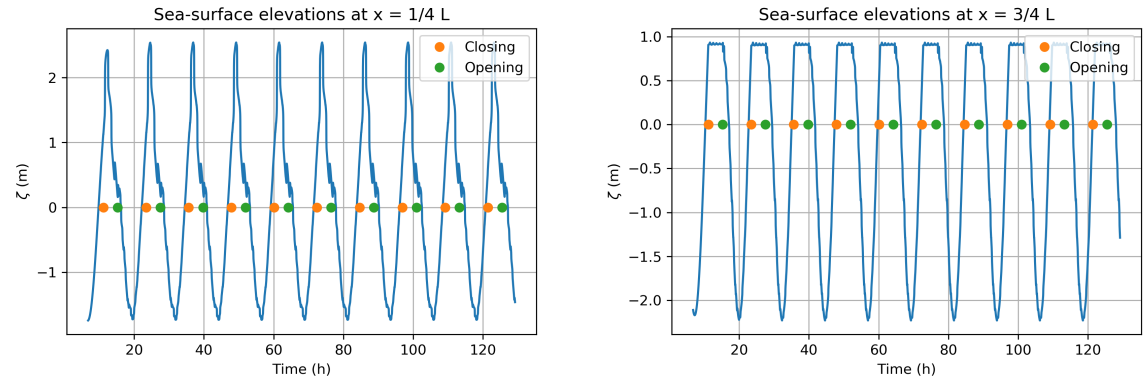

Figure 4.5: At the left the sea-surface elevations is shown at $x = 1/4L$ and at the right at $x = 3/4L$.

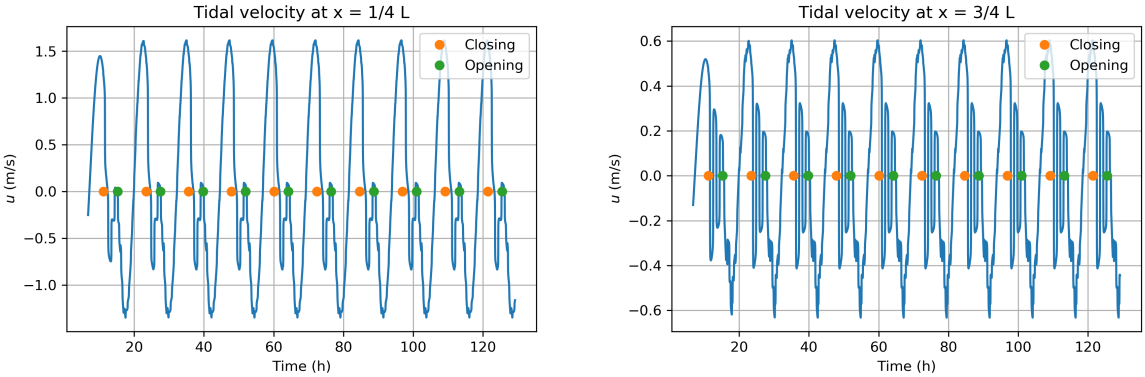

Figure 4.6: At the left the tidal velocity is shown at $x = 1/4L$ and at the right at $x = 3/4L$.

In the figures above, the orange and green dots are the closing and opening time respectively. At $x < L_1$ and $t < T_{close}$ (before the first orange dot i.e. before closing the estuary at $x = L_1$) the sea-surface elevations and tidal velocity are described by the forcing at the seaward boundary. When the estuary is closed at $t = T_{close}$ the sea-surface elevations and tidal velocity evolve in time. Consequently when the estuary is opened again at $t = T_{open}$ (the first green dot) the sea-surface elevation and tidal velocity have a different amplitude and phase then initially prescribed by the tidal forcing at $t < T_{close}$. At $x > L_1$ and $t < T_{close}$ the sea-surface elevation and tidal velocity are described by the tidal forcing. When the estuary is closed at $t = T_{close}$ the sea-surface elevations oscillates around the height it attained when the barrier was closed and the tidal velocity dampens while oscillating. The tidal velocity and sea-surface elevation are still T-periodic. To confirm this the FFT of ζ and u are calculated at $x = 0.25L$ and at $x = 0.75L$. The FFT of the sea-surface elevations and tidal velocity at $x = 1/4L$ is shown in Figure 4.7 and at $x = 3/4L$ in Figure 4.8

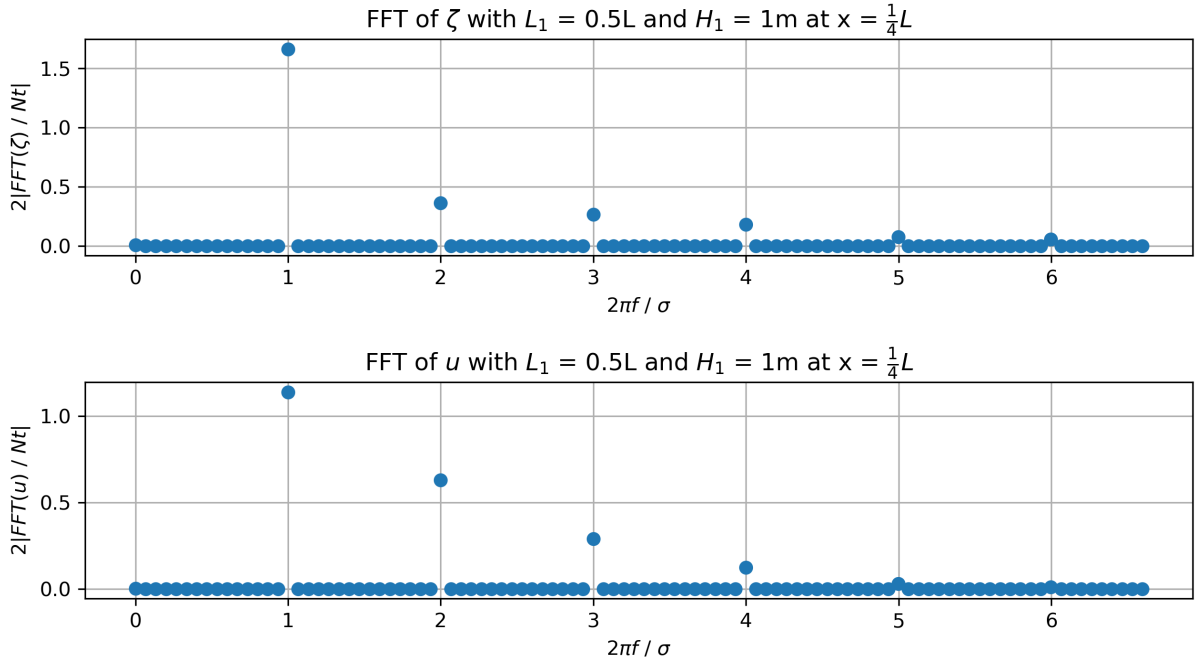

Figure 4.7: Plot of the FFT of the sea-surface elevations and tidal velocity at $x = 0.25L$. Note that the vertical axis shows the corresponding amplitude and the horizontal axis the non-dimensional angular frequency.

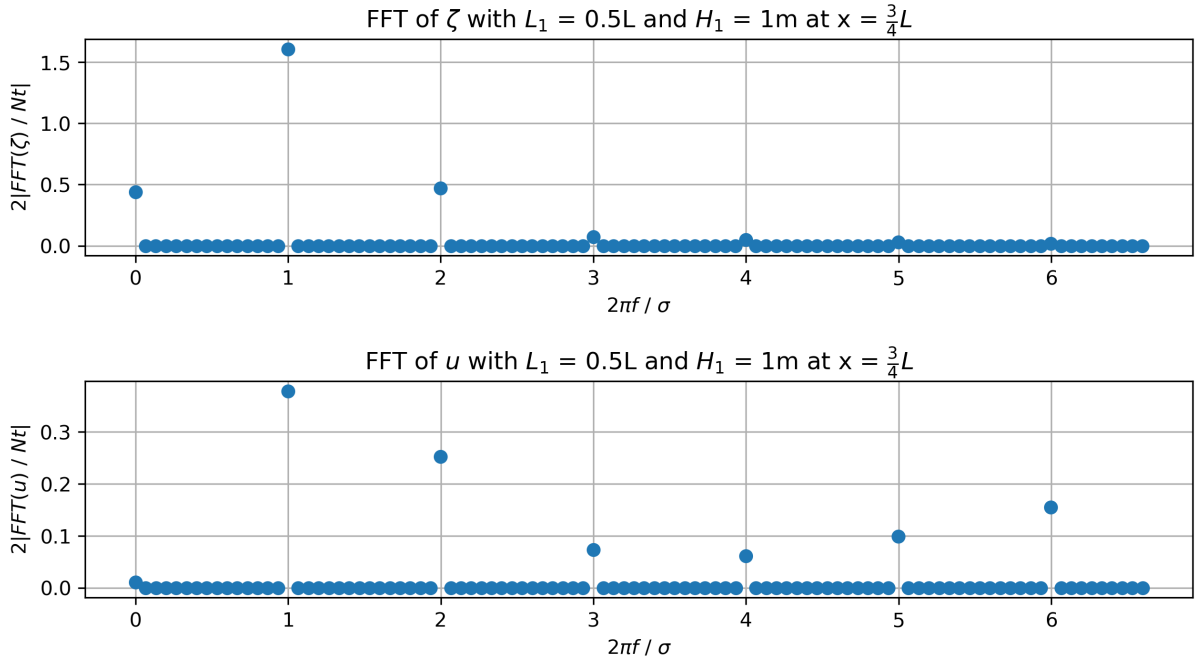

Figure 4.8: Plot of the FFT of the sea-surface elevations and tidal velocity at $x = 0.75L$. Note that the vertical axis shows the corresponding amplitude and the horizontal axis the non-dimensional angular frequency.

The various peaks of the FFT of ζ and u are found to be multiples of σ. Furthermore, there is a finite number of peaks when the full spectrum is considered (see Figure C.1 and C.2 in

appendix C) showing that ζ and u are T-periodic. Comparing the FFT's in Figure 4.7 and 4.8 with the FFT's shown in Figure 4.2, we observe that the angular frequency σ still dominates the total amplitude of ζ and u. This is expected, since we have a time-periodic boundary with an angular frequency of σ at the sea-ward boundary. At $x = 0.75L$ the sea-surface elevations ζ and tidal velocity u have an $\sigma = 0$ contribution i.e. a residual contribution, due to the closing of the estuary for a period of ΔT.
To determine the frequencies in the closed estuary the Fourier transform of the spectral solution of ζ in the closed estuary is calculated (the exact same can be done for the tidal velocity but for illustration only the sea-surface elevation is considered):

$$
\begin{aligned}
\mathcal{F}\{\zeta(x,t)\} =& \mathcal{F}\{A_0 + C_0 e^{-\lambda t} + \sum_{n=1}^{\infty} \left[A_n e^{s_{n_+} t} + C_n e^{s_{n_-} t}\right] \phi_n(x)\}, \\
=& A_0\delta(f) + \mathcal{F}\{C_0 e^{-\lambda t}\} + \sum_{n=1}^{\infty} \mathcal{F}\{\phi_n(x) A_n e^{\mathrm{Re}(s_{n_+})t + i\mathrm{Im}(s_{n_+})t}\} + \mathcal{F}\{\phi_n(x) C_n e^{\mathrm{Re}(s_{n_-})t + i\mathrm{Im}(s_{n_-})t}\}, \\
=& A_0\delta(f) + \mathcal{F}\{C_0 e^{-\lambda t}\} + \sum_{n=1}^{\infty} \phi_n(x) A_n \mathcal{F}\{e^{\mathrm{Re}(s_{n_+})t}\} * \mathcal{F}\{e^{i\mathrm{Im}(s_{n_+})t}\} \\
&+ \phi_n(x) C_n \mathcal{F}\{e^{\mathrm{Re}(s_{n_-})t}\} * \mathcal{F}\{e^{i\mathrm{Im}(s_{n_-})t}\}, \\
=& A_0\delta(f) + \mathcal{F}\{C_0 e^{-\lambda t}\} + \sum_{n=1}^{\infty} \phi_n(x) A_n \mathcal{F}\{e^{\mathrm{Re}(s_{n_+})t}\} * \delta(f - \frac{\mathrm{Im}(s_{n_+})}{2\pi}) \\
&+ \phi_n(x) C_n \mathcal{F}\{e^{\mathrm{Re}(s_{n_-})t}\} * \delta(f - \frac{\mathrm{Im}(s_{n_-})}{2\pi}),
\end{aligned}
$$

where $s_{n_\pm} = -\frac{\lambda}{2} \pm \frac{1}{2}\sqrt{\lambda^2 - 4c_0^2\lambda_n}$, $'*'$ is a convolution, δ the Dirac Delta function and f the frequency. The location of the peaks (i.e. the frequencies) that emerge in the closed estuary are dependent on the imaginary part of the eigenvalues of the differential operator of equation (3.13). Using the parameters in Table 3.1 the eigenvalues and the location of the peaks are determined. In Figure 4.9 the eigenvalues of the first 10 modes are plotted in the complex plane and in Table 4.2 the angular frequencies corresponding to each mode number are listed. All the modes have the same real part except mode number zero which has a zero real part. This means that all the frequencies are damped-out at the same rate except for mode number zero, in this case over a time interval of ΔT. Because ζ and u are T periodic these frequencies are not observed in the FFT of ζ and u.

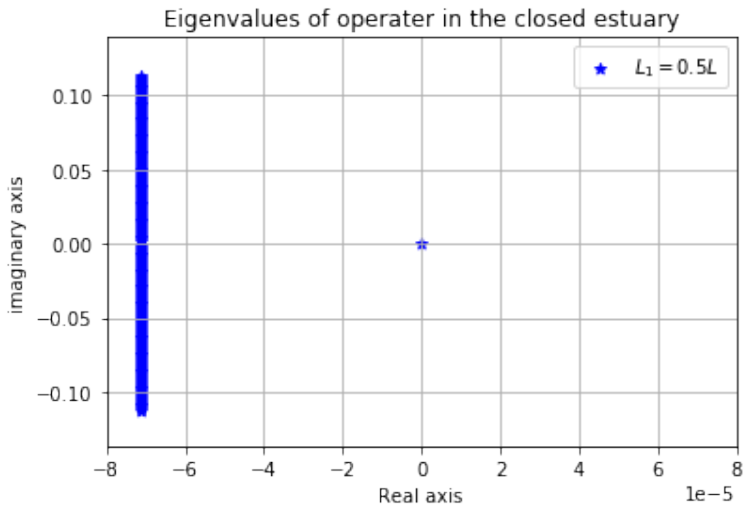

Figure 4.9: The eigenvalues of the differential operator of equation (3.13) are plotted in the complex plane.

mode-number	corresponding angular frequency = Im $\left(\frac{s_{n-}}{\sigma}\right)$
0	0
1	6.60
2	13.23
3	13.23
4	19.85
5	26.47
6	33.09
7	39.71
8	46.32
9	52.94

Table 4.2: List of mode numbers with their corresponding angular frequencies.

To analyse the closing height and closing position we fix one parameter and vary the other parameter. Let $H_1 = 1$ m and vary L_1 from $0.2L$ to $0.8L$ in steps of $0.1L$. This means that we close the estuary at high water as seen in Figure 4.4 and we move the closing position from the seaward boundary to the landward boundary.

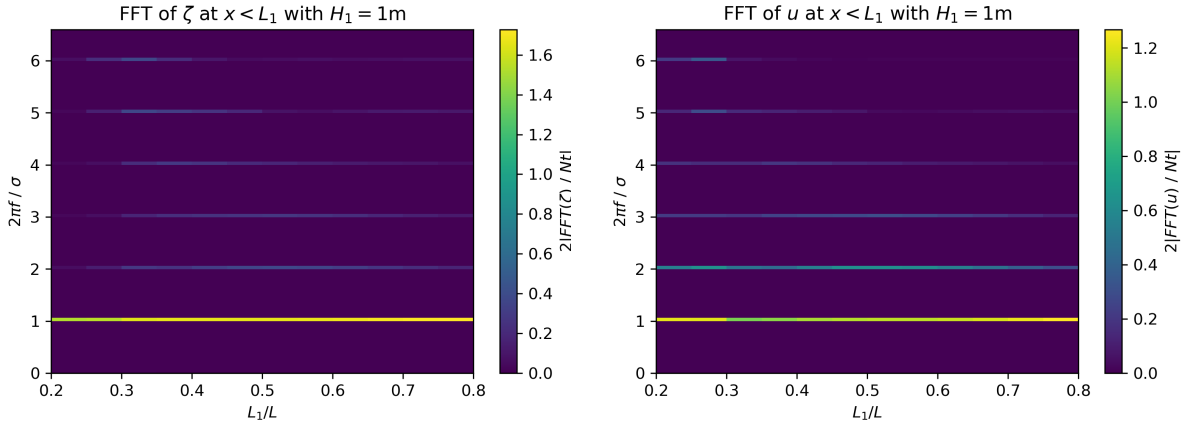

Figure 4.10: FFT of ζ and FFT of u with $H_1 = 1\text{m}$ at $x < L_1$. On the horizontal axis the non-dimensional closing positions are shown and on the vertical axis the non-dimensional angular frequencies.

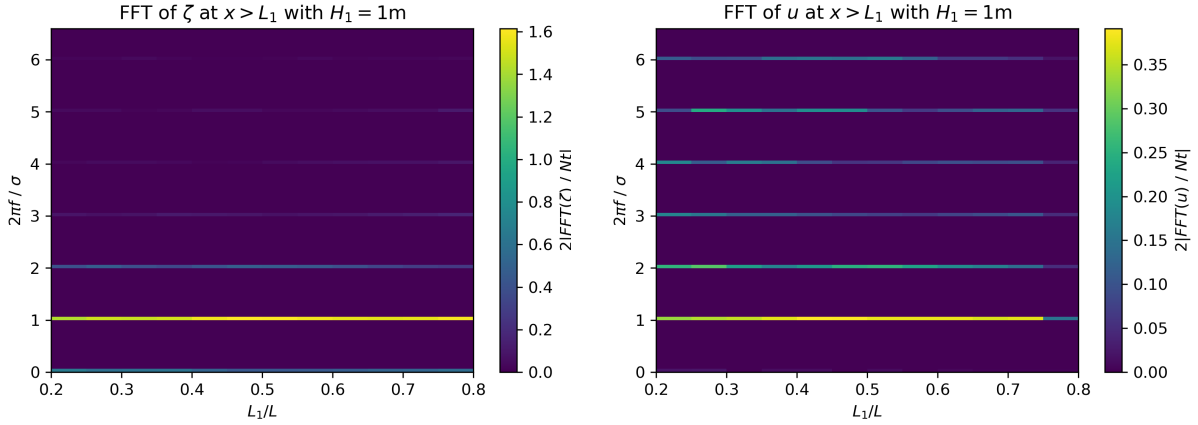

Figure 4.11: FFT of ζ and FFT of u with $H_1 = 1\text{m}$ at $x > L_1$. On the horizontal axis the non-dimensional closing positions are shown and on the vertical axis the non-dimensional angular frequencies.

In Figure 4.10 the FFT of ζ and u are shown at $x < L_1$ and in Figure 4.11 at $x > L_1$. On the horizontal axis different closing positions L_1 are chosen. Again a spacing of σ and a finite amount of peaks (see also Figure C.3 for the full spectrum) are observed, showing again that ζ and u are T periodic. In Figure 4.10 and 4.11 the σ angular frequency is dominating for every closing position, since we have a time-periodic boundary forcing with angular frequency σ. The amplitude and the phase of the other frequencies are not the same for every closing position L_1. The solution for the tidal velocity u with $H_1 = 1\text{m}$ and $L_1 = 0.2L, \ldots, 0.8L$ in steps of $0.1L$ can be approximately written as the following finite sum:

$$u = \sum_{i=0}^{N} U_{M_{2i}} \cos(i\sigma t + \phi_{M_{2i}}),$$

where $U_{M_{2i}}$ are the amplitudes and $\phi_{M_{2i}}$ the phases that follow from the FFT. Note that the subscript M_{2i} refers to the different type of tides (e.g. semi-diurnal, quarter-diurnal etc.). New angular frequencies have emerged and therefore residual sediment transport is induced as

discussed in section 3.6, since calculating the proxy $\langle u^3 \rangle$ results in cross terms that prevents $\langle u^3 \rangle$ from vanishing. We have confirmed that the tidal velocity is T =12h25m periodic for $H_1 = 1$m and $L_1 = 0.2L, \ldots, 0.8L$ therefore the residual sediment transport proxy $\langle u^3 \rangle$ is calculated and shown in Figure 4.12. On the horizontal axis different closing positions L_1 are chosen and on the vertical axis the distance to the seaward boundary is shown.

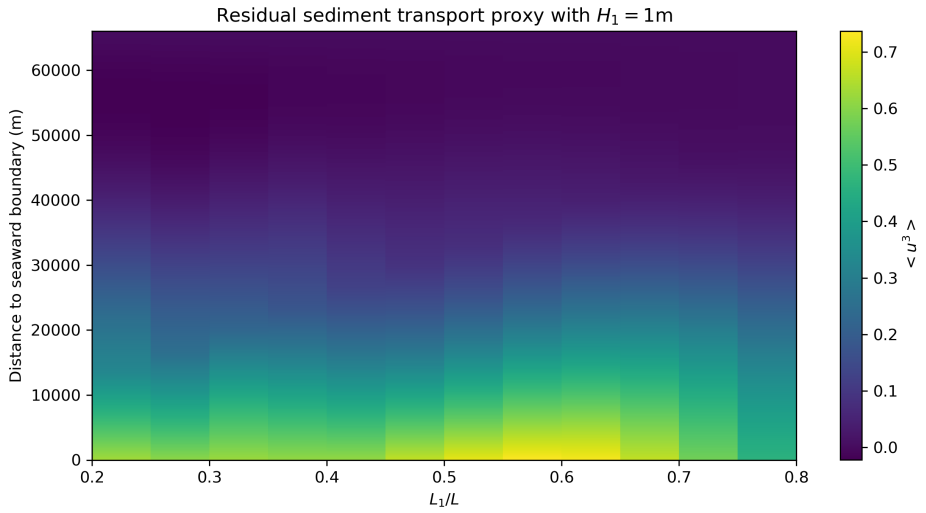

Figure 4.12: Plot of the sedimentation proxy which is given by $< u^3 >$ for $H_1 = 1$m. On the vertical axis the distance to the seaward boundary is shown and on the horizontal axis $\frac{L_1}{L}$.

Comparing the residual sediment transport shown above with the reference case in Figure 4.3, a strong increase in residual sediment transport is observed for all closing positions L_1 at $x <$ 30000m. In Figure 4.13 the residual sediment transport is plotted differently to investigate the magnitude of the residual sediment transport.

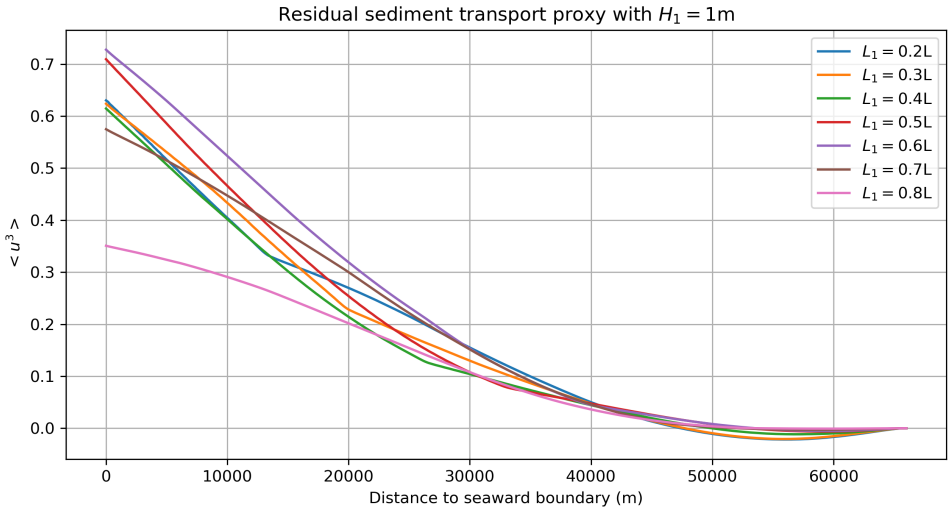

Figure 4.13: Plot of the sedimentation proxy which is given by $\langle u^3 \rangle$ for $H_1 = 1$m. On the vertical axis the residual sediment transport is shown.

At the landward boundary the residual sediment transport is zero which is what we expect since the landward boundary condition is $u = 0$. The highest residual sediment transport at the seaward boundary is observed when the barrier is located at $L_1 = 0.6L$. Now we fix the closing position L_1 and vary the closing height H_1. Let $L_1 = 0.6L$ and $H_1 = -1, 0.75, -0.5, 0.5, 0.75$ and 1 meter. FFT of ζ and FFT of u are calculated and shown in Figure 4.14 at $x < L_1$ and in Figure 4.15 at $x > L_1$.

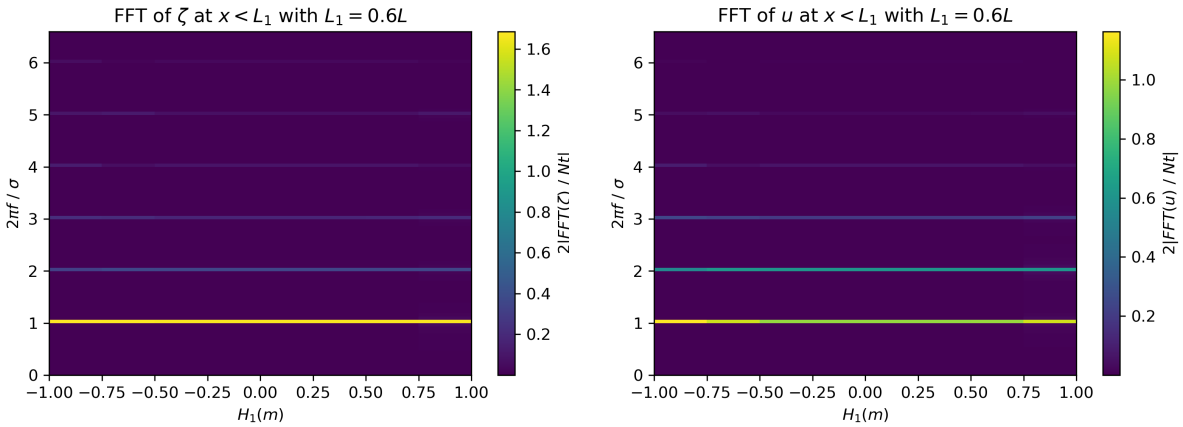

Figure 4.14: FFT of ζ and FFT of u with $L_1 = 0.5L$ is shown at $x < L_1$. On the horizontal axis the closing heights in meters are shown and on the vertical axis the non-dimensional angular frequencies.

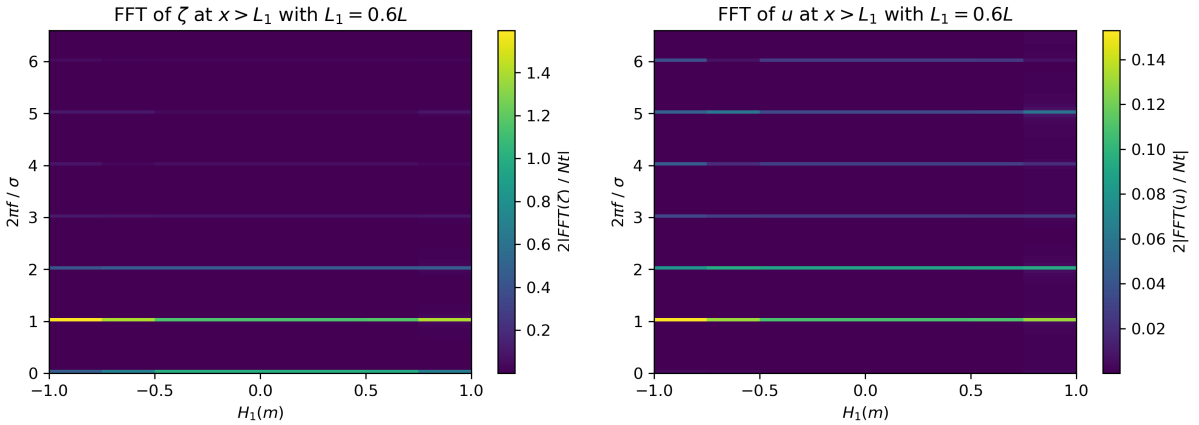

Figure 4.15: FFT of ζ and FFT of u with $L_1 = 0.5L$ is shown at $x > L_1$. On the horizontal axis the closing heights in meters are shown and on the vertical axis the non-dimensional angular frequencies.

For all cases u and ζ are T-periodic allowing for the calculation of the residual sediment transport. We do not use equation (3.26), but calculate $\langle u^3 \rangle$ numerically because of the large number of generated overtides and generated residual contribution. In Figure 4.16 the residual sediment transport for $L_1 = 0.6L$ and $H_1 = -1, -0.75, -0.5, 0.5, 0.75$ and -1 meter is shown. For high water there is a landward residual sediment transport and for low water there is a seaward residual sediment transport. The residual sediment transport is symmetric around $\langle u^3 \rangle = 0$ for different closing heights H_1. This is because the transport is mainly a result of the emerging first overtide.

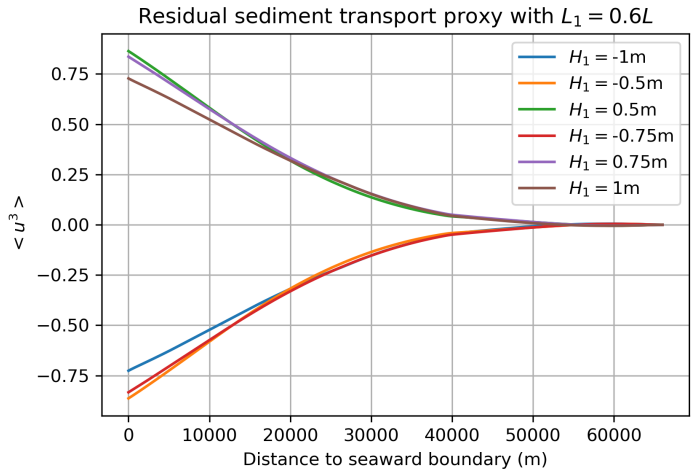

Figure 4.16: Plot of the sedimentation proxy which is given by $\langle u^3 \rangle$ for $L_1 = 0.6L$. On the vertical axis residual sediment transport is shown and on the horizontal axis the distance to the seaward boundary .

4.2 Ems-Dollard estuary

In this section the first overtide is implemented along with the semi-diurnal tide, following section 3.5, together with the parameters of the Ems-Dollard estuary listed in Table 4.3.

Parameter		Value
Gravitational acceleration	g	9.81 ms^{-2}
Height of Estuary	H	12.2 m
Angular frequency of semi-diurnal tide	σ	1.424E-4 $rad{\cdot}s^{-1}$
Angular frequency of the overtide	2σ	2.848E-4 $rad{\cdot}s^{-1}$
Length of estuary	L	6.37E4 m
Frictional damping	λ	σ
Amplitude of semi-diurnal tide	$\hat{Z}_1$	1.35m
Amplitude of semi-diurnal tide	$\hat{Z}_2$	0.19m
phase difference between semi-diurnal tide and overtide at the seaward boundary	ϕ_ζ	$-175°$
Number of modes	n	100

Table 4.3: List of values for the parameters of the Ems-Dollard estuary Chernetsky (2012)

First we investigate the open estuary which is our reference case. Given the sea-surface elevation ζ and u in the open estuary, the residual sediment transport is calculated with equation (3.27) for different phases $\phi_\zeta(x = 0) = 0, \frac{\pi}{2}$ and π, where ϕ_ζ denotes the phase difference between the sea-surface elevation of the semi-diurnal tide and overtide at the entrance of the estuary. The residual sediment transport is shown in Figure 4.17.

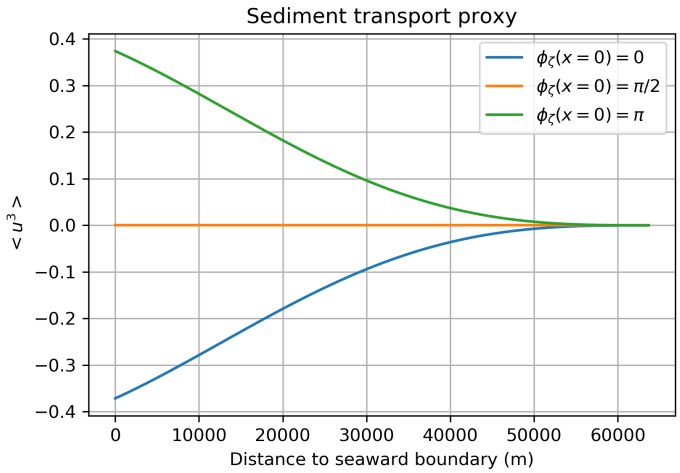

Figure 4.17: Plot of the sedimentation proxy which is given by $\langle u^3 \rangle$ as shown on the vertical axis. Furthermore on the horizontal axis the distance to the seaward boundary is shown.

For $\phi_\zeta(x=0) = \frac{\pi}{2}$ the residual sediment transport is equal to zero. For $\phi_\zeta(x=0) = \pi$ we have a landward directed residual sediment transport and for $\phi_\zeta(x=0) = 0$ a seaward directed residual sediment transport is observed. The sea-surface elevation lags the tidal velocity by $\pi/2$ at $x = 0$. Thus Figure 4.17 corresponds with the theory described in section 3.6. The Ems-Dollard estuary has a phase difference of $\phi_\zeta = -175°$ at the seaward boundary therefore we have a land-inward directed residual sediment transport. Now the periodically opened and closed estuary is implemented and the residual sediment transport is determined for $H_1 = 1$ and $L_1 = 0.2L, \ldots, 0.8L$ in steps of $0.1L$. The result is shown in Figure 4.18.

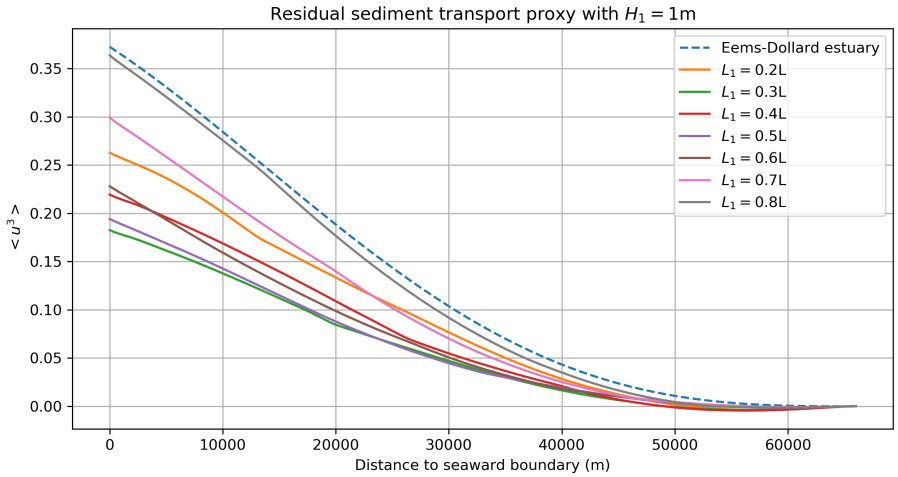

Figure 4.18: Plot of the sedimentation proxy which is given by $\langle u^3 \rangle$ as shown on the vertical axis. Furthermore on the horizontal axis the distance to the seaward boundary is shown.

Comparing the residual sediment transport of the periodically opened and closed estuary with the reference case a decrease in sediment transport is observed for all closing position. From Figure 4.18 we conclude that the highest residual sediment transport occurs at $L_1 = 0.8L$. Locating the barrier at $L_1 = 0.8L$ and closing the estuary at $H_1 = -1, -0.75, 0.5, 0.5, 0.75$ and

1 meter results in Figure 4.19.

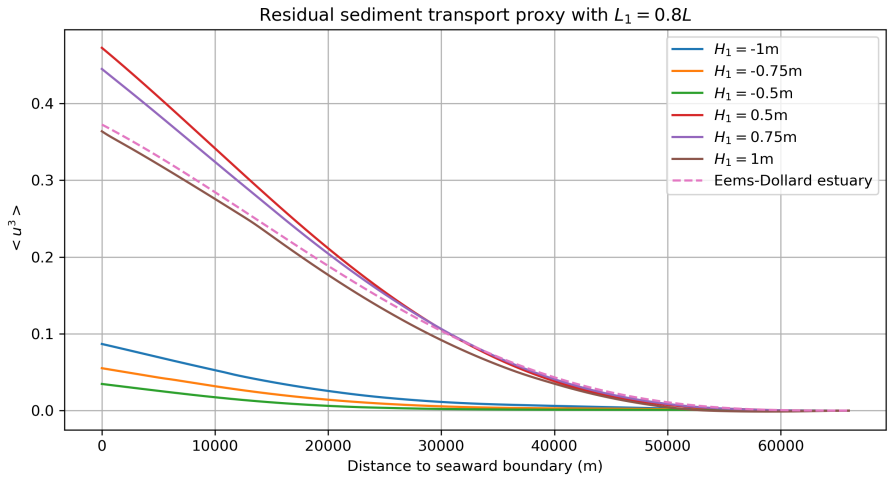

Figure 4.19: Plot of the sedimentation proxy which is given by $\langle u^3 \rangle$ as shown on the vertical axis. Furthermore on the horizontal axis the distance to the seaward boundary is shown.

From Figure 4.19 we conclude that closing the estuary at $H_1 = 0.5$ and 0.75 meters causes an increase in residual sediment transport and at $H_1 = 1$ meters a decrease. For low water there is always a decrease of residual sediment transport but the residual sediment transport is still landward directed. We want to determine for what closing height and closing position the residual sediment transport is seaward directed. In Figure 4.18 the smallest residual sediment transport is observed for $L_1 = 0.3L$ and in Figure 4.19 for $H_1 = -0.5$m. Using these values the residual sediment transport is shown in Figure 4.20. We observe a seaward directed residual sediment transport for $x < 40000$m and a landward directed residual sediment transport for $x > 40000$m. This results in accumulation of sediment (ETM) at $x > 40000$m and therefore an infeasible situation.

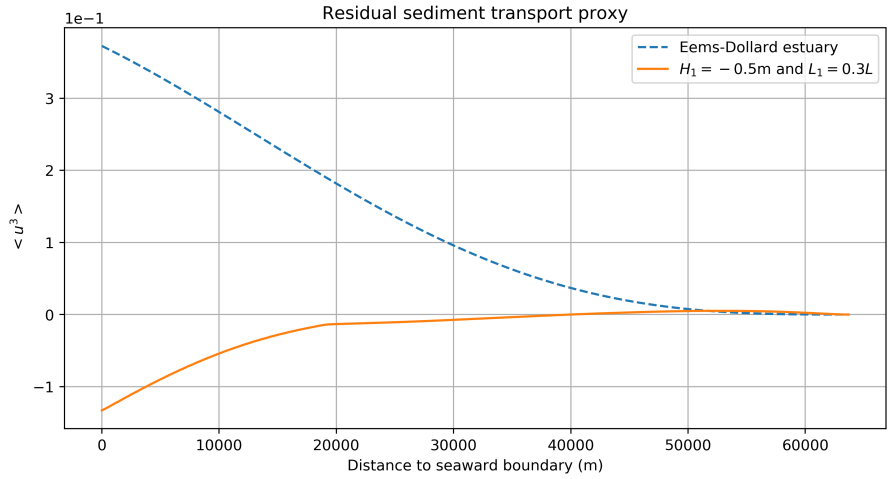

Figure 4.20: Plot of the sedimentation proxy which is given by $\langle u^3 \rangle$ as shown on the vertical axis. Furthermore on the horizontal axis the distance to the seaward boundary is shown.

Chapter 5

Conclusion

In this thesis, we investigated the water motion and sediment dynamics in an estuary. Several assumptions have been made that lead to the cross-sectionally averaged equations in chapter 2. A periodically opened and closed estuary was introduced and the equations were solved with the eigenfunction expansion method in chapter 3. In this chapter the postulated research questions are answered with the obtained results and corresponding discussion of chapter 4.

Can the sea surface elevation/tidal velocity in an estuary that is periodically opened and closed be accurately modeled with a limited number of Fourier modes in time?

In a periodically opened and closed estuary where no overtide was considered, we have three free parameters the closing position, closing height and closing time. The closing time is related to the closing height and position therefore only the closing height and closing position are varied to determine if it is possible to model a periodically opened and closed estuary with a finite number of Fourier modes. Closing the estuary at high water and varying L_1 gives us a sea-surface elevation ζ and tidal velocity u. Calculating the FFT of ζ and u gives us a finite spectrum (see Figure C.3) with peaks at angular frequencies which are multiples of σ (see Figures 4.10 and 4.11) therefore ζ and u are 12h25m periodic. If L_1 is fixed and H_1 is varied between high and low water the resulting ζ and u are again 12h25m periodic. We conclude that ζ and u can be written as a finite Fourier series for all closing positions and closing heights.

What is the influence of introducing a barrier on the residual sediment transport of an estuary?

The parameters L_1, the location of the barrier, and H_1, the closing height, describe the introduction of a barrier's influence. When no overtide is considered, it was found that the closing height H_1 determines the direction of the residual sediment transport. Closing the estuary at high water results in an landward directed residual sediment transport and closing the estuary at low water results in a seaward directed residual sediment transport. The closing position influences the magnitude of the residual sediment transport. It was found that the largest increase in landward directed residual sediment transport occurs at $L_1 = 0.6L$ and $H_1 = 0.5$m and the largest increase in seaward directed residual sediment transport occurs at $L_1 = 0.6L$ and $H_1 = -0.5$m. In the case that an overtide was introduced in the forcing of the system it was found that the closing height no longer determines the direction of the residual sediment tranport. The closing height and the location of the barrier determine the magnitude and the direction of the residual sediment transport.

The Ems-Dollard estuary has a landward directed residual sediment transport. By introducing a barrier that periodically closes and opens we intended to achieve a seaward directed residual sediment transport. The result of our research suggest that this is not possible. Further research is needed with more extensive models to confirm this. For future Research we recommend to extend the model to a two-dimensional model with the eigenfunction expansion method. Other possibilities may be to consider a spatial dependent erodible bed.

Appendix A

Initial conditions

In this section the asymptotic contribution of the initial condition for the sea-surface elevations (note that for the tidal velocity a similar derivation is possible) is derived given the following PDE with boundary and initial conditions:

$$\begin{aligned} &\frac{\partial^2\zeta}{\partial t^2} + \lambda\frac{\partial\zeta}{\partial t} - c_0^2\frac{\partial^2\zeta}{\partial x^2} = 0, \quad c_0^2 = gH, \\ &\zeta = \Re\left\{\hat{Z}e^{-i\sigma t}\right\} \quad \text{at} \quad x = 0, \quad \frac{\partial\zeta}{\partial x} = 0 \quad \text{at} \quad x = L, \\ &\zeta = f(x) \quad \text{at} \quad t = 0 \quad \frac{\partial\zeta}{\partial t} = g(x) \quad \text{at} \quad t = 0. \end{aligned} \tag{A.1}$$

Since the problem is linear the partial differential equation can be split into two parts. For the first part the initial conditions are taken zero of the same type and for the second part the boundary are taken zero of the same type. The latter part is the contribution of the initial conditions and therefore the only case considered and reads:

$$\begin{aligned} &\frac{\partial^2\zeta}{\partial t^2} + \lambda\frac{\partial\zeta}{\partial t} - c_0^2\frac{\partial^2\zeta}{\partial x^2} = 0, \quad c_0^2 = gH, \\ &\zeta = 0 \quad \text{at} \quad x = 0, \quad \frac{\partial\zeta}{\partial x} = 0 \quad \text{at} \quad x = L, \\ &\zeta = f(x) \quad \text{at} \quad t = 0 \quad \frac{\partial\zeta}{\partial t} = g(x) \quad \text{at} \quad t = 0. \end{aligned} \tag{A.2}$$

To solve Equation (A.2) the method of eigenfunction expansion method Haberman (1983) is considered. Assume that the solution $\zeta(x, y)$ is continuous together with $\frac{\partial\zeta}{\partial x}$, $\frac{\partial^2\zeta}{\partial x^2}$, $\frac{\partial\zeta}{\partial t}$ and $\frac{\partial^2\zeta}{\partial t^2}$. The eigenfunctions $\phi_n(x)$ and eigenvalues λ_n follow from the eigenvalue problem given by:

$$\begin{aligned} &\frac{d^2\phi(x)}{dx^2} = -\lambda\phi(x), \\ &\phi(x) = 0 \quad \text{at} \quad x = 0, \\ &\frac{d\phi(x)}{dx} = 0 \quad \text{at} \quad x = L. \end{aligned} \tag{A.3}$$

Solving the eigenvalue problem, the eigenfunctions and eigenvalues read:

$$\begin{aligned} &\lambda_n = \left(\frac{\pi(2n-1)}{2L}\right)^2 \quad n \in \{1, 2, \ldots\}, \\ &\phi_n(x) = \sin\left(\frac{\pi(2n-1)}{2L}x\right) \quad n \in \{1, 2, \ldots\}. \end{aligned} \tag{A.4}$$

The solution can be expanded as a Fourier sine series:

$$\zeta(x,t) \sim \sum_{n=1}^{\infty} B_n(t) \sin\left(\frac{\pi(2n-1)}{2L}x\right), \tag{A.5}$$

where $B_n(t)$ are the time-dependent coefficients. Since $\zeta(x,t)$ and $\frac{d\zeta}{dx}$ are continuous and $\zeta(0,t) = 0$ and $\frac{d\zeta(L,t)}{dx} = 0$, the Fourier sine and cosine series can be differentiated term by term:

$$\frac{\partial u}{\partial x} = \sum_{n=1}^{\infty} B_n(t) \left(\frac{\pi(2n-1)}{2L}x\right) \cos\left(\frac{\pi(2n-1)}{2L}x\right), \tag{A.6}$$

$$\frac{\partial^2 u}{\partial x^2} \sim -\sum_{n=1}^{\infty} \left(\frac{\pi(2n-1)}{2L}\right)^2 B_n(t) \sin\left(\frac{\pi(2n-1)}{2L}\right)^2. \tag{A.7}$$

According to the theorem on page 120 of Haberman (1983) the Fourier sine series can be differentiated term by term with respect to the parameter t, if $\frac{d\zeta}{dt}$ is piecewise smooth. Therefore assuming $\frac{d\zeta}{dx}$ and $\frac{d^2\zeta}{dx^2}$ are piecewise smooth the following can be stated:

$$\frac{\partial u}{\partial t} \sim \sum_{n=1}^{\infty} \frac{dB_n}{dt}(t) \sin\left(\frac{\pi(2n-1)}{2L}x\right), \tag{A.8}$$

$$\frac{\partial^2 u}{\partial t^2} \sim \sum_{n=1}^{\infty} \frac{d^2B_n}{dt^2}(t) \sin\left(\frac{\pi(2n-1)}{2L}x\right). \tag{A.9}$$

All the tools have been gathered to apply the eigenfunction expansion to the PDE stated in equation (A.2). Substituting the expansion in equation (A.2) and using the assumption stated in equation (A.6), (A.7), (A.8) and (A.9):

$$\sum_{n=1}^{\infty} \frac{d^2B_n}{dt^2}(t)\phi_n(x) - c_0^2 \sum_{n=1}^{\infty} B_n(t)\lambda_n \frac{d^2\phi_n(x)}{dx^2} + \hat{\lambda} \sum_{n=1}^{\infty} \frac{dB_n(t)}{dt}\phi_n(x) = 0. \tag{A.10}$$

Using the orthogonality of the eigenfunction and using the boundary conditions of the eigenvalue problem and our original are zero therefore being able to interchange integration and summation and substituting the term $\frac{d^2\phi_n(x)}{dx^2}$ for $-\lambda_n\phi_n(x)$ using equation (A.3), equation (A.10) reduces to an ODE .

$$\frac{d^2B_n}{dt^2}(t) + c_0^2 B_n(t)\lambda_p + \hat{\lambda}\frac{dB_n(t)}{dt} = 0. \tag{A.11}$$

The solution depends on the roots μ_+ and μ_- of the characteristic equation and read:

$$\mu_{\pm} = \frac{-\hat{\lambda} \pm \hat{\lambda}\left[1 - \frac{4\lambda_n c_0^2}{\hat{\lambda}^2}\right]^{\frac{1}{2}}}{2}. \tag{A.12}$$

An important question is: will the solution dampen out for $t \to \infty$? This is true if the following inequality is satisfied, where the biggest possible root of the characteristic equation is considered:

$$
\begin{aligned}
&\mu_- < 0, \\
&-\hat{\lambda}\left[1-\left[1-\frac{4\lambda_n c_0^2}{\hat{\lambda}^2}\right]^{\frac{1}{2}}\right] < 0, \\
&1-\left[1-\frac{4\lambda_n c_0^2}{\hat{\lambda}^2}\right]^{\frac{1}{2}} > 0, \\
&1-\frac{4\lambda_n c_0^2}{\hat{\lambda}^2} < 1, \\
&\frac{4\lambda_n c_0^2}{\hat{\lambda}^2} > 0.
\end{aligned}
\tag{A.13}
$$

The inequality is satisfied because λ_n, c_0^2 and $\hat{\lambda}^2$ are positive. Therefore the contribution of the initial condition to the solution of equation (A.1) are zero for $t \to \infty$ and no initial conditions are needed to solve equation (A.1) asymptotically.

Appendix B

Finite difference method

In this section the linearised cross-sectionally averaged equations for an open and closed estuary are solved with the finite difference method. To solve for the water motion, equation (3.2) and (3.3) are going to be solved to obtain the sea surface elevations and the tidal velocity.

B.1 The open estuary

$$\begin{aligned} &\frac{\partial^2\zeta}{\partial t^2} + \lambda\frac{\partial\zeta}{\partial t} - c_0^2\frac{\partial^2\zeta}{\partial x^2} = 0, \quad c_0^2 = gH, \\ &\zeta = \Re\left\{\hat{Z}e^{-i\sigma t}\right\} \quad \text{at} \quad x = 0, \quad \frac{\partial\zeta}{\partial x} = 0 \quad \text{at} \quad x = L, \\ &\zeta = f(x) \quad \text{at} \quad t = 0, \quad \frac{\partial\zeta}{\partial t} = g(x) \quad \text{at} \quad t = 0. \end{aligned} \tag{B.1}$$

The sea-surface elevation is computed numerically by discretizing equation (B.1). The following grid points are defined $x_i = i\Delta x$ with $i = 0, 1, \ldots, N$ and $t_n = n\Delta t$ with $n = 0, 1, \ldots, M$ where $\Delta x = L/N$, $\Delta t = T/M$, L is the estuary length and T is the final time. Furthermore $x_0 = 0$ and $x_N = L$. The values for the sea-surface elevations on an arbitrarily grid point and at a certain time are denoted as $\zeta_i^n = \zeta(i\Delta x, n\Delta t)$. For $i = 1, \ldots, N$ and $n = 1, \ldots, M$ the following discretizations are chosen for the derivatives in equation (3.2):

$$\begin{aligned} \left.\frac{\partial^2\zeta}{\partial t^2}\right|_i^n &= \frac{\zeta_i^{n+1} - 2\zeta_i^n + \zeta_i^{n-1}}{\Delta t^2} - \frac{(\Delta t)^2}{12}\left.\frac{\partial^4\zeta}{\partial t^4}\right|_i^n + O\left(\Delta t^4\right), \\ \left.\frac{\partial\zeta}{\partial t}\right|_i^n &= \frac{\zeta_i^{n+1} - \zeta_i^{n-1}}{2\Delta t} - \left.\frac{\partial^3\zeta}{\partial t^3}\right|_i^n + O\left(\Delta t^4\right), \\ \left.\frac{\partial^2\zeta}{\partial x^2}\right|_i^n &= \frac{\zeta_{i+1}^n - 2\zeta_i^n + \zeta_{i-1}^n}{\Delta x^2} - \frac{(\Delta x)^2}{12}\left.\frac{\partial^4\zeta}{\partial x^4}\right|_i^n + O\left(\Delta t^4\right). \end{aligned}$$

Substituting the discretization and omitting all terms of $\mathcal{O}(\Delta x^2, \Delta t^2)$ the finite difference scheme is derived:

$$\zeta_i^{n+1} = \frac{1}{1 + \frac{\lambda}{2}\Delta t}\left[2(1-s)\zeta_i^n - (1 - \frac{\lambda}{2}\Delta t)\zeta_i^{n-1} + s\left(\zeta_{i+1}^n + \zeta_{i-1}^n\right)\right].$$

Next the boundary conditions are considered. The numerical scheme is simplified for $i = 1$ and $N - 1$ and $n = 1, \ldots, M$ by using the boundary condition. the boundary condition at $x = 0$ can be rewritten as $\zeta_0^n = \hat{Z}\cos(\sigma n\Delta t)$ for $n = 1, \ldots, M$. For the other boundary condition a second order accurate backward difference is used:

$$\zeta_x(L,t)=0 \Rightarrow \frac{\partial \zeta_N^n}{\partial x}=0 \Rightarrow \frac{3\zeta_N^n-4\zeta_{N-1}^n+\zeta_{N-2}^n}{2\Delta x}=0 \Rightarrow \zeta_N^n=\frac{3}{4}\zeta_{N-1}^n-\frac{1}{3}\zeta_{N-2}^n \quad \text{for} \quad n=1,\ldots,M.$$

The full numeric scheme for $n=1,\ldots,M$ is given by:

$$\begin{aligned}
\zeta_i^{n+1} &= \frac{1}{1+\frac{\lambda}{2}\Delta t}\left[2(1-s)\zeta_i^n-(1-\frac{\lambda}{2}\Delta t)\zeta_i^{n-1}+s\left(\zeta_{i+1}^n+\zeta_{i-1}^n\right)\right] \quad \text{for} \quad i=2,\ldots,N-2,\\
\zeta_1^{n+1} &= \frac{1}{1+\frac{\lambda}{2}\Delta t}\left[2(1-s)\zeta_1^n-(1-\frac{\lambda}{2}\Delta t)\zeta_1^{n-1}+s\left(\zeta_2^n+\hat{Z}\cos(\sigma n\Delta t)\right)\right],\\
\zeta_{N-1}^{n+1} &= \frac{1}{1+\frac{\lambda}{2}\Delta t}\left[2(1-\frac{1}{3}s)\zeta_{N-1}^n-(1-\frac{\lambda}{2}\Delta t)\zeta_{N-1}^{n-1}+\frac{1}{3}s\zeta_{N-2}^n\right],
\end{aligned}$$

where $s=c^2\frac{\Delta t^2}{\Delta x^2}$. There is still a problem for $n=1$. To calculate ζ_i^1 the value ζ_i^{-1} is needed. Using the initial conditions the following relation is derived for $i=1,\ldots,N-1$:

$$\zeta_t(x,0)=g(x) \Rightarrow \frac{\partial \zeta_i^0}{\partial t}=g(x_i) \Rightarrow \frac{\zeta_i^1-\zeta_i^{-1}}{2\Delta t}=g(x_i) \Rightarrow \zeta_i^{-1}=\zeta_i^1-2\Delta t g(x_i).$$

With the above relation ζ_i^1 is derived:

$$\begin{aligned}
\zeta_i^1 &= \frac{1}{2}\left[2(1-s)\zeta_i^0+s\left(\zeta_{i+1}^0+\zeta_{i-1}^0\right)\right]+(1-\frac{1}{2}\lambda\Delta t)\Delta t g(x_i) \quad \text{for} \quad i=2,\ldots,N-2,\\
\zeta_1^1 &= \frac{1}{2}\left[2(1-s)\zeta_1^0+s\left(\zeta_2^0+\hat{Z}\right)\right]+(1-\frac{1}{2}\lambda\Delta t)\Delta t g(x_1),\\
\zeta_{N-1}^1 &= \frac{1}{2}\left[2(1-\frac{1}{3}s)\zeta_{N-1}^0+\frac{2}{3}s\zeta_{N-2}^n\right]+(1-\frac{1}{2}\lambda\Delta t)\Delta t g(x_{N-1}).
\end{aligned} \tag{B.2}$$

The sea-surface elevations can now be calculated with given initial condition $\boldsymbol{\zeta^0}=\boldsymbol{f(x)}$. First $\boldsymbol{\zeta^1}$ is calculated and consequently $\boldsymbol{\zeta^{n+1}}$ for $n=1,\ldots,M$:

$$\boldsymbol{\zeta^1}=\begin{pmatrix}\zeta_1^1\\ \vdots\\ \vdots\\ \zeta_{N-1}^1\end{pmatrix}=\tfrac{1}{2}\begin{pmatrix}2(1-s) & s & & \\ s & \ddots & \ddots & \\ & \ddots & \ddots & s\\ & & \frac{2}{3}s & 2(1-\frac{1}{3}s)\end{pmatrix}\boldsymbol{\zeta^0}+\begin{pmatrix}\frac{s\hat{Z}}{2}\\ 0\\ \vdots\\ 0\end{pmatrix}+\begin{pmatrix}(1-\frac{1}{2}\lambda\Delta t)\Delta t g(x_1)\\ (1-\frac{1}{2}\lambda\Delta t)\Delta t g(x_2)\\ \vdots\\ (1-\frac{1}{2}\lambda\Delta t)\Delta t g(x_{N-1})\end{pmatrix}$$

,

$$\begin{aligned}
\boldsymbol{\zeta^{n+1}}=\begin{pmatrix}\zeta_1^{n+1}\\ \vdots\\ \vdots\\ \zeta_{N-1}^1\end{pmatrix} &= \tfrac{1}{1+\frac{1}{2}\lambda\Delta t}\begin{pmatrix}2(1-s) & s & & \\ s & \ddots & \ddots & \\ & \ddots & \ddots & s\\ & & \frac{2}{3}s & 2(1-\frac{1}{3}s)\end{pmatrix}\boldsymbol{\zeta^n}\\
&+\tfrac{\frac{1}{2}\lambda\Delta t-1}{1+\frac{1}{2}\lambda\Delta t}\boldsymbol{\zeta^{n-1}}+\begin{pmatrix}\frac{s\hat{Z}\cos(\sigma n\Delta t)}{1+\frac{1}{2}\lambda\Delta t}\\ 0\\ \vdots\\ 0\end{pmatrix}.
\end{aligned}$$

Similarly a finite difference scheme is derived for the tidal velocity given by equation (3.3). Again the initial condition are $\boldsymbol{u^0} = \boldsymbol{f(x)}$:

$$\boldsymbol{u^1} = \begin{pmatrix} u_1^1 \\ \vdots \\ \vdots \\ u_{N-1}^1 \end{pmatrix} = \frac{1}{2} \begin{pmatrix} 2(1-\frac{1}{3}s) & \frac{2}{3}s & & \\ s & 2(1-s) & s & \\ & s & \ddots & \ddots \\ & & \ddots & \ddots \end{pmatrix} \boldsymbol{u^0} + \begin{pmatrix} (1-\frac{1}{2}\lambda\Delta t)\Delta t g(x_1) \\ (1-\frac{1}{2}\lambda\Delta t)\Delta t g(x_2) \\ \vdots \\ (1-\frac{1}{2}\lambda\Delta t)\Delta t g(x_{N-1}) \end{pmatrix},$$

$$\boldsymbol{u^{n+1}} = \begin{pmatrix} u1^{n+1} \\ \vdots \\ \vdots \\ u_{N-1}^1 \end{pmatrix} = \frac{1}{1+\frac{1}{2}\lambda\Delta t} \begin{pmatrix} 2(1-\frac{1}{3}s) & \frac{2}{3}s & & \\ s & 2(1-s) & s & \\ & s & \ddots & \ddots \\ & & \ddots & \ddots \end{pmatrix} \boldsymbol{u^n} + \frac{\frac{1}{2}\lambda\Delta t - 1}{1+\frac{1}{2}\lambda\Delta t} \boldsymbol{u^{n-1}} + \begin{pmatrix} -\frac{2\Delta x s \hat{Z} \cos(\sigma n \Delta t)}{3H(1+\frac{1}{2}\lambda\Delta t)} \\ 0 \\ \vdots \\ 0 \end{pmatrix}.$$

Given the above schemes both the sea-surface elevations and the tidal velocity can be calculated. The values given in Table B.1 are used. Furthermore for the initial conditions $\boldsymbol{f(x)}$ and $\boldsymbol{g(x)}$ the analytic solution stated in equation (3.7) is used at $t = 0$. For stability reasons the value of s must lie between zero and one, therefore $\Delta t = 0.99 \cdot \frac{\Delta x}{c}$. This can be intuitively understand by rewriting $s = c^2 \frac{\Delta t^2}{\Delta x^2} < 1 \iff c\Delta t < \Delta x$. This means that the distance that is travelled by ζ or u is bounded by the chosen grid step size. In Figure B.1 a comparison between the FDM and analytical solution for the sea-surface elevation and tidal velocity is shown for different time t.

Parameter		Value
Gravitational acceleration	g	9.81 $\frac{m}{s^2}$
Height of Estuary	H	10 m
Angular frequency of semi-diurnal tide	σ	2π/12h25m s^{-1}
Length of estuary	L	6.6E4 m
Frictional damping	λ	14.25E-5
Amplitude of semi-diurnal tide	$\hat{Z}$	1.5m
Grid step size	Δx	54.6 m
Time step size	Δt	$0.99 \cdot \frac{\Delta x}{c}$

Table B.1: List of values for the parameters that are used for the numerical computation.

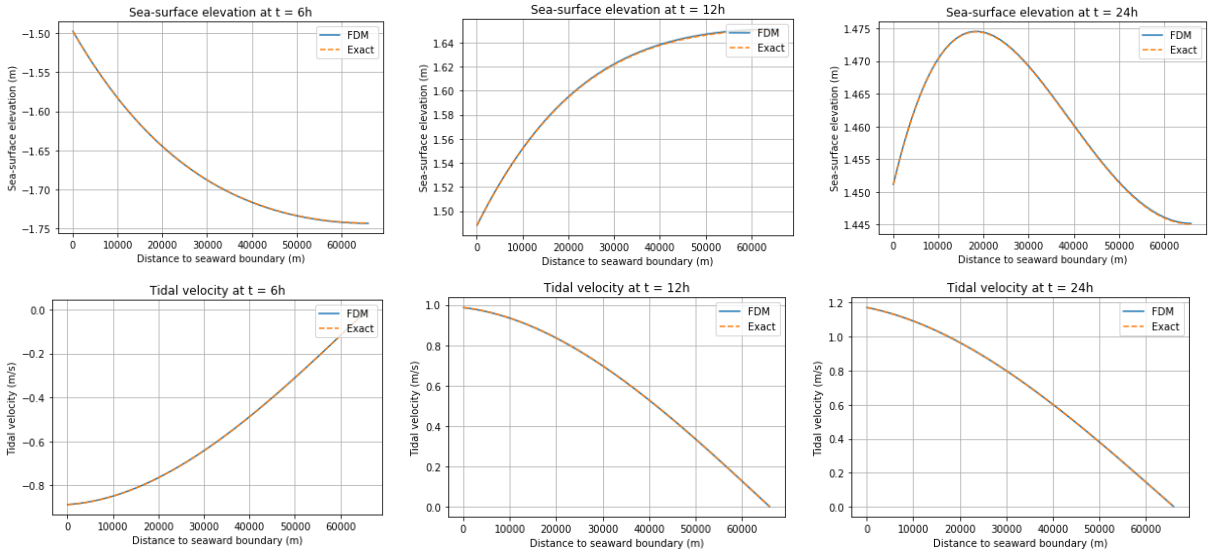

Figure B.1: In the first row the sea-surface elevations in meters is plotted against the distance to the seaward boundary in meters. In the second row the tidal velocity in meters per second is plotted against the distance to the seaward boundary in meters.

In Figure B.2 the L_2 norm of the error is shown for both the sea-surface elevation and the tidal velocity. There is a clear oscillation present with a maximum error of order 10^{-3} for the tidal velocity and 10^{-4} for the sea-surface elevation.

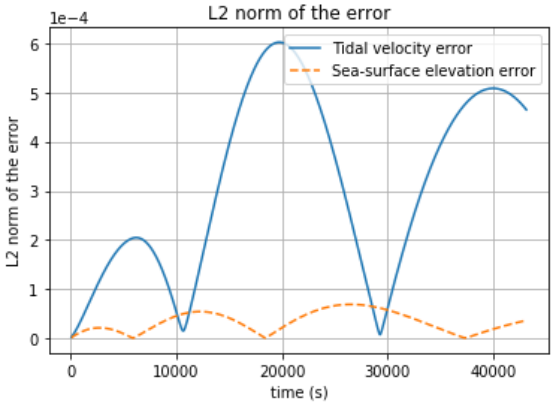

Figure B.2: The L_2 norm of the error for both the Tidal velocity (blue line) and the Sea-surface elevations (orange dashed line) is plotted against the time in seconds.

B.2 The closed estuary

$$\begin{aligned} &\frac{\partial^2\zeta}{\partial t^2} + \lambda\frac{\partial\zeta}{\partial t} - c_0^2\frac{\partial^2\zeta}{\partial x^2} = 0, \quad c_0^2 = gH, \\ &\frac{\partial\zeta}{\partial x} = 0 \quad \text{at} \quad x = L_1, \quad \frac{\partial\zeta}{\partial x} = 0 \quad \text{at} \quad x = L \\ &\zeta = f(x) \quad \text{at} \quad t = 0, \quad \frac{\partial\zeta}{\partial t} = g(x) \quad \text{at} \quad t = 0. \end{aligned} \tag{B.3}$$

For a closed Estuary, a Neumann boundary condition is imposed at $x = L_1$. This is summarized in equation (B.3). The discretization is almost the same as in section B.1 the only things to

reconsider are the discretized domain, the new boundary condition and the initial conditions. In the new domain the first and last grid point are defined as $x_0 = L_1$ and $x_N = L$. From the newly imposed boundary condition a relation is derived to simplify ζ_1^n for $n = 1 \dots M$ as follow:

$$\zeta_x(L_1, t) = 0 \Rightarrow \frac{\partial \zeta_1^n}{\partial x} = 0 \Rightarrow \frac{-3\zeta_0^n + 4\zeta_1^n - \zeta_2^n}{2\Delta x} = 0 \Rightarrow \zeta_0^n = \frac{3}{4}\zeta_1^n - \frac{1}{3}\zeta_2^n. \tag{B.4}$$

At last the initial condition $\boldsymbol{f(x)}$ is obtained from the open estuary scheme at $t = 12h$ and $\boldsymbol{g(x)}$ is obtained by recalling equation (3.1b) and noticing that both u and ζ are coupled, therefore:

$$g(x) = \left.\frac{\partial \zeta}{\partial t}\right|_{t=0} = -H\frac{\partial u}{\partial x} \Rightarrow g(x_i) = -H\left(\frac{u\left(x_{i+1}\right) - u\left(x_{i-1}\right)}{2\Delta x}\right) \quad \text{for i} = 1, 2, \dots N-1. \tag{B.5}$$

For the boundaries the forward/backward approximation are used to finalize $\boldsymbol{g(x)}$. Applying the above insights to the previous scheme and defining the new grid points $x_i = i\Delta x$ with $i = 0, 1, \dots, N$ on a smaller domain where Δx is the same as before and $N = (L - L_1)/\Delta x$. The sea-surface elevation is again calculated by a three stepping scheme. With the given initial condition $\boldsymbol{\zeta^0} = \boldsymbol{f(x)}$ first $\boldsymbol{\zeta^1}$ is calculated and consequently $\boldsymbol{\zeta^{n+1}}$ for $n = 1, \dots, M$:

$$\boldsymbol{\zeta^1} = \begin{pmatrix} \zeta_1^1 \\ \vdots \\ \vdots \\ \zeta_{N-1}^1 \end{pmatrix} = \frac{1}{2}\begin{pmatrix} 2(1-\frac{1}{3}s) & \frac{2}{3}s & & \\ s & 2(1-s) & s & \\ & \ddots & \ddots & \ddots \\ & & \frac{2}{3}s & 2(1-\frac{1}{3}s) \end{pmatrix}\boldsymbol{\zeta^0} + \begin{pmatrix} (1-\frac{1}{2}\lambda\Delta t)\Delta t g(x_1) \\ (1-\frac{1}{2}\lambda\Delta t)\Delta t g(x_2) \\ \vdots \\ (1-\frac{1}{2}\lambda\Delta t)\Delta t g(x_{N-1}) \end{pmatrix}, \tag{B.6}$$

$$\boldsymbol{\zeta^{n+1}} = \begin{pmatrix} \zeta_1^{n+1} \\ \vdots \\ \vdots \\ \zeta_{N-1}^1 \end{pmatrix} = \frac{1}{1+\frac{1}{2}\lambda\Delta t}\begin{pmatrix} 2(1-\frac{1}{3}s) & \frac{2}{3}s & & \\ s & 2(1-s) & s & \\ & \ddots & \ddots & \ddots \\ & & \frac{2}{3}s & 2(1-\frac{1}{3}s) \end{pmatrix}\boldsymbol{\zeta^n} + \frac{\frac{1}{2}\lambda\Delta t - 1}{1+\frac{1}{2}\lambda\Delta t}\boldsymbol{\zeta^{n-1}}. \tag{B.7}$$

In the same fashion the tidal velocity is discretized. The newly imposed Dirichlet boundary condition at $x = L_1$ is shown in the following equation:

$$\begin{aligned} &\frac{\partial^2 u}{\partial t^2} + \lambda\frac{\partial u}{\partial t} - c_0^2\frac{\partial^2 u}{\partial x^2} = 0, \quad c_0^2 = gH, \\ &u = 0 \quad \text{at} \quad x = L_1, \quad u = 0 \quad \text{at} \quad x = L, \\ &u = f(x) \quad \text{at} \quad t = 0, \quad \frac{\partial u}{\partial t} = g(x) \quad \text{at} \quad t = 0. \end{aligned} \tag{B.8}$$

The only things to reconsider from the previous scheme are u_1^n for $n = 1, \dots, M$ and $\boldsymbol{g(x)}$. From the boundary condition it is clear that $u_0^n = 0$ for $n = 1, \dots, M$. Next $\boldsymbol{g(x)}$ is derived by recalling equation (3.1b):

$$g(x) = \left.\frac{\partial u}{\partial t}\right|_{t=0} = -g\frac{\partial \zeta}{\partial x} - \lambda u \Rightarrow g(x_i) = -g\left(\frac{\zeta\left(x_{i+1}\right) - \zeta\left(x_{i-1}\right)}{2\Delta x}\right) - \lambda u_i \quad \text{for i} = 1, 2, \dots N-1. \tag{B.9}$$

Applying these relations gives the following three stepping scheme for the tidal velocity. Given the initial condition $\boldsymbol{u^0} = \boldsymbol{f(x)}$ first $\boldsymbol{u^1}$ is calculated and consequently $\boldsymbol{u^{n+1}}$ for $n = 1, \dots, M$:

$$\boldsymbol{u^1} = \begin{pmatrix} u_1^1 \\ \vdots \\ \vdots \\ u_{N-1}^1 \end{pmatrix} = \tfrac{1}{2} \begin{pmatrix} 2(1-s) & s & & \\ s & 2(1-s) & s & \\ & s & \ddots & \ddots \\ & & \ddots & \ddots \end{pmatrix} \boldsymbol{u^0} + \begin{pmatrix} (1-\frac{1}{2}\lambda\Delta t)\Delta t g(x_1) \\ (1-\frac{1}{2}\lambda\Delta t)\Delta t g(x_2) \\ \vdots \\ (1-\frac{1}{2}\lambda\Delta t)\Delta t g(x_{N-1}) \end{pmatrix}, \tag{B.10}$$

$$\boldsymbol{u^{n+1}} = \begin{pmatrix} u1^{n+1} \\ \vdots \\ \vdots \\ u_{N-1}^1 \end{pmatrix} = \tfrac{1}{1+\frac{1}{2}\lambda\Delta t} \begin{pmatrix} 2(1-s) & s & & \\ s & 2(1-s) & s & \\ & s & \ddots & \ddots \\ & & \ddots & \ddots \end{pmatrix} \boldsymbol{u^n} + \tfrac{\frac{1}{2}\lambda\Delta t - 1}{1+\frac{1}{2}\lambda\Delta t} \boldsymbol{u^{n-1}}. \tag{B.11}$$

We want to test our scheme, but there is no analytic solution therefore another method is needed. In section 3.2 the eigenfunctions are derived these can be used to test the scheme by noticing that, if a eigenfunction is used as an initial condition then the output of the scheme gives a rescaled eigenfunction. The eigenfunctions $\phi_n^\zeta(x)$ of equation (B.1) and $\phi_n^u(x)$ of equation (B.8) are given by:

$$\phi_n^\zeta(x) = \cos\left(\frac{\pi n(x-L)}{L_1 - L}\right), \quad \phi_n^u(x) = \sin\left(\frac{\pi n(x-L)}{L_1 - L}\right). \tag{B.12}$$

To test the correctness of the finite difference method for a closed estuary, a specific eigenfunction is used as initial condition and the ratio between the initial condition and the resulting sea-surface elevation after a specific time is checked to be constant. The plots of the ratio of the eigenfunctions are shown in Figure B.3. We see that the output of the finite difference method gives a re-scaled eigenfunction back, suggesting the finite difference method gives correct results.

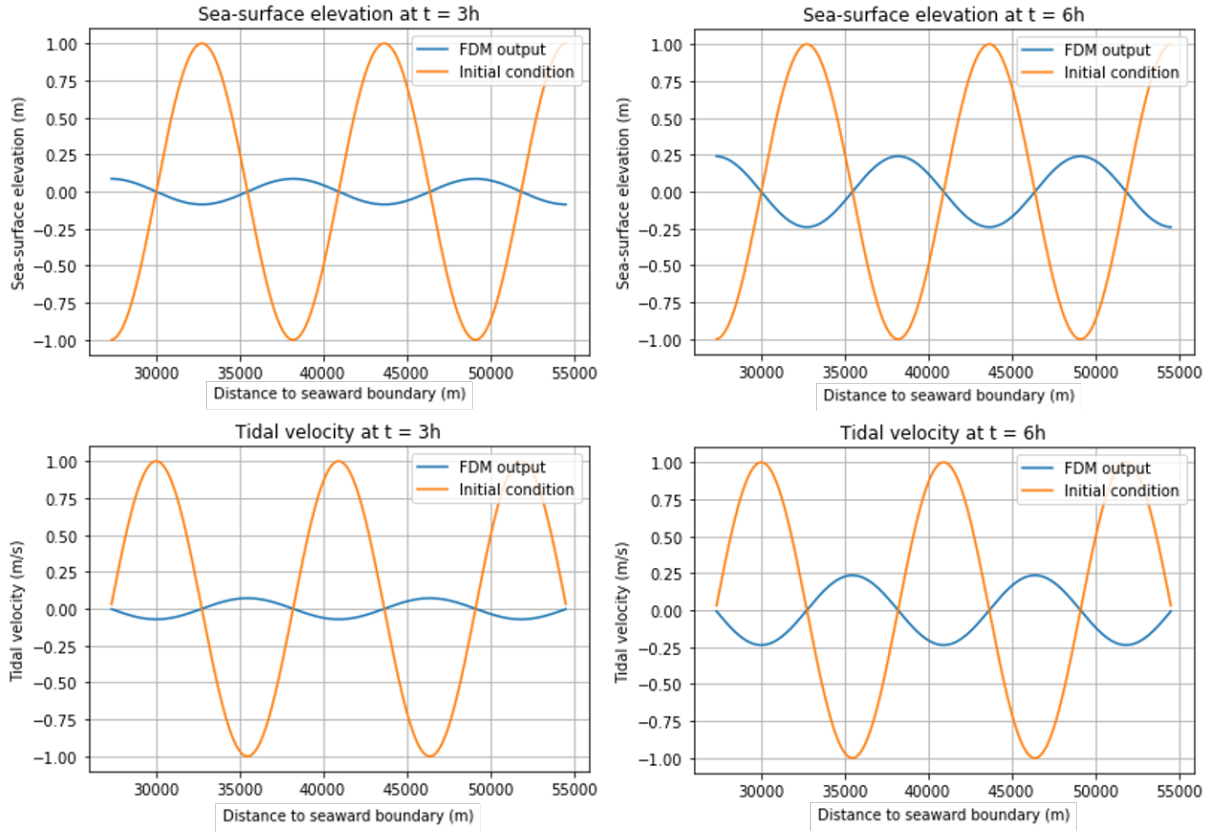

Figure B.3: In the first row the sea-surface elevations, colored orange, is plotted with its corresponding eigenfunctions with mode number $n = 5$, colored blue, as initial condition. In the second row the tidal velocity

Appendix C

Supplementary figures for results

C.1 Full spectra

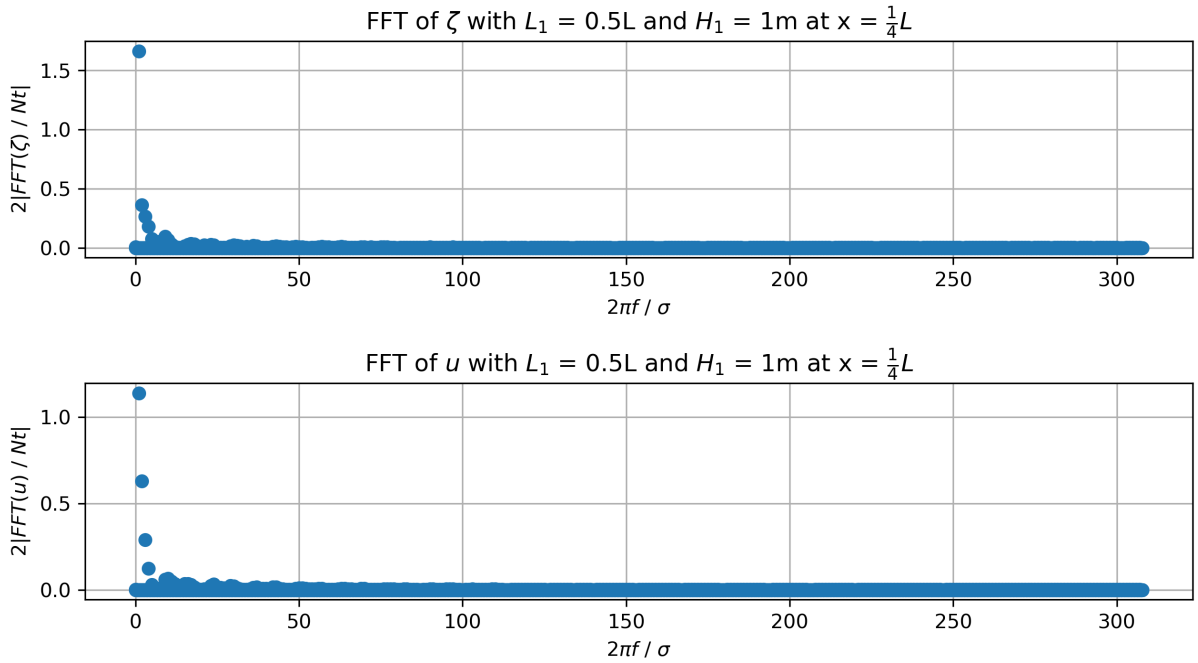

Figure C.1: Plot of the FFT of the sea-surface elevations and tidal velocity at $x = 0.25L$.

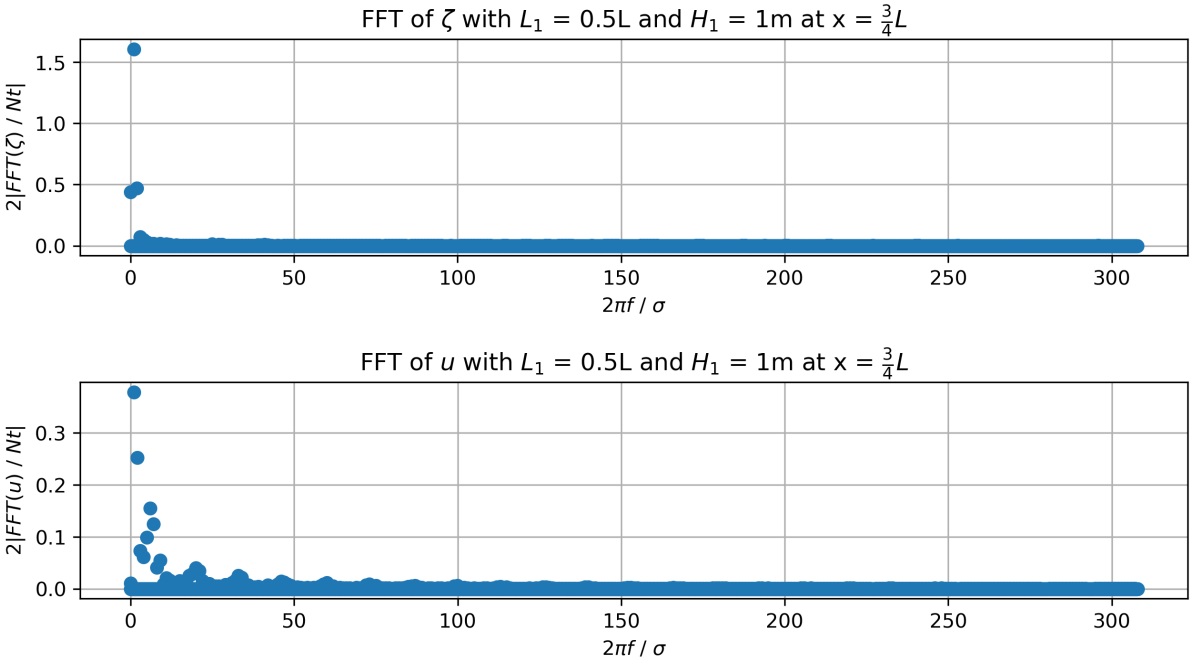

Figure C.2: Plot of the FFT of the sea-surface elevations and tidal velocity at $x = 0.75L$.

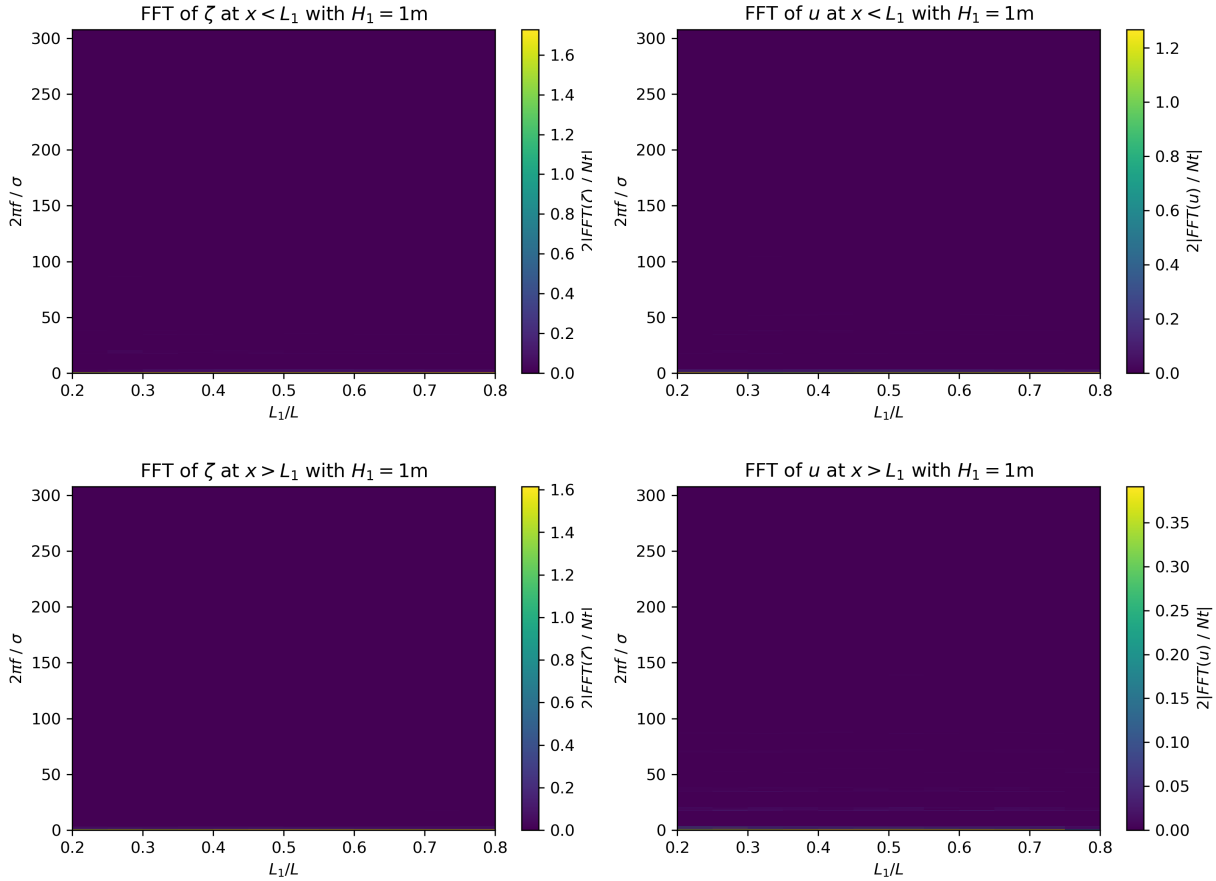

Figure C.3: In the first row the FFT at a fixed $x < L_1$ of ζ and u are shown. In the second row the FFT is shown for $x > L_1$.

C.2 Convergence

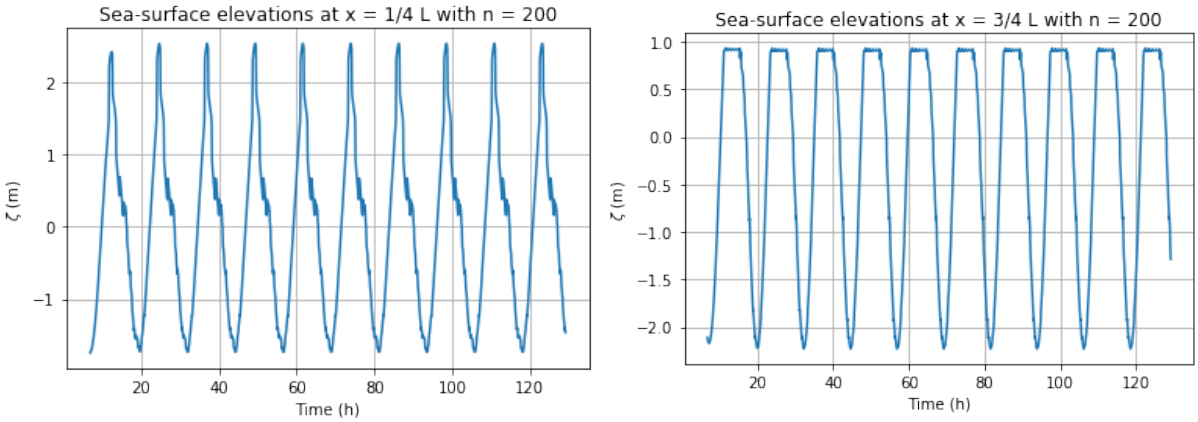

Figure C.4: At the left the sea-surface elevations is shown at $x = 1/4L$ and at the right at $x = 3/4L$

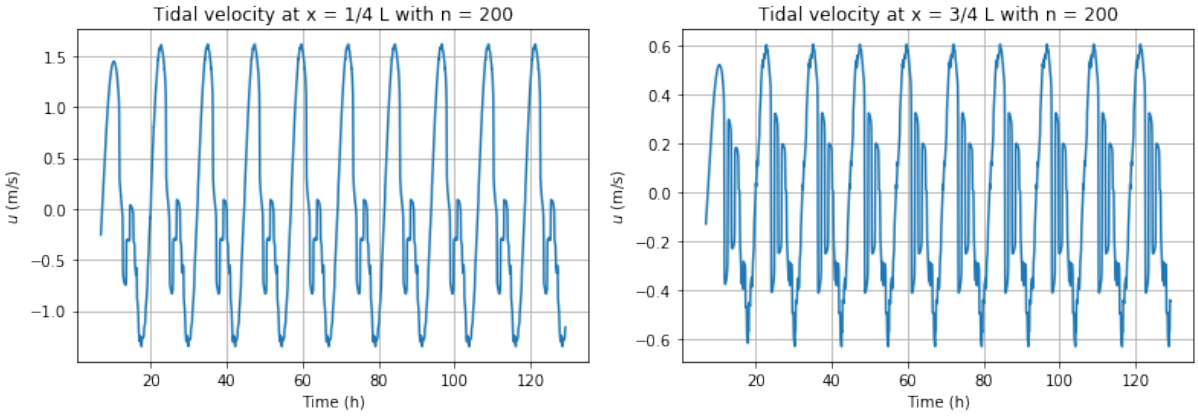

Figure C.5: At the left the tidal velocity is shown at $x = 1/4L$ and at the right at $x = 3/4L$

Bibliography

Boesch et al. Scientific assessment of coastal wetland loss, restoration and management in louisiana. *Journal of Coastal Research*, pages 1–103, 1994.

Burchard et al. Sediment trapping in estuaries. 2018.

Geórgenes H. Cavalcante. *Well-Mixed Estuary*, pages 737–738. Springer Netherlands, Dordrecht, 2016. ISBN 978-94-017-8801-4. doi: 10.1007/978-94-017-8801-4_184. URL https://doi.org/10.1007/978-94-017-8801-4_184.

A Chernetsky. Trapping of sediment in tidal estuaries. 2012.

Benoit Cushman-Roisin and Jean-Marie Beckers. *Introduction to geophysical fluid dynamics: physical and numerical aspects*. Academic press, 2011.

Thijs de Jongh. Idealised tidal dynamics in an estuary with a horizontally movable time dependent barrier: A contribution to one of the possible solutions of the sludge problem in the eems estuary. 2020.

HE De Swart. Physics of coastal systems. 2006.

Richard Haberman. *Elementary applied partial differential equations*, volume 987. Prentice Hall Englewood Cliffs, NJ, 1983.

Krebs et al. Ems-dollart estuary. *Die Küste, 74 ICCE*, (74):252–262, 2008.

Robert H Meade. Landward transport of bottom sediments in estuaries of the atlantic coastal plain. *Journal of Sedimentary Research*, 39(1):222–234, 1969.

Jacques CJ Nihoul. *Modelling of marine systems*. Elsevier, 2011.

Joseph Pedlosky. *Geophysical fluid dynamics*. Springer Science & Business Media, 2013.

Donald W Pritchard. *What is an estuary: physical viewpoint*. 1967.

Marco Rozendaal. An idealised morphodynamic model of a tidal inlet and the adjacent sea. 2019.

HM Schuttelaars and HE De Swart. Cyclic bar behaviour in a nonlinear model of a tidal inlet. In *Managing Water: Coping with Scarcity and Abundance*, pages 28–33. ASCE, 1996.

HM Schuttelaars and HE De Swart. An idealized long-term morphodynamic model of a tidal embayment. 1997.

HM Schuttelaars and HE De Swart. Multiple morphodynamic equilibria in tidal embayments. *Journal of Geophysical Research: Oceans*, 105(C10):24105–24118, 2000.

Miriam Carolien Ter Brake. Tidal embayments: modelling and understanding their morphodynamics. 2011.

van Albada et al. A comparative study of computational methods in cosmic gas dynamics. 1982.

Joop van Houdt. Groningen. *defotograaf.eu*.

Cornelis Boudewijn Vreugdenhil. *Numerical methods for shallow-water flow*, volume 13. Springer Science & Business Media, 2013.

Wang et al. Tidal asymmetry and residual sediment transport in estuaries. *Delft Hydraulics report Z2749*, 1999.